DISSERTATION

THE MICROBIOME SURROUNDING DEATH AND DECAY: MICROBIAL ECOLOGY OF FOOD PROCESSING, MEAT SPOILAGE, AND HUMAN DECOMPOSITION ENVIRONMENTS

Submitted by

Aeriel D. Belk

Department of Animal Sciences

In partial fulfillment of the requirements

For the Degree of Doctor of Philosophy

Colorado State University

Fort Collins, Colorado

Summer 2021

Doctoral Committee:

Advisor: Jessica L. Metcalf

Jennifer Martin
Kelly Wrighton
Asa Ben-Hur

This resource was prepared by the author(s) using Federal funds provided by the U.S. Department of Justice. Opinions or points of view expressed are those of the author(s) and do not necessarily reflect the official position or policies of the U.S. Department of Justice.

This resource was prepared by the author(s) using Federal funds provided by the U.S. Department of Justice. Opinions or points of view expressed are those of the author(s) and do not necessarily reflect the official position or policies of the U.S. Department of Justice.

ABSTRACT

THE MICROBIOME SURROUNDING DEATH AND DECAY: MICROBIAL ECOLOGY OF FOOD PROCESSING, MEAT SPOILAGE, AND HUMAN DECOMPOSITION ENVIRONMENTS

The primary processes associated with spoilage and decomposition are driven by microorganisms present on and near the decomposing tissues. Therefore, to better understand the decomposition processes, it is critical that we evaluate the microbial ecology of these systems. In this dissertation, I apply questions related to the vertebrate decomposition environment to several systems: the built environment, meat spoilage, and human decomposition for forensic sciences. The overarching goal of this dissertation is to demonstrate the patterns with which microbial communities assemble and progress in these specific environments, and to show the applications of this knowledge to the larger industry and research fields.

Given the diversity of these environments and systems, I begin this dissertation with a review of literature for each of the areas in the first chapter. This chapter summarizes the current knowledge of built environments with a specific focus on the sources of microorganisms in these environments, how the microbial communities assemble, and the ecology of the communities in food processing facilities specifically. Then, I describe the current knowledge related to meat spoilage-associated microorganisms, with specific focus on their role in poultry processing and spoilage. Finally, I introduce terrestrial, outdoor vertebrate decomposition environments. I specifically describe how vertebrate decomposition research can be applied to forensic science, as the patterns of microbial succession in these environments can be used to predict the postmortem interval (PMI).

The second chapter, titled “The microbiome of a newly constructed meat processing facility establishes over time by room function and microbial source”, describes a research project investigating the microbiome of the built environment of a meat processing facility. We conducted this study to investigate knowledge gaps surrounding how microbial communities initially form in a food processing

environment. Specifically, we investigated three major research questions: (1) Is a stable microbiome established in a meat processing facility? (2) What factors are associated with the facility microbial composition? (3) What are the major sources of microbes present in the facility microbiome? To address these questions, we collected samples of the microbial communities from drains and door handles in the newly constructed meat processing facility at Colorado State University approximately monthly spanning the first 18 months of operation. We used 16S rRNA gene sequencing following Earth Microbiome Project protocols to elucidate the content of the microbial communities, and further investigated the patterns using QIIME2 and R. Results indicated that stable microbial communities begin to form throughout the processing facility within the first eight to nine months of consistent production. However, these communities appeared subject to perturbation when major conditions in the facility change, such as a large shift in production volume. Additionally, different communities form within spaces, likely selected for by microbial source, room temperature, general use, and nutrient availability. Interestingly, it also appeared that physical barriers within the facility prevented specific organisms from being transmitted between spaces. Overall, this study demonstrates the importance of deliberate facility design and regular cleaning and sanitation practices to control the microbial communities in the food processing space.

Chapter 3, “Air versus water chilling of chicken: a pilot study of quality, shelf-life, microbial ecology, and economics”, describes an experiement evaluating the microbial communities associated with chicken breasts that were chilled using two different methods and how the communities from these two treatments lead to different patterns in spoilage over time. In this study, we assessed the meat quality, shelf-life, microbial ecology, and techno-economic impacts of chilling methods on chicken broilers in a university meat laboratory setting. We discovered that air-chilling methods resulted in superior chicken odor and shelf-life, especially prior to 14 days of dark storage. Moreover, we demonstrated that air chilling resulted in a more diverse microbiome that we hypothesize may delay the dominance of the spoilage organism *Pseudomonas*. Finally, a techno-economic analysis highlighted potential economic advantages to air chilling when compared to water-chilling in facility locations where water costs are a

more significant factor than energy costs. Overall, we demonstrated that the method used during chilling (air vs water chilling) influences the final product microbial community, quality, and physiochemistry. Notably, the use of air chilling appeared to delay the bloom of *Pseudomonas* spp that are the primary spoilers in packaged meat products. By using air chilling to reduce carcass temperatures instead of water chilling producers may extend the time until spoilage of the products and, depending on costs of water in the area, may have economic and sustainability advantages.

The fourth and fifth chapters describe studies in which we used patterns in microbial succession in decomposition environments to investigate how decomposition changes the microbial ecology and methods by which these patterns can be used to predict PMI. In chapter four, "Microbiome data accurately predict the postrmortem interval using random forest regression models", we explored how to build the most robust Random Forest regression models for prediction of PMI by testing models built on different sample types (gravesoil, skin of the torso, skin of the head), gene markers (16s rRNA, 18s rRNA, ITS), and taxonomic levels (Sequence Variants, Species, Genus). We also tested whether particular suites of indicator microbes were informative across different datasets. Generally, results indicate that the most accurate models for predicting PMI were built using gravesoil and skin data using the 16s rRNA genetic marker at the taxonomic level of phyla. Additionally, several phyla consistently contributed highly to model accuracy and may be candidate indicators of PMI.

In chapter five, "Patterns of microbial succession in skin and decomposition-associated soils are predictive of the postmortem interval of human remains", we sought to improve the understanding of microbial communities in postmortem human environments by evaluating the patterns of microbial succession associated with human remains at three geographically distinct locations. The primary objectives were to (1) identify patterns in microbial diversity and taxonomy during human decomposition in skin and decomposition-associated soils across distinct environments and (2) determine the utility of amplicon sequencing-derived microbiome data in predicting the postmortem interval within the first 21 days of decomposition. To achieve these, we decomposed a total of 36 donated human remains across three anthropological research facilities (three per season per facility for four seasons) in distinct climactic

regions of the United States. We collected microbial samples from the skin of the face, skin of the hip, soil near the face, and soil near the hip daily for the first 21 days of decomposition. These were then sequenced for the 16S and 18S rRNA genes to evaluate the microbial community composition, and generated models to estimate PMI using the Random Forest algorithm with nested cross-validation. We showed that the microbial diversity of decomposition soils decreased over time, likely due to environmental selection for specific organisms such as *Clostridiales, Pseudomonodales*, and *Xanthamonadales*. The environmental conditions of the anthropological research facilities used in this study led to distinct differences in microbial communities by location, but patterns of succession were still present. Models constructed to predict PMI from the microbial community were accurate within 49 to 92.33 ADD, which is equivalent to 3 to 5.82 days. Models were more accurate when greater taxonomic resolution was used in training. Overall, these results demonstrate that the patterns of microbial succession are predictive of PMI, even across different environments.

In summary, in this dissertation I present the results of a series of studies, all of which describe the microbial community development and succession in distinct environments. All of these environments have the potential to influence the decomposition patterns of vertebrate remains. In food processing and meat environments, the microbes present in the community are connected to meat spoilage, which can shorten the product shelf life and contribute to the global food waste problem. In human decomposition, these patterns can be used by forensic investigators to estimate PMI and gain crucial evidence about the death event. In this dissertation, I demonstrate real-world applications of microbial ecology that can protect human health and well-being, and potentially solve crimes.

ACKNOWLEDGMENTS

"It is the long history of humankind (and animal kind, too) those who learned to collaborate and improvise most effectively have prevailed." - Charles Darwin

Though I am proud of the work I was able to accomplish during my graduate program, I would not have been able to do any of it without the incredible mentors, collaborators, teachers, and friends that helped and supported me.

First and foremost, I need to thank my incredible advisor, Dr. Jessica Metcalf. She is the best mentor an aspiring scientist can hope to find. She helped me not only elevate my science, but taught me life skills, like advocacy and negotiations. She offered me incredible opportunities to teach and travel and learn from experts in the field, far beyond what I ever expected. I never imagined that a PhD could be so much more than research, but Jessica created a healthy and supportive environment that let me enjoy everything I participated in. I joined clubs, tried new fields, and went on adventures because of what Jessica did for me. She also taught me the basic skills, like how to write like a scientist. Every topic sentence in this dissertation exists thanks to Jessica's training and the opportunities she gave me to practice. I had to save this paragraph for last, because it is so difficult to put into words how grateful I am for her mentorship and friendship.

I am also incredibly grateful for the support and guidance of my committee members. I spent a lot of time in Dr. Jennifer Martin's office over the last few years, planning out how to make a miniature chicken plant in a meat lab in another state and going over how to analyze meats data. She was also always there if I just needed some help or advice. Dr. Kelly Wrighton provided incredible scientific expertise and advise and taught me how to think ecologically and put together a good story. Beyond academics, Kelly helped us build a community of graduate students in microbiome sciences that became an incredibly important part of my support system, and for that support I'll be eternally grateful. And Dr. Asa Ben-Hur taught me everything I know about machine learning, both in classes and when helping me

workshop my own data. He also taught me mindfulness, a skill that I take advantage of often. Taking breaks to meditate is a practice that will continue to benefit me even when the rest of my work becomes obsolete. I could not have wished for a better committee to guide me through this program! I also need to thank all of the mentors I had during my undergraduate and master's programs: Dr. Jason Bruemmer, Dr. Gina Geornaras, Dr. Jeff Savell, Dr. Matt Taylor, Dr. Kerri Gehring, Dr. Ashley Arnold, and each and every professor I've ever taken a class with were all instrumental in building the foundation I now walk on.

Support from mentors is critical to anyone's success but support from peers is just as important. I was immeasurably lucky to have the best peer network anyone could hope for. When I started my program, I had Maggie Weinroth to teach me everything she could about sequencing, coding, and writing science. Even after she graduated, she continued to help me as I tried to fill her shoes here at CSU, watching me practice every presentation and giving me feedback on every poster. She more than anyone understands my love of research competitions. I was also so blessed to have Heather Deel as a lab mate and adventure partner. We explored conferences, braved a Baltimore snowfall, tag-teamed presentations, and taught more classes and workshops than I can count. She'll always answer my questions, even when they're stupid, and one time even dreamed the answer to a problem I had.

The other graduate students in the meats group at CSU were support systems, troubleshooting buddies, and best friends during my program. So, thank you to Sara Gonzales, Emily Rice, Nathan Frazier, Tyler Thompson, Chaoyu Zhai, Caleb Swing, Chloe Carlson, Jordan Roggen, Fae Dong, Sunny Liu, Mo Jia, Michael Hernandez, Haley Davis, Joanna Swenson, Luke Fuerniss, Ashley Corona, and Arquimides Reyes for being not just colleagues but friends as well. Thank you for our international cooking lessons, wine nights, hot pots, and potlucks. I never would have survived without you.

Each of my projects was the work of a team, and none of the projects would have been completed without people way smarter than me. The food processing facility project required many hands to complete, most of whom I've already mentioned. But it also took the help and cooperation of Dr. Robert Delmore and the CSU meat lab team, who were always willing to let me interfere with their processing

schedule and to provide me with whatever extra information I needed. I also especially appreciate Dr Georgnaras and Nathan Frazier for their help in designing and leading the project and conducting lab work.

My chicken chilling project was multi-disciplinary, and as such was made up of a huge research team. I couldn't have done it without my co-leader Toni Duarte who helped organize and plan the experiment, set up the facilities, and helped with writing. I'd also like to thank Dr. David Coil, Dr. Jonathan Eisen for their help with the microbiome analysis and phylogenetics and for loaning us their students for sampling help. Dr. Casey Quinn and Dr. Jason Quinn did the work on the technoeconomic analysis and give me a tour of their energy lab. Dr. Crystal Yang and her group to lead the sampling and microbiology experiments, and she was also a mentor to me when she was in her PhD and I was just an undergrad. Last but not least, I'd like to thank the meat lab team at UC Davis for loaning us their facility and spending a full day cutting up chickens for me.

Vertebrate decomposition research also requires huge teams, and for a project with so much geographic diversity the teams were spread across the country. At Colorado Mesa University, Melissa Connor and her students made sure the bodies were placed and recorded. At Sam Houston State University, Sibyl Bucheli and Aaron Lynne were the greatest, and they even gave me my first visit to a body farm before I'd finished my masters, getting me excited to start my research. And at the University of Tennessee, Knoxville we had the fantastic collaborators Dawnie Steadman and Giovanna Vidoli. We also had help from Zhenjiang Xu, Gail Ackermann, Greg Humphrey, and Rob Knight at the University of California San Diego who helped us with sample processing and sequencing. Lastly, I would like to acknowledge the donors of human remains and their families, without whom this work would not be possible.

I would also like to thank the members of the Metcalf lab. Our postdocs, Alex Emmons and Zach Burcham, have been incredible instructors and provided so much guidance for me, especially as I constantly ran into problems that they have more experience solving. I also had the chance to work with several lab managers, all of whom made my research possible, including Holly Archer, Andy Esterle, and Kris Otto (who is truly a science superhero, as I tell her all the time).

Finally, I want to thank my family. I grew up surrounded by knowledge and books and knowing I could do anything I wanted to. I was so lucky to know I could dream big because I has so much support behind me. I always knew they wanted me to achieve my goals, since every time I saw my dad, he asked me “when are you going to graduate?” Well, here I am, and it’s all thanks to them and their constant support.

TABLE OF CONTENTS

ABSTRACT ii
ACKNOWLEDGMENTS vi
REVIEW OF LITERATURE 1
MICROBIAL COMMUNITIES OF THE BUILT ENVIRONMENT 1
Microbial Movement in Built Environments 1
Microbes in Food Processing Environments 4
Impact of Cleaning and Sanitation 7
Conclusions 8
THE CHICKEN PROCESSING AND SPOILAGE MICROBIOME 8
The Poultry Processing Industry 8
Impacts of Processing Parameters on Aerobic Chicken Product Quality and Microbiota 10
Chicken Product Spoilage 18
Conclusions 24
MICROBIAL CONTRIBUTIONS TO VERTEBRATE DECOMPOSITION 24
Vertebrate Decomposition 24
Microbiology of Decomposition Environments 25
Nutrient Cycling in Decomposition Soils 27
Estimating the Postmortem Interval 29
Conclusions 32
REFERENCES 33
THE MICROBIOME OF A NEWLY CONSTRUCTED MEAT PROCESSING FACILITY ESTABLISHES OVER TIME BY ROOM FUNCTION AND MICROBIAL SOURCE 45
SUMMARY 45
INTRODUCTION 46
RESULTS AND DISCUSSION 47
Sequencing results 47
Establishment of a Stable Microbial Community 48
Microbial Communities are Shaped by Room Conditions 51
Spatial Movement of Microbes Through the Facility 54
CONCLUSIONS 57
MATERIALS AND METHODS 58
The Global Food Innovation Center 58
Experimental Design and Sample Collection 59
DNA Extraction and Sequencing 61
Microbial Community Analysis 61
REFERENCES 64
AIR VERSUS WATER CHILLING OF CHICKEN: A PILOT STUDY OF QUALITY, SHELF-LIFE, MICROBIAL ECOLOGY, AND ECONOMICS 70
SUMMARY 70
INTRODUCTION 71
RESULTS 72
Experimental Results 72
Quality and shelf-life implications of chilling strategy 73
Microbial ecology of chilled, fabricated, and packaged chicken 76
Phylogeny, diversity, and spoilage potential of Pseudomonas 79
Chilling system techno-economic analysis 80
DISCUSSION 80

CONCLUSION 84
MATERIALS AND METHODS 85
Experimental design 85
Chicken processing 86
Microbial sample collection/processing 89
Phylogenetic trees 91
Chilling system techno-economic analysis 94
REFERENCES 96
MICROBIOME DATA ACCURATELY PREDICT THE POSTRMORTEM INTERVAL USING RANDOM FOREST REGRESSION MODELS 104
SUMMARY 104
INTRODUCTION 104
RESULTS 106
Cross-validation error rates: comparison of sample types 106
Cross-validation error rates: comparisons of genetic markers across taxonomic levels. 107
Cross-study error rates 109
Important feature taxa 111
DISCUSSION 112
CONCLUSIONS 115
MATERIALS AND METHODS 116
Amplicon sequencing data processing 116
Assigning taxonomy 117
Model testing 118
REFERENCES 120
PATTERNS OF MICROBIAL SUCCESSION IN SKIN AND DECOMPOSITION-ASSOCIATED SOILS ARE PREDICTIVE OF THE POSTMORTEM INTERVAL OF HUMAN REMAINS 125
SUMMARY 125
INTRODUCTION 126
RESULTS AND DISCUSSION 127
Sequencing results 127
Patterns of microbial succession over time 128
Decomposition microbiomes are differentiated by environment 134
Predictive models to estimate postmortem interval 135
Amplicon data compared to metagenomic data to represent microbial succession 138
CONCLUSIONS 140
MATERIALS AND METHODS 140
Experimental Design and Sample Collection 140
DNA Extraction and Sequencing 141
Data Analysis 142
REFERENCES 146
CONCLUSIONS 152
APPENDIX A: CHAPTER 3 SUPPLEMENTARY MATERIALS 155
APPENDIX B CHAPTER 4 SUPPLEMENTARY MATERIALS 162

REVIEW OF LITERATURE

Microbial Communities of the Built Environment

Microbial Movement in Built Environments

In enclosed spaces with human occupants, the microbial communities that form in the environment are closely related to their use and occupancy. These spaces, which are designed, constructed, and managed by humans, are generally referred to as the built environment. Humans are generally the primary organism occupying these spaces, but they can also house animals (pets), plants, rodents, insects, and more, depending on the specific environment [1]. All of these occupants interface with the space, and can interact with microorganisms in the space itself, both by introducing new organisms from outside the space and by taking up or moving organisms present in the built space. Both of these instances can have impacts on the humans, especially from a health perspective. Many pathogenic organisms can persist in these spaces, for instance *Legionella pneumophila* can reside in water systems [2], opportunistic non-tuberculous mycobacteria can reside in shower head biofilms [3], and methicillin-resistant *Staphylococcus aureus* can reside on environmental surfaces [4]. Conversely, the hygiene hypothesis proposes that the reduction of the non-pathogenic microorganisms in environments may be responsible for an increase in allergies and asthma in children due to a lack of exposure in early life [5]. For these reasons, the microbiome of built environments is a critical area of research; in fact, in 2017 the National Academies of Science published a research agenda and identified a series of knowledge gaps in this area [1].

The majority of research in the built environment microbiome field focus on home and house microbial communities, as these are the spaces with which humans most frequently interact. In 2015, Lax *et al* conducted the Home Microbiome Project, in which they evaluated the microbial interactions between humans and their homes over a period of six weeks [6]. During this time, they obtained samples from the occupants and environment from seven families living in ten houses, as three of the families moved to a new home during the experimental period. They reported several interesting observations

regarding the movement of microbes between the occupants and the space. It appeared that the microbial signature of the built environment was influenced by the humans, as the microbiome of the new homes quickly began to resemble that of the human occupants, rather than the environment influencing the humans. The floor samples in particular resembled the microbial communities of the occupants, perhaps due to less frequent cleaning than surfaces and because the foot samples were more differentiated across households than hand samples. Overall, they concluded that homes contain distinct microbial communities that are influenced by their occupants, and the differences between households was stronger than differences from different samples within a household [6]. Similarly, Dunn *et al*., in a study of forty households in North Carolina, demonstrated that human-associated sources (skin, mouth, feces) were important contributors to the microbial communities of most household surfaces, especially the toilet seat, pillowcase, television screen, door handle, and interior door trim [7]. They also reported that the alpha diversity of the surface communities was higher in locations where aerosols are more likely to collect, such as the television screen and interior door trim, which suggests that aerosols may be a route by which the human microbiota colonize the built environment. This study also evaluated external home surfaces, which were less similar to the human occupant microbiome, further demonstrating how the occupancy of a space is what allows humans to influence the formation of microbial communities in built environments [7].

Similar patterns have been observed in other sites of occupation. One area of interest for understanding habitat microbial communities is in the implications for long-term space travel and occupancy. Malli *et al*. conducted a study of surfaces in the NASA submerged habitat and determined that, during occupancy, microbial cells could be isolated from all surfaces, many of which have also been isolated from the international space station [8]. The major finding of this study was that the surface material was an important driver of microbial community formation, which has major implications for the ability of surface design to prevent colonization [8]. Singh *et al*. also demonstrated that international space station surfaces could harbor microbial communities, though they also demonstrated that pathogens and antibiotic resistance genes were present in them [9]. They also linked these communities to the

astronaut occupants and described their similarity to earth communities, which shows that the general trends in built environment microbiome assembly are not limited to earth-based environments [9]. The overall trends are also not limited to human-occupied spaces, as demonstrated by Hyde *et al* in a study of Komodo dragon zoo habitats [10]. The microbiome of the dragon enclosures was strongly influenced by the dragon saliva, skin, and fecal organisms. Interestingly, the sources of these communities differed based on specific source; the dragon saliva was the main source of microbes on soil, rock, and glass surfaces while skin was the main source for metal microbial communities [10]. Overall, it is clear that the occupant of a built environment is the primary driver for microbial community assembly, at least in the case of homes and habitats.

Humans also consistently interact with built environments outside their home habitats, and the microbial communities of these spaces have also been widely studied. For example, students may spend similar amounts of time at school campuses as they do at the home, so the microbial community patterns seen with human occupation should extend to these spaces. Indeed, a study of dust microbiomes in kindergarten classrooms demonstrated that a quarter of the bacterial relative abundance in the samples were human associated [11]. The experiment began before the opening of the Kindergarten and continued through the first year of occupation, which allowed researchers to show where the initial microbial communities arose from. This provided some interesting observations. The early timepoints, when the spaces were primarily occupied by adults preparing the space, saw communities with a high abundance of *Propionibacterium*, an adult-associated organism, which decreased in relative abundance over time. They also reported a seasonal effect, where the abundance of human-associated organisms increased in the winter when the children spend more time indoors [11]. A study of a college campus door handle microbiomes drew similar conclusions [12]. They found that handle microbiomes were associated with human skin, though these were outdoors and therefore also affected by soil, plants, and food sources. The found that stable communities actually formed on the door handles, which was unexpected, and hypothesized that this was due to dead skin, oils, soil, and other organic matter providing enough moisture to maintain a microbial environment [12]. Office buildings, too, are spaces where humans spend

long periods of time and therefore influence the microbial communities. Chase *et al*. showed that human skin microbes contribute to the communities of all surfaces in an office environment [13]. They also showed that communities assembled differently based on room, but not by surface type, which directly contradicts other studies of built environments. Additionally, the microbiome of hospital rooms has been shown to be strongly influenced by their occupants [14]. In fact, Lax *et al* showed that while initially, on the first day of occupancy, the patient community may be influenced by room-associated taxa, after one night the patient microbiome began to alter the microbial communities in the room. Even though a hospital is a highly sanitized space, this study shows that environmental communities still form and are influenced by the occupants, similar to a home microbiome [14]. Clearly, in spaces occupied primarily by humans, the microbiome of these occupants is the primary driver of built environment community formation, even within a short occupancy or interaction period.

Another important built space is athletic facilities, where humans may spend less time but interact strongly with the environment. These spaces are interesting, because the occupants are not consistent as they are in a home, school, or office. Wood *et al* showed that athletic equipment surfaces frequently in contact with human skin housed highly dynamic microbial communities, likely because organisms from new sources were being deposited so frequently [15]. Furthermore, a study of climbing wall microbiomes showed that the most important source of organisms was soil, though human skin was also important [16]. This study also suggested that the microbial communities deposited by humans may be of fecal origin, so perhaps the individual human contributions of organisms were overshadowed by the source type [16]. These study types suggest that perhaps built environments without consistent occupants do not form a stable microbial community.

Microbes in Food Processing Environments

The built environments associated with food and beverage production are also critical, yet understudied, spaces that may influence human health. The microbial communities of these spaces can harbor pathogens of human concern including *Escherichia coli*, *Salmonella spp.*, and, notably, *Listeria*

monocytogenes. Though food processing facilities have testing and sanitation protocols, a greater understanding of how the microbial communities assemble in these spaces could have major food safety implications. Moreover, a greater proportion of the microbes found in these environments, such as *Pseudomonas*, *Moraxellaceae*, and Lactic Acid Bacteria, are not pathogenic, but if transferred to the product are responsible for spoilage and a shortened shelf-life. These environments are understudied in comparison to human-oriented spaces, but recent research has begun to elucidate the value of research on this community.

Meat processing facilities present a unique challenge in regard to managing the environmental microbial communities due to the constant introduction of organisms from live animals, and as such should be closely monitored. Regulations require monitoring and control plans for several important pathogens or their indicators, but little is actually known about the other organisms in the microbial communities [17]. Hultman *et al.* published one of the only studies to profile the microbial community of a meat processing facility [18]. They evaluated the communities of product-contact surfaces and found that the microbial communities of the spaces did not cluster with the final sausages but were similar to raw materials. The organism most prevalent in the final sausage product, *Leuconostoc*, was found in low abundance on processing surfaces, which indicates it could be a source. The study did not, however, speculate on the original sources of the facility communities [18]. More recently, Zwirzitz *et al* evaluated the transmission routes of microbes through a pork processing facility [19]. They were able to follow specific organisms through the facility to determine where they originated and whether they impacted the final product. They were able to identify the contamination routes of several organisms, for example *Moraxella* spp. likely moved from polishing tunnels, gloves, and railing to carcasses, and the splitting saw may transfer *Lactococcus.* Additionally, they reported distinct shifts in the facility communities, which occurred after singeing, when a flame is used to removed hairs from the skin, and at the truck, or transportation, step. This suggests that decontamination procedures reduce the bacterial load and diversity, which alters the basic microbiome. Overall, the major origins of microbes were the animals themselves, with organisms such as *Enterobacteriaceae* originating from feces and others arising from

skin and gut sites. This is likely a common theme in food processing, as the major ingredients and raw materials are likely the best vectors for carrying organisms into the facility.

Within meat processing facilities, biofilms are one of the major structures that maintain a resident microbial community. These biofilms are especially notable for allowing *Listeria spp*. to persist in these environments. Hassan *et al*. showed that *Pseudomonas putida* biofilms can harbor *Listeria* on stainless steel surfaces, and in these environments, *Listeria* could grow even under starvation conditions [20]. Also, in these conditions, they showed that these cells could detach from the surface and potentially contaminate food products. Within biofilms, *Listeria* can actually interact with other resident organisms in the facilities, and if the community contains *Kocuria varians*, *Staphylococcus capitis*, *Stenotrophomonas melophilia*, or *Comamonas testosterone* it could actually increase *Listeria* growth [21]. However, *Listeria* in these biofilms could also potentially be controlled by other organisms. Zhao *et al* demonstrated that competitive bacteria could remove *Listeria monocytogenes* from biofilms in a poultry plant, so perhaps the built environment communities could also be harnessed to prevent negative food safety outcomes [22].

The microbial communities of other food processing environments have been more fully described. Tan *et al* evaluated the microbial communities of three different fruit tree processing facilities [23]. These communities consisted of *Flavobacteriaceae, Moraxellaceae, Weeksellaceae, Xanthomonadaceae,* and *Burkholderiaceae*, though in different abundances at each facility. The three locations displayed different levels of visual cleanliness, and this was associated with the composition of the community. The facility noted to be dirtiest also had the highest occurrence of *Listeria*, which was found in 100% of the samples taken, and a predominance of *Pseudomonadaceae* and *Dipodascaceae*. Additionally, the communities differentiated based on the place in the process clustered separately, with the areas associated with fruit waxing had a higher abundance of *Mycobacteria*. These results demonstrate how the microbial community can harbor pathogens that can be transferred to products, and how cleanliness impacts the communities [23]. In a cheesemaking plant, Bokulich and Mills also demonstrated the assembly of a community in the facility that could be introduced to the product, though

in these facilities that community may actually improve the product quality due to the importance of microbes in the cheese fermentation process [24]. In a brewery environment the communities assembled differently based on the function of the space [25]. Primarily, this meant clustering based on the substrate type in the space; the fermenter samples were associated with *Bacillaceae*, the cellar production areas associated with *Micrococcaceae*, the wort, malt, and hotside areas associated with *Enterobacteriaceae* and *Leuconostocaceae*, barrel-room samples with *Lactobacillaceae* and *Enterobacteriaceae*, and coolship and barrel rooms with *Cryptococcus* and *Cladosporium*. These clustering patterns show that the microbial communities of this facility were driven not by the human occupants, but by the ingredients and products in the spaces [25]. It appears to be a common trend in food processing facilities for the microbial communities to assemble based on the raw ingredients or products and the cleanliness, as opposed to the humans present in the space.

Impact of Cleaning and Sanitation

It is well established that microbial communities can be altered by cleaning and sanitation. In built environments, this is the primary option for controlling microorganisms. In general, cleaning and sanitation reduces the human fingerprint in the built environment microbiome, even in homes [26]. The increase of cleaning and sanitation in home environments may be, in fact, tied to changes in urbanization [27]. McCall *et al* found that the number of distinct chemicals used in the environments increased with urbanization, lipid and lipid-like compounds that may be associated with cleaning products were more dominant in cities [27]. The greater use of these sanitizing products was associated with a lower abundance of yeasts and higher abundance of skin-associate bacteria than rural areas. Thus, the sanitation was associated with a shift in the microbiome, from more environmental organisms to human-associated. This follows trends previously reported, and it follows that the readily introduced human-associated microbes would thrive in an environment in which other organisms have been removed. In food processing facilities, sanitation has been shown to reduce the presence of pathogens, especially *Listeria*. A study by Stessl *et al*, multiple sanitizers were tested against strains of *Listeria* that had previously

caused contamination in the facility as well as several test strains [28]. A hypochlorite solution impacted all strains present in the facility, a chelating alkylamine disinfectant test substance was effective against all *Listeria* strains in the experiment, and a sanitizer based on nitric and phosphoric acid was most effective against one of the test strains. This study outlined the importance of using effective sanitizers in an environment, as they are not all equally effective [28]. In a similar study, Martín *et al* actually recovered some strains after cleaning and sanitation, which were then traced to meat products [29]. Clearly, the importance of sanitation protocols on the built environment cannot be overstated.

Conclusions

The built environment microbiome is a critical area of research. These communities persist in locations with which humans interact every day, and as such can have lasting impacts on human health. Even food processing environments, with which very few individuals interact, have the potential to impact everyone. The research conducted in this area has provided important insights that could lead to advances in microbial control. This includes more knowledge of the origins of microbes in these communities, how they interact with the human occupants, and how cleaning and sanitation can alter them.

The Chicken Processing and Spoilage Microbiome

The Poultry Processing Industry

The United States is the largest producer of poultry meat worldwide, processing approximately 9 billion chickens a year in a 495.1-billion-dollar industry [30]. Over the last 50 years, the industry has concentrated to approximately 27,000 production facilities in just 15 states, while the size of an individual operation has increased to 600,000 birds [31]. Along with an increase in size and concentration of facilities, the processing procedures have become more industrialized and automated. The basic procedure for poultry harvest and processing begins with electrical stunning prior to exsanguination. After the birds

are dead, they are placed in scalding tanks to soften the cartilage around the feathers, enabling their removal by feather-picking machines. Then, the head, legs, oil gland, and viscera are removed, at which point the bird becomes a carcass [32]. After evisceration, the carcasses must be cooled to below 4°C within two hours of harvest per USDA regulation, as a microbiological safety intervention [33]. Finally, the chilled carcasses are fabricated, or cut, into parts based on various specifications and packaged [32]. Though individual facilities vary in how these steps are conducted, the US poultry industry is fairly homogenous, and these basic processing steps describe the majority of chicken production in the US.

There are several points in the poultry processing that alter the microbiological makeup of the product, either intentionally as a food safety measure or unintentionally as a consequence of carcass conditions. Before harvest, muscle tissue should be considered sterile; any interaction with this tissue that could deliver microbes to these surfaces serves to create the initial product microbiome [34]. Sticking, or using a knife to begin exsanguination, is the first point in which microbes can be introduced to the carcass. If the knife is not properly sanitized microbes can be introduced to the bloodstream and circulated through the body before exsanguination is complete, and even if it is this step could introduce microbes on the exterior of the chicken into the interior [35]. Scalding and defeathering have been noted as important steps for carcass contamination in several studies, as the scalding water can transfer microbes from the feathers to the carcass [36–39]. After these preliminary steps, when the exterior sources of contamination such as feathers are removed, the ingestia becomes the primary source of microbes. During evisceration, gut microbes can be transferred to product surfaces and the processing environment, where it can continuously re-contaminate other carcasses. Finally, the chilling step has been implicated as a source of cross-contamination between carcasses, where microbes on one carcass can spread to all the others in the batch.

Carcasses must be rapidly chilled after harvest to prevent the growth of pathogens; there are several methods by which this can be achieved, with most common being air chilling, water immersion chilling, and evaporative air chilling. In the United States, water immersion chilling is the most commonly used method. In this procedure, carcasses are moved through a tank, or series of tanks,

containing cold water, usually kept near 1-2 °C [40]. This method is very effective in rapidly cooling the carcasses with relatively low energy input, but has several drawbacks including high water use, the potential for carcasses to gain weight during the process, and the potential for cross-contamination between carcasses, a phenomenon which has been previously documented in literature [40–44]. Processing facilities will often include antimicrobial compounds in the chiller water in order to prevent this contamination. Air chilling methods are more common in other countries, especially in the European Union. In this method, cooled air is blown over the carcasses, usually in a single room or tunnel [40]. Carcasses may be hung on rails as the air passes over, or they may be placed on conveyors and moved through the room as they chill [40]. Using this method, chilling times may be longer than in water immersion chilling, chilling requires more space in the facility, and carcasses may lose some weight due to evaporation, but it is less likely to be a source of microbial contamination as the carcasses do not share contact spaces during the process. Finally, some facilities employ a method called spray or evaporative chilling. This method, essentially a combination of the first two, involves spraying the carcasses with cold water as they undergo air chilling [40]. This decreases the chilling time and potential water loss from carcasses without the cross-contamination risks of water immersion chilling. This has also been shown to be the most efficient method for chilling, with heat loss at 1.8 kcal/kg greater than in air chilling [45]. However, this method is at an energy and resource use disadvantage, as it requires large amounts of energy and water both. In the United States, regulations do not specify which method should be used by a facility as long as it effectively reduces temperatures, and therefore the decision for which method to use depends on the resources available and priorities of an individual processor or company.

Impacts of Processing Parameters on Aerobic Chicken Product Quality and Microbiota

A wide variety of methods have been utilized throughout scientific study to evaluate the quality and microbial composition of chicken products. However, while techniques used to evaluate quality are well-established and applied relatively consistently throughout the literature, the field of microbial ecology has changed rapidly over the past decades, and as a result has led to dramatic differences in how

the microbial composition has been quantified. To evaluate quality, researchers have generally looked at the physiochemistry and sensory aspects of a product. The physiochemical attributes can be quantified through a suite of biochemical tests such as pH, moisture content, chromatography, and mass spectrometry. The sensory attributes include color, texture, flavor, tenderness, and odor, and can be measured through objective instruments such as a portable spectrophotometer to analyze color, mass spectrometry to evaluate odor compounds, and shear force to analyze tenderness. Additionally, these measurements can be collected through human panelists, either trained or untrained, who capture perceptions of these attributes using a given scale, perhaps with references. While not all studies employ all of these methods, in general the proper technique to capture each aspect of product quality is well-established. In investigating microbial composition, though, the methods are less consistent. Many researchers use culture-based methods to enumerate organisms on the product, and if these methods are selective, they can be used to identify specific organisms. The presence of specific microorganisms has also been demonstrated through quantitative PCR tests and immunoassays. However, while these can be applied to specific research questions, the evaluation of single organisms or groups of organisms does not describe the full microbiota of the product. More recently, Next Generation Sequencing technologies have been used to more fully elucidate the product microbiome, though this is still a recent area of research and not yet consistently applied in meat science literature. Sequencing analyses provide a fuller picture of the microbial composition, but do not generally provide an enumeration of microbial numbers, so the use of multiple microbial methods is highly valuable. Currently, however, the high variation in methodologies makes it difficult to compare results across literature in this field. Therefore, in describing the literature it is important to consider the methods used and their limitations.

There are clear choices made by processors in the facility design and product treatments that impact the ultimate product quality and microbiology. The chilling method has been shown to directly impact the product quality, but perhaps has a lesser impact on the microbiological composition of products. Sanchez *et al.* compared the microbial composition of carcasses chilled at two separate facilities, one that used air and one that used water immersion chilling methods [46]. Unfortunately, the

use of an entirely separate facility for each chilling method slightly confounds the results, but there were still a few conclusions to be drawn about the impacts of the processing parameters. Water immersion chilling resulted in a microbiological profile with more psychrotrophs, which is important as these organisms are often associated with product spoilage and may cause a shorter shelf-life, or the time until the product is rendered inedible. Additionally, *Salmonella* spp. and *Campylobacter* spp. were isolated less frequently from the air chilled carcasses, indicating that this method may result in better food safety outcomes, though this could also be a result of facility sanitation protocols. Within these populations, the authors reported high incidence of antimicrobial resistance, which was also higher in the water immersion chilled carcasses [46]. The addition of antimicrobial compounds to the chilling water may play a role in this outcome, though it is also possible it is driven by other features of this facility that were not measured by the researchers. Indeed, Berrang *et al.* found conflicting results in a more controlled study [47]. In this study, researchers obtained carcasses and cut them in half along the dorsal line, then subjected one half to air chilling and one half to water immersion chilling before conducting microbiological analyses. The difference in microbial colony counts due to chilling method was only approximately 0.5 log CFU/mL, which is not enough to be biologically important. However, in this study the *Campylobacter* counts were higher in the air chilled carcass halves, in contradiction to the Sanchez *et al.* results [46,47]. Moreover, Berrang *et al* concluded that there was no evidence of selection for antibiotic resistance in either chilling method [47]. A study by Zhang *et al.* agreed with these results and also determined there was little microbiological difference between chilling methods; they reported no difference in the incidence rates for *Salmonella* spp. or *Campylobacter* on carcasses between air and water immersion chilling methods [48]. The only difference reported in this study was that air chilling may actually be less effective in reducing *Campylobacter* counts on carcasses than water immersion chilling, as the process of water chilling may physically remove the bacterial cells from carcasses [48]. Tuncer and Sireli also reported few differences in microbiological counts between air and water immersion chilling methods [49]. They obtained carcasses after air or water chilling in a commercial processing facility, then placed them under storage in one of several packaging methods at either 0, 4, or 7 °C. Though there were significant changes

in microbiological counts over time for all treatments, there were not differences in counts between chilling methods. At the end of the experiment on day 10, air chilling and water immersion chilling resulted in final microbial counts of 7.64 and 7.51 log CFU/mL, respectively [49]. In general, it appears that the chilling method may not have a substantial impact on the microbiological profile of chicken products, or at least on the presence and number of potential pathogens on the products. Given contrasting results in the studies, though, it is difficult to draw strong conclusions as to the microbiological advantages of one chilling method over another.

Other studies that focus on the quality and sensory aspects of the product rather than the microbiological safety, did find distinct differences between air and water chilled products. In an early comparison study, Mielnik *et al.* chilled 100 carcasses using either air chilling or evaporative air chilling, then stored the product at either 4 or -1 °C for either 15 or 19 days [45]. At the end of the storage period, they evaluated a plethora of quality and microbiological techniques to evaluate the impacts of these methods. The greatest impact of chilling method was in the final product color; the air chilled breasts had a darker and more yellow color than those subjected to evaporative chilling. However, between these two similar methods there was no difference in moisture content, pH, or cook loss. Moreover, the microbial composition was similar between the two methods, with *Pseudomonas* dominating the flora from all samples, along with *Brochothrix thermosphacta* at 100-fold lower levels [45]. Zhuang *et al.* chilled carcasses using either air or water immersion methods, then fabricated them into breast fillets and tenders at 4 hours postmortem [50]. Both chilling methods impacted carcass weight, but in different directions; air chilling reduced weight by 2.4% while water immersion chilling increased weight by 4.6%. Air chilling reduced the tenderness as measured by Warner-Bratzler shear force when compared to hot-boned products but was not significantly different from the water immersion chilled products. Chilling method also did not impact water holding capacity or drip loss, which indicate that the chilling method will not impact marinade pickup in these products [50]. In order to investigate the impact of these methods on further processed chicken, Carroll and Alvarado evaluated the impacts air and water immersion chilling had on marinated products [51]. They evaluated the color and pH of breast filets that had been either air

or water immersion chilled, then marinated the products before applying a marinade using a tumbler. After marination they conducted a microbiological analysis of the raw product, then cooked the filets before a sensory analysis with shear force and consumer panels. Researchers found that air chilled filets were darker, had a lower pH, and were more tender than the water chilled products. Additionally, the air chilled products had an increased marinade pickup and retention, suggesting that this method may be superior for facilities that intend to further process the products. Finally, researchers predicted that the air chilled products would have a longer shelf-life, as they yielded lower aerobic plate counts and coliform counts, though the actual shelf life was not measured in this study [51]. Jeong *et al.* found similar result in a study in which they processed carcasses using either air chilling, water immersion chilling, or evaporative air chilling [52]. Water immersion chilling resulted in the highest pH and numerically the highest shear force values. They also found the air chilled products to have the darkest color and water immersion chilled the lightest. Overall, the objective measurements indicated that air chilling resulted in the highest quality products, though the chilling method did not impact the perceived sensory outcomes by consumers. Water immersion chilling was the most efficient of the tested methods, though, with a chilling time of 57 minutes compared to 125 and 93 minutes for air chilling and evaporative air chilling, respectively [52]. In another report by the same authors, water immersion chilling resulted in the highest yield after chilling, but the lowest moisture retention after fabrication and storage, indicating that these products release more absorbed water during the cutting and storage processes [53]. Water immersion chilling also resulted in the lightest color, likely due to the aforementioned water absorption causing more light scattering. Air chilling was the yellowest, less white than water immersion chilling, had the highest scores for dark spots and white spots, and had the highest dryness score, all likely due to surface desiccation during chilling that would resolve during storage time [53]. Based on these studies, it appears that, though water immersion chilling may have some efficiency advantages, air chilling provides a product quality and shelf-life advantage over the other methods.

Another processing parameter that directly impacts the product quality and microbiological composition is the time and temperature for storage and display. As time increases, the microbiota shifts,

generally to the advantage of spoilage organisms. An increased storage time means the product is closer to the end of the shelf life, though alterations in other aspects of product handling can change how long this period is. Gill and Newton published a review in 1977 that described the early conceptual framework for this [54]. They described a system in which bacterial numbers increased over time, and when these counts exceeded 10^8 CFU/gram ammonia production began and researchers observed decreases in carbohydrates, free amino acids, and nucleotides. This may be due to an increase in *Pseudomonas* growth over time, as in aerobically stored products the growth rate of these organisms increases with decreased storage temperature [54]. Arnaut-Rollier *et al.* confirmed that the main shift in microbial community during an increased storage period is an increased abundance of *Pseudomonas* [55]. They reported that *Pseudomonas* made up only 20% of the microbes on fresh carcasses, but this increased to 44.2% by day 3 and 90% by day 8 of aerobic product storage. This rapid change demonstrates the short shelf life of chicken products when it is aerobically stored and implies that interventions to slow the spoilage rate should be made prior to the third day of storage. The rate at which these microbes grow can be slowed by maintaining low temperatures in the storage environment. In a 2012 review, Doulgeraki *et al*. described conditions of temperature abuse in meat product, showing that *Enterobacteriaceae*, *Pseudomonas*, and *Acinetobacter* were dominant [56]. *Pseudomonas* are psychrotrophic, so do not grow as effectively at warmer temperatures, which may be what allowed other groups of organisms to persist on the product. Handley *et al.* also evaluated the impact of temperature abuse on poultry carcasses, specifically of carcasses stored in large combo bins kept at ambient temperature after chilling [57]. Researchers did not see an increase in aerobic bacterial counts, *E. coli* counts, or total coliform counts until after the first 26 hours of temperature abuse, likely due to a long recovery period from the lag phase after antimicrobial treatments. However, in the second 26-hour period each of these microbial groups increased significantly to a final mean count of 7.19, 4.45, and 4.81 log CFU/mL, respectively. The *Enterobacteriaceae* counts increased consistently throughout the experimental period, from 0.66 to 7.19 log CFU/mL. Within approximately two days of temperature abuse conditions (elevated storage temperatures) the microbiological counts were at spoilage-associated levels, demonstrating how quickly these organisms

can grow at elevated levels [57]. In another experiment testing storage conditions, Katiyo *et al*. collected and packaged raw chicken legs (thighs), then placed them in cold storage under aerobic packaging for 1, 3, 7, 10, or 14 days before microbiological sampling and taking sensory measurements [58]. Under these cold storage conditions, it was *Pseudomonas* that became the dominant organism on the legs. *Enterobacteriaceae* and Lactic Acid Bacteria (LAB) were present throughout storage, but at much lower levels and without much change in population over time. The *Enterobacteriaceae* population did not change after 10 days, and the LAB population did not change after three days. Interestingly, this study also took into account quality and consumer acceptability changes over this time as well, showing that detectable slime on the product appeared after 10 and 14 days of storage, when the total viable microbial counts had reached 8.66 and 9.13 log CFU/g, respectively. They also showed that the color became less pink, more faded, and more undesirable after 10 days of storage [58]. Overall, it is clear that advanced storage times decreases the physical and microbiological quality of chicken products as it moves closer to a spoilage state. This process can be slowed by using lower storage temperatures but continues over time regardless of other treatments.

There are other factors that impact the product quality; as the product moves through the processing facility the microbial composition is altered by the treatments, and the final product might be impacted by intentional changes to the pH. Handley *et al*. conducted a study in 2018 to establish the microbiome of commercially processed broilers and to evaluate the reduction in microorganisms during processing by collecting chicken rinseates from carcasses at commercial plants after distinct stages in processing [59]. In this study, each stage in processing (rehang after exsanguination, pre-chill, and post-chill) showed significantly reduced microbial populations coupled with reductions to the microbial diversity [59]. It is likely that the processing steps are mechanically removing bacterial cells from the carcasses, but perhaps selecting for certain organisms such as *Pseudomonas* and *Enterobacteriaceae*. In a similar study, Chen *et al*. reported slightly diverging results [39]. In this study, researchers collected carcass rinseates from a processor in Australia at distinct processing timepoints but included more than were used in Handley *et al.*: before scalding, after scalding, before immersion chilling, after immersion

chilling, and after air chilling. In contrast to Handley, they reported an increase in bacterial richness, or the number of microbial species, after each intervention, most notably a shift from 51.7 to 100.1 in before and after scalding steps [39,59]. With this, they saw no difference in evenness or Shannon's diversity calculations between any processing timepoint groups. They did, however, show a change in beta diversity, with shifts in the microbial community composition after scalding and water chilling, possibly due to physical wash-off of bacterial cells. The final measured step in the process, air chilling, also resulted in a large increase in microbial diversity, which may indicate this step as a potential site of cross-contamination for carcasses and the processing chain. Despite these increases in microbial diversity, the researchers reported a decrease in microbial cell counts, especially during the two chilling steps. In other words, the number of bacterial ASVs was increasing as the total number of bacterial cells decreased; perhaps the reduction in competition allowed more individual organisms to prosper in this system [39]. Rothrock *et al.* also considered the impacts of processor steps on the chicken microbiota, though they focused primarily on the changes in the waters of the scalder and chiller tanks throughout the day [60]. Water was collected from the tanks prior to entry of the first bird, after 9 hours of processing, and after the end of the processing day but before cleaning. They found microbial diversity to remain relatively consistent in the tanks throughout the day. However, other chemical attributes that indicate dirtiness did increase; the chemical oxygen demand, biological oxygen demand, oil and grease, and total solids all increased significantly in the chiller tanks after starting production, with highest values occurring at the midpoint sampling time. During this time, the relative abundances of the major bacterial phyla (*Proteobacteria*, *Firmicutes*, *Actinobacteria*, *Bacteroidetes*) returned to their starting levels by the end of the processing day, most likely due to the effectiveness of the chlorination of the waters. Only a few organisms increased in relative abundance throughout the processing day; *Anoxybacillus* and *Erysipelotrichaceae* showed the greatest increase and *Pseudomonas* increased over time but recovered to starting levels by the final sampling timepoint. It is clear that processing stages have an impact on the final product microbiome, but without more study it is unclear exactly how this change manifests.

Any processing step that otherwise alters the physiochemistry of the chicken product will have an impact on the final product quality. In a review article, Gram *et al*. again confirmed that *Pseudomonas* and similar organisms will dominate proteinaceous foods, especially when stored aerobically at low temperatures, but noted that *Shewanella putrefaciens*-like organisms will also grow quickly in products with a higher pH [61]. For this reason, the acidity of a product is altered during production, to reduce the growth of these bacteria and increase shelf-life. Gram *et al*. also describe the impacts of using salt to decrease the water activity, which can actually shift the microbiome to an anaerobic condition, with LAB, *Enterobacteriaceae*, and *Brochothrix* dominating the community [61].

Chicken Product Spoilage

After death, the muscles of a carcass begin to break down through autolysis reactions and the influence of external microbes. When this process occurs in meat products, it is referred to as spoilage, and the time until the product is rendered inedible by the spoilage process is the shelf-life and is generally defined as when the microbial load on the product reaches 7 log CFU/mL [58,62]. In aerobically stored meat products, the outcome of spoilage is generally the formation of a slime on the product surface, off-odors (pungent, fishy, rotten-egg, ammonia), and a distinct microbial profile generally dominated by *Pseudomonas* [58,61]. The rate of spoilage can be slowed by the application of specific conditions, as described in the previous section, but is an inevitable process. The spoilage rate of fresh meats is rapid compared to other food products, and the volume of product that spoils before being purchased or consumed is a major contributor to food waste in the United States [63]. Therefore, it is critical to understand this phenomenon.

The main driver of spoilage is the presence of microorganisms on the surface of the product. The main bacteria involved in chicken spoilage are well-documented: *Enterobacteriaceae* including *Acinetobacter*, *Enterobacter*, *Hafnia*, *Proteus*, *Serratia*, *Aeromonas*, *Alcaligenes*, and *Providencia*. *Pseudomonadaceae* organisms, especially *P. lundensis*, *P. fragi*, and *P fluorescens*, and *Firmicutes* including *Brochothrix*, *Carnobacterium*, *Enterococcus*, *Leuconostoc*, *Weissella*, *Lactobacillus*, and

Lactococcus, and *Shewanellaceae* species *S. putrefaciens* [34,45,54,56,58,59,61,64–67]. These organisms are important for spoilage because they thrive in the conditions in which products are stored; namely, these are psychrotrophic organisms that are capable of growing under refrigerated conditions (4 °C). There are several mechanisms through which these organisms drive spoilage. Simply a large amount of bacterial growth can begin to cause sensory defects such as sliming, but the products of microbial metabolism cause the majority of chemical changes in the product as it spoils, with the major compounds being alcohols, aldehydes, ketones, esters, and sulfur compounds [34]. Casaburi *et al* provided a review of research describing the volatile compounds produced by microorganisms during spoilage [65]. Initially, the microbes will use glucose as a substrate, which can lead to production of acetate, acetoin, diacetyl, acetic acid, iso-butyric acid, iso-valeric acid, and ethanol. After consumption of glucose, proteins will be broken down into amines, sulphides, and esters and fatty acids into aldehydes, all of which have negative sensory impacts on the product. These products have been directly linked to specific microorganisms, as reported in this review. *Pseudomonas* and *Carnobacterium* appear to be most involved in the production of the alcohols, while these organisms plus *Enterobacteriaceae* aldehydes. *Pseudomonas fragi* specifically has also been associated with the production of esters; in one case of 45 esters detected in a spoiled product at least 27 were produced by *P. fragi*. Finally, *Brochothrix thermosphacta* and *Carnobacterium spp.* were the major producers of volatile fatty acids. Overall, this paper describes specific changes in volatiles present in meat products that authors propose could be potentially used to describe or predict degrees of spoilage [65]. In a similar review, Gram *et al.* evaluate the microbes involved in spoilage by specifically analyzing their interactions and communication [61]. These authors also provide connections between organisms and spoilage products that agrees with the Casaburi *et al*. review; they show that *Pseudomonas*, *Aeromonas,* and many *Enterobacteriaceae* are likely to produce ammonia and biogenic amines from the breakdown of proteins and amino acids, *Pseudomonas* and *Shewanella putrefaciens* can break down cysteine to hydrogen sulphides, *Pseudomonas*, *Enterobacteriaceae*, and LAB can break methionine down into sulfhydryl, and *B. thermosphacta*, *Enterobacteriaceae*, and homofermentative LAB can metabolize glucose into acetoin, diacetyl, and 3-

methylbutanoyl. However, they also go beyond simply summarizing these compounds and also explain how combinations of these organisms in a community may change the dynamics. In a community, *Pseudomonas* is likely to act competitively with other organisms by producing a range of antibacterial and antifungal compounds including antibiotics and cyanide. Plus, they efficiently chelate iron, giving them an advantage when competing for substrates. This explains why *Pseudomonas* often comes to dominate spoilage communities, and why the diversity of these communities may be reduced. Other organisms perform more efficiently in collaboration; when ornithine-decarboxylase-positive *Enterobacteriaceae* were cultured with arginine-deaminase-positive LAB the production of putrescine was 10 – 15 times higher than when these organisms were cultured individually. If *Clostridium botulinum*, and important pathogen especially in anaerobically stored products, interacts with some aerobic bacteria it can enhance the toxin production, as these aerobic organisms remove oxygen from the environment more quickly and create better conditions for *C. botulinum*. Finally, the authors describe the production of quorum sensing molecules as likely to be very important in understanding these interactions, but there is not currently enough literature to fully support this [61]. This focus on interaction makes it very clear that, while only a few organisms may actively contribute to the spoilage outcomes, the entire community is important to fully understanding microbial food spoilage.

In addition to general reviews, several studies focus on specific aspects of the microbial communities and their metabolic activities. Lee *et al*. characterized the putrefactive bacteria that were isolated from chicken meat during cold storage [66]. They compared the taxonomic results from culture dependent and Next Generation Sequencing methods and found similar results from both. Culture-dependent methods revealed 118 strains of psychrotrophic bacteria, which were primarily associated with three major organisms: *Pseudomonas* (58.48%), *Serratia* (10.17%), and *Organella* (6.78%). The sequencing method showed similar taxonomies, but more microbial diversity. They did not fully describe the spoilage mechanisms of these organisms but did note that two-thirds of the *Pseudomonas* isolates showed some proteolytic activity, which is expected compared to the other literature [66]. Morales *et al*. specifically focused on the products of *Pseudomonas* metabolism, evaluating both the phenotypic and

genotypic diversity of *Pseudomonas* strains in marinated poultry products [67]. Researchers identified 42 *Pseudomonas* isolates in these products that associated with three previously described species: *P. fragi* (57% of isolates), *P. fluorescens* (33%), *P. lundensis* (7%), and one isolate did not associate with a tested species. Within these isolates they described three basic metabolic profiles related to spoilage activity that were detected through biochemical testing. Most isolates had proteolytic metabolisms without lecithinase production ability (14/24 isolates tested), some were non-proteolytic and had not lecithinase production ability (7/24) and some had proteolytic and lecithinase positive ability (2/24). No tested isolates had biosurfactant or lipolytic capabilities, which does suggest that there is a metabolic niche for non-*Pseudomonas* organisms in the microbial community [67]. In another study profiling the spoilage compounds in meat, Argyri *et al*. correlated the volatile compounds of minced beef with microbiological and sensory data under different storage temperatures and packaging conditions [64]. Though this study focused on beef, not chicken, the results are still comparable to the chicken spoilage results. The initial microbiota of these minced beef products consisted of LAB, *Pseudomonas*, *B. thermosphacta*, *Enterobacteriaceae*, and yeasts and molds. Under aerobic storage conditions the fast-growing *Pseudomonas* dominated the community and accelerated spoilage at all storage temperatures, though the growth of *B. thermosphacta* was also favored at low temperatures. After analyzing the microbiota, the researchers compared these to the volatile compounds detected by mass spectroscopy and determined that the alcohols derived from proteolytic activity in the breakdown of amino acids which may be due to *Pseudomonas* activity, though LAB and *B. thermosphacta* could also be involved. *Pseudomonas* is also involved in aldehyde and ketone production. Interestingly, the predominant spoilage products shift as the spoilage time increases. Alcohols increased early in the spoilage period until the midpoint, then decreased in abundance toward the end. Most ketones increased over time, though 2-butanone decreased over time. Esters increased as well, except in storage at 0 and 5 °C at which propanoate, butanoate, and lactate decreased over time. Though the dominance of *B. thermosphacta* is less reported in chicken literature, the general patterns reported here seem to carry through to chicken products as well [64]. All of the spoilage

organisms and metabolites reported in the literature cause the degradation of product quality to the point of inedibility.

The off-odor is the primary indicators of spoilage in meat products as consumers make purchasing and cooking decisions [68]. Numerous off-odors have been described in the literature, which include putrid, rancid, cabbage-like, floral/citrus, and sulfur [34,69]. In their study the spoilage volatilome, Casaburi *et al.* connected the products of microbial metabolism to specific odor outcomes [65]. Glucose is used first by psychrotrophic bacteria and is the precursor to many volatile compounds that cause strong negative odors, including acetate, acetoin, diacetyl, acetic acid, iso-butyric acid, iso-valeric acid, 2-methylbutryic acid, 3-methylbutanol, 2-methylpropanol, ethanol. After the depletion of glucose, proteins are broken down and the products of amino acid metabolism are malodorous sulfides, esters, and amines. The acetic acid and ethyl acetate can cause sharp, acrid odors, while the sulfides cause the sulfurous and putrid odors. The more complex alcohols cause distinct odors as well: 2-ethyl-1-hexanol can cause resin, flower and green odors, 1-heptanol leads to fragrant, woody, oily, green, fatty, winey, sap and herb odors, 1-octen-3-ol is associated with mushroom odors, 1-hexanol with chemical wine, fatty, fruity and weak metallic, 3 methyl-1-butanol can be associated with a whiskey-like odor [65]. In a similar study, Argyri *et al.* identified compounds that were prevalent both in non-spoiled and spoiled products, though they were not tied to specific odors from sensory study [64]. They found compounds associated with acceptable products to be 2-butanone, 2,3-pentanedione, 2,5-octanedione, pentanal, hexanal, trans-2-heptanal, and trans-2-octanal and products associated with spoilage to be 2-pentanone, 2-nonanone, 2-methyl-1-butanol, 3-methyl-butanol, ethyl hexanoate, ethyl propanoate, ethyl lactate, ethyl acetate, ethanol, 2-heptanone, 3-octanone, diacetyl, and acetoin. Several of these compounds align with those identified by Casaburi *et al*. and others were distinct but similar volatiles, adding to the list of potential odor-causing compounds that are produced by microbes during product spoilage [64,65]. Other compounds have previously been associated with spoilage odors, including biogenic amines cadaverine and putrescine, which are produced through the decarboxylation of amino acids, but these occur more frequently in anaerobic packaging [34]. To summarize, microbial metabolism results in numerous volatile

products, especially alcohols and amines; when microbial populations grow large enough these products are sufficient to contribute off-odors associated with product spoilage and inedibility by consumers.

Discoloration of meat and other foods is another major indicator of product spoilage that occurs through both chemical and microbiological pathways. These color changes have been characterized in poultry products. Katiyo *et al.* measured these color changes over storage period using both instrument and panel scoring [58]. In this study, as storage time increased the product became less pink and less intense by instrumental measurements, with days 10 and 14 having significantly lower values than previous study days. Interestingly, the human panel was more informative than the instrument measures, detecting color changes earlier in the storage period [58]. These changes may be induced by physiochemical changes in the product, including surface desiccation reducing product chroma. Additionally, the storage conditions may alter the state of the myoglobin compound in the muscle tissue. Extended oxygen exposure can cause the molecule to oxidize to metmyoglobin, which produces a brown color [34]. Smolander *et al*, in a study describing freshness indicators in poultry, also demonstrated how hydrogen sulfide compounds produced by microbes can bind with myoglobin to produce a greening [70]. Due to a lower myoglobin concentration in chicken compared to other meats, though, these chemical discolorations may be less obvious, which is perhaps why odor is a stronger indicator of spoilage. Off-colors in chicken may also be due to pigments produced by microbes, specifically *Pseudomonas* that grow abundantly in spoiled products. *P. fluorescens* produces of blue, green, and yellow pigments, with the yellow being a siderophore that is a product of iron metabolism [34]. Andreani *et al*. found two copies of genes involved in tryptophan biosynthesis, and up-regulation of genes involved in iron uptake, and down-regulation of genes involved in primary metabolism in pigmenting *P. fluorescens* strains as opposed to the non-pigmenting strains, which may show why these strains thrive in food products [71]. These pigments were not specifically associated with spoilage observations in consumer studies, but may still be important in overall product impressions, and likely is related to quality degradation.

Conclusions

The spoilage, through physiochemical and microbiological means, of chicken products is complex. There are numerous microorganisms that take advantage of a matrix of high-quality nutrients, though *Pseudomonas* tend to dominate the microbial ecosystem. The metabolisms of these microbes produce alcohols, aldehydes, amines, esters, ketones, and sulfides, which contribute to negative odors, discoloration, and off-flavors in the products that render them non-consumable. This has a massive impact on the amount of food waste produced globally when these products spoil before being sold or consumed, and that also contributes to major economic consequences for food production companies. Therefore, researchers have sought to reduce the incidence of spoilage through modification of product conditions. These include decreased storage temperatures, changing harvesting, chilling, and other processing parameters, and modifying packaging, though this review focused on aerobic conditions. Despite this increased body of knowledge, further research is still necessary to determine the exact relationship between the microbial community and spoilage outcomes in order to increase the shelf life and further reduce food loss due to inedibility.

Microbial Contributions to Vertebrate Decomposition

Vertebrate Decomposition

The process of decomposition is crucial for nutrient cycling in the environment, and therefore has undergone extensive study. While a large portion of the literature on the subject investigates the impact of the decay of leaf litter and other plant materials, the decomposition islands generated by vertebrate decomposition have been shown to have major impacts on the biogeochemical cycling [72–74]. The process of vertebrate decomposition is well-described. It proceeds in distinct stages, which are defined by the physical description of the remains; however, several different classifications of these stages have been proposed. One of the highly recognized early systems, proposed by Payne, divides decomposition into six stages: fresh, bloat, active decay, advanced decay, dry, and remains [75]. Subsequent descriptions use similar categories but may merge several together. For example, Megyesi *et al*. consider four stages:

fresh, early decomposition, advanced decomposition, and skeletonization [76], and other have combined dry and remains to one stage instead of separating them [77]. Regardless of the terminology, the descriptions of the stages are similar. Fresh is associated with the initial death event, the depletion of internal oxygen, and autolysis of cells in the body. Bloat, or early decomposition, is associated with anaerobic metabolism and the production of gasses by internal microbes and the start of purging into the soil. Active decay is the period of high mass loss from the remains, maggot activity, and the transfer of fluids from the remains to the soil or surrounding environment. Advanced decay is determined by the migration of fly larvae and comprises a slower rate of mass and fluid deposition. Finally, the dry remains stage is associated with growth of plants and fungi on or near the remains and full exposure of bones [78].

Microbiology of Decomposition Environments

The microorganisms that become active during the decomposition period are essential to the nutrient breakdown during decay. Though cell autolysis is an important part of the early decomposition process, the larger portion of physical remains breakdown is regulated by the activity of scavengers and insects, which serves to deposit the associated material into the soil and release the nutrients [78]. After the remains are reduced, the microorganisms actively cycle the materials, especially the carbon and nitrogen compounds. Given the importance of microbes to this system, there are several studies investigating the organisms that drive the breakdown of decomposition products in the soil and on and within the remains themselves.

The microbial composition of soil is significantly altered by the sudden release of high-quality nutrients that occurs during decomposition. Indeed, it has been demonstrated that the soil community is the primary source of the decomposer microbes [79]. During the initial stages of decomposition (fresh, bloat), the microbial communities are generally comprised of typical soil organisms, including *Proteobacteria, Acidobacteria,* and *Bacteroidetes*, with a lower abundance of *Actinobacteria, Planctomycetes, Chloroflexi, Gemmatimonadetes, Crenarchaeota,* and *Nitrospirae* [80]. Interestingly, different studies reported opposite trends in the abundance of *Verrucomicrobia*, with one study showing it

in high abundance in all soils and another describing a low abundance during this early stage [80,81]. The former, conducted by Carter *et al*, used swine as a host species, was evaluating the microbial composition across seasons, and was conducted in a tallgrass prairie [81], while the latter, conducted by Adserias-Garriga *et al*. was conducted using human remains in a subtropical forested area [80]. Any of these factors could have influenced the distinct result. The Adserias-Garriga paper continued to observe the changes in these organisms over time, showing a sudden increase in Firmicutes and a decrease in Proteobacteria after days 6 to 7, likely associated with the onset of active decay, and then associated a high abundance of *Clostridiales* with advanced decay and dry remains [80]. Other organisms reported to increase in abundance during this period are *Sphingobacteriaceae*, *Brucellaceae*, *Phyllobacteriaceae*, *Hyphomicrobiaceae*, and *Alcaligenaceae*. Weiss *et al*. [82] and Metcalf *et al.* [83] demonstrated a decrease in relative abundance of *Acidobacteria,* which is inversely related to soil pH, and several microbial eukaryotes across the decomposition period.

The microbial community associated with the host remains themselves is influenced not only by the availability of nutrients and oxygen, but also by the breakdown of tissues, allowing generally internal microbes to influence the external spaces. Metcalf *et al* showed that organisms associated with the gut microbiome increase in relative abundance within the abdominal cavity during the early stages of decomposition, through bloat [83]. After rupture, the relative abundance of these organisms decrease due to the shift in oxic conditions as the body cavity is exposed to air. This shift allows other organisms to dominate the community, including several families of Alphaproteobacteria, *Serratia*, *Escherichia*, *Klebsiella*, and *Proteus* [83]. Other studies further investigated the changes in gut microbiota during decomposition. Debruyn and Hauther sampled the gut microbiome daily through an incision sealed with tape to preserve the anoxic conditions [84]. They demonstrated that communities in early decomposition contained a high abundance of *Bacteroides*, *Parabateroides*, *Faecalibacterium*, *Phascolarectobacterium*, *Blautia*, and *Lachnospiraceae*, while late decomposition communities had a higher abundance of *Clostridium*, *Peptosterptococcus*, *Anaerosphaera*, and Gammaproteobacteria coupled with a decrease in Bacteroidetes. Interestingly, they identified distinctions between individuals in the early timepoints, but

all individual remains followed a similar trajectory towards a decrease in community richness and dominance by just a few genera [84]. Hauther *et al*. saw a similar pattern in the human cecum, reporting a decrease in the abundance of *Bacteroides* and *Lactobacillus* over the first 20 days of decomposition [85]. Additional body sites tested in the literature include the mouth, ear, eye, nose, umbilicus, and rectum. The mouth, or buccal cavity, of rats was investigated by Guo *et al*, who found that *Moraxellaceae* increased in abundance over the first day of decomposition, but then decreased as *Xanthamonadaceae* and *Enterobacteriaceae* increased in abundance [86]. Additionally, from day 4 onwards the abundance of *Strepotcocaceae* and *Pasteurellaceae* decreased, and *Pseudomonadaceae* increased rapidly on the sixth day postmortem [86]. Pechal *et al* investigated all of these sites on a large scale [87]. They found that all the sampling sites had distinct microbial communities, and this remained discrete throughout the decomposition period. The mouth samples demonstrated the most variability over decomposition period, compared with the rectum that harbored a consistent community. In remains discovered in the first 48 hours, the authors detected a higher functional redundancy coupled with a higher taxonomic diversity compared to later decomposition periods, showing that during the fresh stage of decomposition there are similar functions being conducted by a variety of organisms [87]. Overall, while there are taxa that create distinct microbiomes at different sample sites, the changes in the abundance of specific microbe groups over times demonstrates clear microbial succession in both the gravesoils and host tissues during decomposition.

Nutrient Cycling in Decomposition Soils

The deposition of a high-quality nutritional resource to an environment can trigger a dramatic change in the nutrient cycle of a soil environment. The remains of vertebrates provide an excellent example of this phenomenon, as the decomposition of some large vertebrates may be contributing more than 1% of the organic matter in some ecosystems [78]. These remains are excellent sources of carbon and nitrogen, which, when released to the soil, are recycled by the microorganisms described above. Other compounds shown to increase in concentration in decomposition-associated soils include

ammonium, phosphorus, calcium, potassium, sulphate, magnesium, chloride, sodium, and base cations [78].

Keenan *et al* investigated the specific contributions of vertebrate decomposition to nitrogen cycling using beavers as a model organism [74]. They concluded that there were three primary biogeochemical phases during decomposition. From placement through early decay, the soil conditions remained aerobic and the equilibrium between nitrogen and carbon cycling continued. Then, during active and advanced decay soil oxygen is depleted; the environment becomes anaerobic due to the deposition of decomposition fluids and remaining oxygen is consumed by the aerobic organisms. The depletion of oxygen was coupled with an increase in cellular respiration, which provided evidence that the oxygen was being utilized by microorganisms. This process led to an overall increase in total nitrogen and carbon in the soil. Moreover, during active decay there was an increase in phosphodiesterase, an enzyme for protein degradation, which could be associated with the breakdown of the phospholipids and nucleic acids from the remains. The third biogeochemical phase, during skeletonization, was indicated by a return to oxygenated condition due to consumption of the fluids, a decrease in microbial respiration rates, and enhanced nitrification and denitrification processes due to the decrease in concentration of free ammonia. From this, researchers hypothesized that the anaerobic conditions during active decay may be inhibiting nitrification. Interestingly, throughout decomposition there was no increase in soil protein, which suggests that these compounds are rapidly broken down, likely by maggots and microbial activity. All of these processes increased the soil pH, which remained elevated until four months after active decay, which was also observed in other similar studies [74,88]. Similarly, Cobaugh *et al* report that the respiration rates and biomass production increased during bloat and were the highest during active decay, showing the high amount of microbial activity in the soils [89]. They also report an overall increase in organic carbon, ammonia, and phosphate as a result of this activity. Conversely, Benninger *et al*. demonstrated no overall change in soil carbon over 100 days of swine decomposition [88]. However, they did report an increase in total nitrogen, especially during the first 14 days of decomposition, and an increase in in soil-extractable phosphorus over the entire 100-day period [88].

Fatty acids are also deposited from the remains to the soil. One study showed a variety of both saturated and unsaturated fatty acids in soil samples collected directly below swine carcasses, which included myristic, palmitic, palmitoleic, stearic, and oleic acids [90]. Benninger *et al* also described an increase in the amount of lipid-associated phosphorus in the soils, especially during early decomposition when the body tissues were being deposited into the soil [88]. The presence of these compounds in the soil may not greatly impact larger trends of biogeochemical cycling, but clearly influence the microbial activity in the soil. In fact, it has been demonstrated that an adipocere, a lipid bulk in the soils surrounding remains, forms due to a lack of microbial degradation [91]. It has been demonstrated that soils with adipocere formation contain higher levels of dissolved carbon and phosphorus, which indicates a change in microbial production, which demonstrates the importance of fatty acids to nutrient cycling in the decomposition environment [92].

Estimating the Postmortem Interval

The patterns in human decomposition can be noted to generate an estimate of the postmortem interval (PMI), or the time since death. This is a crucial piece of information, both in forensic investigation and to the relations of the decedent. In forensic science, an accurate PMI can allow investigators to validate alibies and to identify witnesses and suspects. Furthermore, it is one of the most frequently requested pieces of information from the relations of the decedent and could be important in distributing contents of wills. Therefore, it is critical to find methods that can accurately estimate PMI, even in cases of late discovery. During the first 48 to 72 hours, several tools are available for this, including body rigor mortis (stiffness), liver mortis (blood pooling), and algor mortis (temperature) [93,94]. However, these become less available as decomposition progresses, so forensic scientists have developed alternative methods in late-term PMI.

There are several methods that have been proposed and studied to estimate PMI in cases of late discovery. The most notable and widely used is forensic entomology, the practice of using the presence and life stages of insects on and around the remains. Investigators collect any insects present on the

remains and soil within two meters of the remains, then collect information including the age, size, and species of insects. Data formulas have been developed to convert this information to a PMI estimation [95]. This is an excellent tool for forensic investigations, but there are several aspects that can limit the accuracy of estimation made with entomology. The knowledge and training of investigators is critical to success as it requires precise identification of the insects, environmental conditions such as temperature, humidity, and indoor vs outdoor spaces impact colonization and growth, and there is always uncertainty regarding the time from death to colonization [95–99].

Other methods have been proposed as an alternative to entomology. For instance, Sabucedo and Furton demonstrated a pseudo-linear relationship between degradation of the cardiac protein Troponin I and PMI, suggesting that the degradation band pattern could be used to determine PMI especially during the first five days postmortem [100]. Additionally, Hunter *et al* evaluated the accuracy of using the expression of upregulated genes [101]. They trained a model to predict PMI using linear regression analysis, then compared the predictions with the actual intervals to determine accuracy. They reported an R^2 of 1 when using zebrafish genes and R^2 of 0.98 and 0.95 for mouse liver and brain genes, respectively. However, this study only evaluated the first 48 or 96 hours postmortem, so this method may be less useful in longer decomposition periods [101]. One additional proposed method for PMI estimation has been very promising as a tool for forensic investigation: microbial succession in the postmortem microbiome. Microbial communities have been demonstrated to change in consistent patterns over time during decomposition on skin [79,83,102], in the gastrointestinal tract and abdominal cavity [79,83–85], mouth [102], and nose [103], and in associated soils [79,81–83,89]. This provides evidence that these patterns can be modeled and used to create estimators of PMI using statistical methods and machine learning. In fact, several studies have demonstrated the accuracy of this method. A study using mice predicted PMI within 3.30 +/- 2.52 days over the first 34 days of decomposition [83]. Another study that included samples from the skin, abdominal cavity, and associated soils of mice and human remains predicted PMI within 2 to 3 days over the first two weeks of decomposition [79]. Finally, as study of skin in nasal an ear

cavity used the *k*-nearest neighbor algorithm to predict PMI within 55 accumulated degree days (ADD), which is equivalent to approximately 2 experimental days.

To generate predictive models that are accurate under multiple conditions, researchers have sought to explore the variables that may alter the microbial succession patterns. Weiss *et al*. decomposed swine carcasses from three different weight groups to evaluate the impact of carcass mass on microbial community structure [82]. When comparing decomposition soils to control soils, they found that the presence of remains and PMI had an impact on the microbial communities, but the mass of the carcass did not significantly impact them, [82]. Additionally, Metcalf *et al*. studied mouse decomposition on soils from distinct environmental sources (desert, shortgrass, forest) and determined that the soil type was not a major driver of microbial community assembly during decomposition [79]. Together, these studies suggest that microbial succession will be similarly predictable regardless of remains mass or soil type, so these variables may not be necessary to include in an accurate predictive model of PMI. In another study, Carter *et al.* compared swine decomposition in the summer and winter to evaluate seasonal variation in decomposition soil microbial communities [81]. They found that, in the winter, the remains froze and had no insect activity, which slowed the decomposition process. Moreover, when comparing the decomposition soils to control soils within a season, they saw larger changes in microbial communities in summer than in winter [81]. Thus, it will be necessary to consider seasonal conditions when estimating PMI from microbial data. Finally, Pechal *et al* considered how antemortem conditions may impact the patterns in decomposition [87]. They concluded that manner of death, sex, death event location, ethnicity, season of death, and body weight were not important in evaluating the structure of the microbial communities. They did report a weak positive relationship between body mass index and the community diversity. However, it is more likely that the microbial communities collected from remains in the first 48 hours can provide information about the antemortem health conditions than the inverse [87], therefore these conditions also may not need to be considered for accurate forensic tools.

Conclusions

The complex process of mammalian decomposition is an important feature of nutrient cycling in soils. The remains deposit important nutrients into the soil during the decomposition process, especially during active and advanced decay, including carbon, nitrogen, phosphorus, and minerals. These nutrients are then utilized during microbial metabolism, which furthers their biogeochemical cycling. As conditions in the soil change, so do the microbial communities, in response to both the nutrient availability and the change in oxygen availability. These shifts occur consistently across environments, within certain conditions such as season, in a process termed microbial succession. After the predictability of these succession was described, it was discovered that these patterns can be harnessed to estimate the postmortem interval. Therefore, a critical and naturally occurring environmental process has the potential to shape both the fields of environmental microbial ecology and forensic science when these concepts are applied.

REFERENCES

1. National Academies of Sciences, Engineering, and Medicine, National Academy of Engineering, Division on Engineering and Physical Sciences, Health and Medicine Division, Division on Earth and Life Studies, Board on Infrastructure and the Constructed Environment, Board on Environmental Studies and Toxicology, Board on Life Sciences, Committee on Microbiomes of the Built Environment: From Research to Application. Microbiomes of the Built Environment: A Research Agenda for Indoor Microbiology, Human Health, and Buildings. National Academies Press; 2017. 318 p.

2. Stout JE, Yu VL, Best MG. Ecology of Legionella pneumophila within water distribution systems. Appl Environ Microbiol. 1985 Jan 1;49(1):221–8.

3. Feazel LM, Baumgartner LK, Peterson KL, Frank DN, Harris JK, Pace NR. Opportunistic pathogens enriched in showerhead biofilms. Proc Natl Acad Sci. 2009 Sep 22;106(38):16393–9.

4. Coughenour C, Stevens V, Stetzenbach LD. An evaluation of methicillin-resistant Staphylococcus aureus survival on five environmental surfaces. Microb Drug Resist. 2011 May 25;17(3):457–61.

5. Okada H, Kuhn C, Feillet H, Bach J-F. The 'hygiene hypothesis' for autoimmune and allergic diseases: an update. Clin Exp Immunol. 2010;160(1):1–9.

6. Lax S, Smith DP, Hampton-Marcell J, Owens SM, Handley KM, Scott NM, Gibbons SM, Larsen P, Shogan BD, Weiss S, Metcalf JL, Ursell LK, Vázquez-Baeza Y, Van Treuren W, Hasan NA, Gibson MK, Colwell R, Dantas G, Knight R, Gilbert JA. Longitudinal analysis of microbial interaction between humans and the indoor environment. Science. 2014 Aug 29;345(6200):1048–52.

7. Dunn RR, Fierer N, Henley JB, Leff JW, Menninger HL. Home Life: Factors structuring the bacterial diversity found within and between homes. PLOS ONE. 2013 May 22;8(5):e64133.

8. Mohan GBM, Parker CW, Urbaniak C, Singh NK, Hood A, Minich JJ, Knight R, Rucker M, Venkateswaran K. Microbiome and metagenome analyses of a closed habitat during human occupation. mSystems. 2020 Aug 25;5(4).

9. Singh NK, Wood JM, Karouia F, Venkateswaran K. Succession and persistence of microbial communities and antimicrobial resistance genes associated with International Space Station environmental surfaces. Microbiome. 2018;6.

10. Hyde ER, Navas-Molina JA, Song SJ, Kueneman JG, Ackermann G, Cardona C, Humphrey G, Boyer D, Weaver T, Mendelson JR, McKenzie VJ, Gilbert JA, Knight R. The oral and skin microbiomes of captive Komodo dragons are significantly shared with their habitat. mSystems. 2016 Aug 30;1(4).

11. Nygaard AB, Charnock C. Longitudinal development of the dust microbiome in a newly opened Norwegian kindergarten. Microbiome. 2018 Sep 15;6(1):159.

12. Ross AA, Neufeld JD. Microbial biogeography of a university campus. Microbiome. 2015 Dec 1;3(1):66.

13. Chase J, Fouquier J, Zare M, Sonderegger DL, Knight R, Kelley ST, Siegel J, Caporaso JG. Geography and location are the primary drivers of office microbiome composition. mSystems. 2016 Apr 26;1(2).

14. Lax S, Sangwan N, Smith D, Larsen P, Handley KM, Richardson M, Guyton K, Krezalek M, Shogan BD, Defazio J, Flemming I, Shakhsheer B, Weber S, Landon E, Garcia-Houchins S, Siegel J, Alverdy J, Knight R, Stephens B, Gilbert JA. Bacterial colonization and succession in a newly opened hospital. Sci Transl Med. 2017 May 24;9(391).

15. Wood M, Gibbons SM, Lax S, Eshoo-Anton TW, Owens SM, Kennedy S, Gilbert JA, Hampton-Marcell JT. Athletic equipment microbiota are shaped by interactions with human skin. Microbiome. 2015 Jun 19;3(1):25.

16. Bräuer SL, Vuono D, Carmichael MJ, Pepe-Ranney C, Strom A, Rabinowitz E, Buckley DH, Zinder SH. Microbial sequencing analyses suggest the presence of a fecal veneer on indoor climbing wall holds. Curr Microbiol. 2014 Nov 1;69(5):681–9.

17. Food and Drug Administration. Current Good Manufacturing Practice, Hazard Analysis, and Risk-Based Preventative Controls for Human Food. Code of Federal Regulations.

18. Hultman J, Rahkila R, Ali J, Rousu J, Björkroth KJ. Meat processing plant microbiome and contamination patterns of cold-tolerant bacteria causing food safety and spoilage risks in the manufacture of vacuum-packaged cooked sausages. Appl Environ Microbiol. 2015 Oct 15;81(20):7088–97.

19. Zwirzitz B, Wetzels SU, Dixon ED, Stessl B, Zaiser A, Rabanser I, Thalguter S, Pinior B, Roch F-F, Strachan C, Zanghellini J, Dzieciol M, Wagner M, Selberherr E. The sources and transmission routes of microbial populations throughout a meat processing facility. Npj Biofilms Microbiomes. 2020 Jul 10;6(1):1–12.

20. Hassan AN, Birt DM, Frank JF. Behavior of Listeria monocytogenes in a Pseudomonas putida biofilm on a condensate-forming surface. J Food Prot. 2004;67(2):322–7.

21. Carpentier B, Chassaing D. Interactions in biofilms between Listeria monocytogenes and resident microorganisms from food industry premises. Int J Food Microbiol. 2004 Dec 15;97(2):111–22.

22. Zhao T, Doyle MP, Zhao P. Control of Listeria monocytogenes in a biofilm by competitive-exclusion microorganisms. Appl Environ Microbiol. 2004 Jul;70(7):3996–4003.

23. Tan X, Chung T, Chen Y, Macarisin D, LaBorde L, Kovac J. The occurrence of Listeria monocytogenes is associated with built environment microbiota in three tree fruit processing facilities. Microbiome. 2019 Aug 21;7(1):115.

24. Bokulich NA, Mills DA. Facility-specific “house” microbiome drives microbial landscapes of artisan cheesemaking plants. Appl Environ Microbiol. 2013 Sep 1;79(17):5214–23.

25. Bokulich NA, Bergsveinson J, Ziola B, Mills DA. Mapping microbial ecosystems and spoilage-gene flow in breweries highlights patterns of contamination and resistance. Kolter R, editor. eLife. 2015 Mar 10;4:e04634.

26. Adams RI, Bateman AC, Bik HM, Meadow JF. Microbiota of the indoor environment: a meta-analysis. Microbiome. 2015 Oct 13;3(1):49.

27. McCall L-I, Callewaert C, Zhu Q, Song SJ, Bouslimani A, Minich JJ, Ernst M, Ruiz-Calderon JF, Cavallin H, Pereira HS, Novoselac A, Hernandez J, Rios R, Branch OH, Blaser MJ, Paulino LC, Dorrestein PC, Knight R, Dominguez-Bello MG. Home chemical and microbial transitions across urbanization. Nat Microbiol. 2020 Jan;5(1):108–15.

28. Stessl B, Szakmary-Brändle K, Vorberg U, Schoder D, Wagner M. Temporal analysis of the Listeria monocytogenes population structure in floor drains during reconstruction and expansion of a meat processing plant. Int J Food Microbiol. 2020 Feb 2;314:108360.

29. Martín B, Perich A, Gómez D, Yangüela J, Rodríguez A, Garriga M, Aymerich T. Diversity and distribution of Listeria monocytogenes in meat processing plants. Food Microbiol. 2014 Dec 1;44:119–27.

30. NAMI. The United States Meat Industry at a Glance [Internet]. Available from: https://www.meatinstitute.org/index.php?ht=d/sp/i/47465/pid/47465

31. Big Chicken: Pollution and Industrial Poultry Production in America [Internet]. PEW; Available from: http://pew.org/2yIxE4p

32. poultry processing | Equipment, Steps, & Facts. In: Encyclopedia Britannica [Internet]. Available from: https://www.britannica.com/technology/poultry-processing

33. Guide: Modernization of Poultry Slaughter Inspection: Amendments to Chilling Requirements [Internet]. FSIS; 2014. Available from: https://www.fsis.usda.gov/wps/portal/fsis/topics/regulatory-compliance/guidelines/2014-0014

34. Zagorec M, Champomier-Vergès M. Meat microbiology and spoilage. In 2017.

35. Guidelines for slaughtering, meat cutting and further processing [Internet]. FAO; Available from: http://www.fao.org/3/t0279e/T0279E04.htm

36. Rivera-Pérez W, Barquero-Calvo E, Zamora-Sanabria R. Salmonella contamination risk points in broiler carcasses during slaughter line processing. J Food Prot. 2014 Dec 1;77(12):2031–4.

37. Berrang ME, Buhr RJ, Cason JA, Dickens JA. Broiler carcass contamination with Campylobacter from feces during defeathering. J Food Prot. 2001 Dec 1;64(12):2063–6.

38. Goksoy EO, Kirkan S, Kok F. Microbiological quality of broiler carcasses during processing in two slaughterhouses in Turkey. Poult Sci. 2004 Aug 1;83(8):1427–32.

39. Chen SH, Fegan N, Kocharunchitt C, Bowman JP, Duffy LL. Impact of poultry processing operating parameters on bacterial transmission and persistence on chicken carcasses and their shelf life. Appl Environ Microbiol. 2020 Jun 2;86(12).

40. James C, Vincent C, de Andrade Lima TI, James SJ. The primary chilling of poultry carcasses—a review. Int J Refrig. 2006 Sep 1;29(6):847–62.

41. Mead GC, Hudson WR, Hinton MH. Use of a marker organism in poultry processing to identify sites of cross-contamination and evaluate possible control measures. Br Poult Sci. 1994 Jul 1;35(3):345–54.

42. Lillard HS. The impact of commercial processing procedures on the bacterial contamination and cross-contamination of broiler carcasses. J Food Prot. 1990 Mar 1;53(3):202–4.

43. Munther D, Sun X, Xiao Y, Tang S, Shimozako H, Wu J, Smith B, Fazil A. Modeling cross-contamination during poultry processing: dynamics in the chiller tank. Food Control. 2016 Jan 1;59:271–81.

44. Karolyi L, Medić H, Vidaček S, Petrak T, Botka-Petrak K. Bacterial population in counter flow and parallel flow water chilling of poultry meat. Eur Food Res Technol. 2003 Nov 1;217:412–5.

45. Mielnik MB, Dainty RH, Lundby F, Mielnik J. The effect of evaporative air chilling and storage temperature on quality and shelf life of fresh chicken carcasses. Poult Sci. 1999 Jul 1;78(7):1065–73.

46. SÁNCHEZ MX, FLUCKEY WM, BRASHEARS MM, McKEE SR. Microbial Profile and Antibiotic Susceptibility of Campylobacter spp. and Salmonella spp. in Broilers Processed in Air-Chilled and Immersion-Chilled Environments. J Food Prot [Internet]. 2002 Jun 1 [cited 2020 Dec 29];65(6):948–56. Available from: https://doi.org/10.4315/0362-028X-65.6.948

47. Berrang ME, Meinersmann RJ, Smith DP, Zhuang H. The effect of chilling in cold air or ice water on the microbiological quality of broiler carcasses and the population of Campylobacter. Poult Sci. 2008 May 1;87(5):992–8.

48. Zhang L, Jeong JY, Janardhanan KK, Ryser ET, Kang I. Microbiological quality of water immersion-chilled and air-chilled broilers. J Food Prot. 2011 Sep;74(9):1531–5.

49. Tuncer B, Sireli UT. Microbial growth on broiler carcasses stored at different temperatures after air- or water-chilling. Poult Sci. 2008 Apr 1;87(4):793–9.

50. Zhuang H, Savage EM, Smith DP, Berrang ME. Effect of dry-air chilling on Warner-Bratzler shear force and water-holding capacity of broiler breast meat deboned four hours postmortem. 2008;

51. Carroll CD, Alvarado CZ. Comparison of air and immersion chilling on meat quality and shelf life of marinated broiler breast fillets. Poult Sci. 2008 Feb;87(2):368–72.

52. Jeong JY, Janardhanan KK, Booren AM, Harte JB, Kang I. Breast meat quality and consumer sensory properties of broiler carcasses chilled by water, air, or evaporative air. Poult Sci. 2011 Mar 1;90(3):694–700.

53. Jeong JY, Janardhanan KK, Booren AM, Karcher DM, Kang I. Moisture content, processing yield, and surface color of broiler carcasses chilled by water, air, or evaporative air. Poult Sci [Internet]. 2011 Mar 1 [cited 2021 Jan 6];90(3):687–93. Available from: http://www.sciencedirect.com/science/article/pii/S0032579119419639

54. Gill CO, Newton KG. The ecology of bacterial spoilage of fresh meat at chill temperatures. Meat Sci. 1978 Jul 1;2(3):207–17.

55. Arnaut-Rollier I, De Zutter L, Van Hoof J. Identities of the Pseudomonas spp. in flora from chilled chicken. Int J Food Microbiol. 1999 May 1;48(2):87–96.

56. Doulgeraki AI, Ercolini D, Villani F, Nychas G-JE. Spoilage microbiota associated to the storage of raw meat in different conditions. Int J Food Microbiol. 2012 Jul 2;157(2):130–41.

57. Handley JA, Hanning I, Ricke SC, Johnson MG, Jones FT, Apple RO. Temperature and bacterial profile of post chill poultry carcasses stored in processing combo held at room temperature. J Food Sci. 2010 Oct;75(8):M515-520.

58. Katiyo W, de Kock HL, Coorey R, Buys EM. Sensory implications of chicken meat spoilage in relation to microbial and physicochemical characteristics during refrigerated storage. LWT. 2020 Jun 1;128:109468.

59. Handley JA, Park SH, Kim SA, Ricke SC. Microbiome profiles of commercial broilers through evisceration and immersion chilling during poultry slaughter and the identification of potential indicator microorganisms. Front Microbiol. 2018;9.

60. Rothrock MJ, Locatelli A, Glenn TC, Thomas JC, Caudill AC, Kiepper BH, Hiett KL. Assessing the microbiomes of scalder and chiller tank waters throughout a typical commercial poultry processing day. Poult Sci. 2016 Oct 1;95(10):2372–82.

61. Gram L, Ravn L, Rasch M, Bruhn JB, Christensen AB, Givskov M. Food spoilage—interactions between food spoilage bacteria. Int J Food Microbiol. 2002 Sep 15;78(1):79–97.

62. Dainty RH, Mackey BM. The relationship between the phenotypic properties of bacteria from chill-stored meat and spoilage processes. Soc Appl Bacteriol Symp Ser. 1992;21:103S-14S.

63. FAO. Overcoming water challenges in agriculture [Internet]. Rome, Italy: FAO; 2020 p. 210. (The State of Food and Agriculture in the World). Available from: http://www.fao.org/state-of-food-agriculture/en/

64. Argyri AA, Mallouchos A, Panagou EZ, Nychas G-JE. The dynamics of the HS/SPME–GC/MS as a tool to assess the spoilage of minced beef stored under different packaging and temperature conditions. Int J Food Microbiol. 2015 Jan 16;193:51–8.

65. Casaburi A, Piombino P, Nychas G-J, Villani F, Ercolini D. Bacterial populations and the volatilome associated to meat spoilage. Food Microbiol. 2015 Feb;45(Pt A):83–102.

66. Lee HS, Kwon M, Heo S, Kim MG, Kim G-B. Characterization of the biodiversity of the spoilage microbiota in chicken meat using Next Generation Sequencing and culture dependent approach. Food Sci Anim Resour. 2017;37(4):535–41.

67. Morales PA, Aguirre JS, Troncoso MR, Figueroa GO. Phenotypic and genotypic characterization of Pseudomonas spp. present in spoiled poultry fillets sold in retail settings. LWT. 2016 Nov 1;73:609–14.

68. Franke C, Höll L, Langowski H-C, Petermeier H, Vogel RF. Sensory evaluation of chicken breast packed in two different modified atmospheres. Food Packag Shelf Life. 2017 Sep 1;13:66–75.

69. Nychas G-JE, Skandamis PN, Tassou CC, Koutsoumanis KP. Meat spoilage during distribution. Meat Sci. 2008 Jan;78(1–2):77–89.

70. Smolander M, Hurme E, Latva-Kala K, Luoma T, Alakomi H-L, Ahvenainen R. Myoglobin-based indicators for the evaluation of freshness of unmarinated broiler cuts. Innov Food Sci Emerg Technol. 2002 Sep 1;3(3):279–88.

71. Andreani NA, Carraro L, Martino ME, Fondi M, Fasolato L, Miotto G, Magro M, Vianello F, Cardazzo B. A genomic and transcriptomic approach to investigate the blue pigment phenotype in Pseudomonas fluorescens. Int J Food Microbiol. 2015 Jun 1;213:88–98.

72. Carter D, Tibbett M. Cadaver Decomposition and Soil. In: Soil Analysis in Forensic Taphonomy: Chemical and Biological Effects of Buried Human Remains. 2008. p. 29–51.

73. Fancher JP, Aitkenhead-Peterson JA, Farris T, Mix K, Schwab AP, Wescott DJ, Hamilton MD. An evaluation of soil chemistry in human cadaver decomposition islands: Potential for estimating postmortem interval (PMI). Forensic Sci Int. 2017 Oct;279:130–9.

74. Keenan SW, Schaeffer SM, Jin VL, DeBruyn JM. Mortality hotspots: Nitrogen cycling in forest soils during vertebrate decomposition. Soil Biol Biochem. 2018 Jun 1;121:165–76.

75. Payne JA. A summer carrion study of the baby pig Sus Scrofa linnaeus. Ecology. 1965;46(5):592–602.

76. Megyesi MS, Nawrocki SP, Haskell NH. Using accumulated degree-days to estimate the postmortem interval from decomposed human remains. J Forensic Sci. 2005 May;50(3):618–26.

77. Parkinson RA, Dias K-R, Horswell J, Greenwood P, Banning N, Tibbett M, Vass AA. Microbial Community Analysis of Human Decomposition on Soil. In: Ritz K, Dawson L, Miller D, editors. Criminal and Environmental Soil Forensics. Dordrecht: Springer Netherlands; 2009. p. 379–94.

78. Carter DO, Yellowlees D, Tibbett M. Cadaver decomposition in terrestrial ecosystems. Naturwissenschaften. 2007 Jan 1;94(1):12–24.

79. Metcalf JL, Xu ZZ, Weiss S, Lax S, Treuren WV, Hyde ER, Song SJ, Amir A, Larsen P, Sangwan N, Haarmann D, Humphrey GC, Ackermann G, Thompson LR, Lauber C, Bibat A, Nicholas C, Gebert MJ, Petrosino JF, Reed SC, Gilbert JA, Lynne AM, Bucheli SR, Carter DO, Knight R. Microbial community assembly and metabolic function during mammalian corpse decomposition. Science. 2016 Jan 8;351(6269):158–62.

80. Adserias-Garriga J, Hernández M, Quijada NM, Rodríguez Lázaro D, Steadman D, Garcia-Gil J. Daily thanatomicrobiome changes in soil as an approach of postmortem interval estimation: an ecological perspective. Forensic Sci Int. 2017 Sep;278:388–95.

81. Carter DO, Metcalf JL, Bibat A, Knight R. Seasonal variation of postmortem microbial communities. Forensic Sci Med Pathol. 2015 Jun;11(2):202–7.

82. Weiss S, Carter DO, Metcalf JL, Knight R. Carcass mass has little influence on the structure of gravesoil microbial communities. Int J Legal Med. 2016 Jan 1;130(1):253–63.

83. Metcalf JL, Wegener Parfrey L, Gonzalez A, Lauber CL, Knights D, Ackermann G, Humphrey GC, Gebert MJ, Van Treuren W, Berg-Lyons D, Keepers K, Guo Y, Bullard J, Fierer N, Carter DO, Knight R. A microbial clock provides an accurate estimate of the postmortem interval in a mouse model system. Kolter R, editor. eLife. 2013 Oct 15;2:e01104.

84. DeBruyn JM, Hauther KA. Postmortem succession of gut microbial communities in deceased human subjects. PeerJ. 2017 Jun 12;5:e3437.

85. Hauther KA, Cobaugh KL, Jantz LM, Sparer TE, DeBruyn JM. Estimating time since death from postmortem human gut microbial communities. J Forensic Sci. 2015 Sep;60(5):1234–40.

86. Guo J, Fu X, Liao H, Hu Z, Long L, Yan W, Ding Y, Zha L, Guo Y, Yan J, Chang Y, Cai J. Potential use of bacterial community succession for estimating post-mortem interval as revealed by high-throughput sequencing. Sci Rep. 2016 Apr 7;6(1):24197.

87. Pechal JL, Schmidt CJ, Jordan HR, Benbow ME. A large-scale survey of the postmortem human microbiome, and its potential to provide insight into the living health condition. Sci Rep. 2018 Apr 10;8(1):5724.

88. Benninger LA, Carter DO, Forbes SL. The biochemical alteration of soil beneath a decomposing carcass. Forensic Sci Int. 2008 Sep 18;180(2):70–5.

89. Cobaugh KL, Schaeffer SM, DeBruyn JM. Functional and structural succession of soil microbial communities below decomposing human cadavers. PLOS ONE. 2015 Jun 12;10(6):e0130201.

90. Larizza M, Forbes SL. Detection of fatty acids in the lateral extent of the cadaver decomposition island. Geol Soc Lond Spec Publ. 2013 Jan 1;384(1):209–19.

91. Schoenen D, Schoenen H. Adipocere formation--the result of insufficient microbial degradation. Forensic Sci Int. 2013 Mar 10;226(1–3):301.e1-6.

92. Fiedler S, Schneckenberger K, Graw M. Characterization of soils containing adipocere. Arch Environ Contam Toxicol. 2004 Nov;47(4):561–8.

93. Madea B. Methods for determining time of death. Forensic Sci Med Pathol. 2016 Dec;12(4):451–85.

94. Shrestha R, Kanchan T, Krishan K. Methods Of Estimation Of Time Since Death. In: StatPearls. Treasure Island (FL): StatPearls Publishing; 2020.

95. Amendt J, Campobasso CP, Gaudry E, Reiter C, LeBlanc HN, Hall MJR, European Association for Forensic Entomology. Best practice in forensic entomology--standards and guidelines. Int J Legal Med. 2007 Mar;121(2):90–104.

96. Wells J, LaMotte L. The role of a PMI-prediction model in evaluating forensic entomology experimental design, the importance of covariates, and the utility of response variables for estimating time since death. Insects. 2017 May 1;8(2).

97. Sharma R, Kumar Garg R, Gaur JR. Various methods for the estimation of the post mortem interval from Calliphoridae: A review. Egypt J Forensic Sci. 2015 Mar 1;5(1):1–12.

98. Faris AM, Wang H-H, Tarone AM, Grant WE. Forensic Entomology: Evaluating Uncertainty Associated With Postmortem Interval (PMI) Estimates With Ecological Models. J Med Entomol. 2016 Sep 1;53(5):1117–30.

99. Anderson GS. Comparison of decomposition rates and faunal colonization of carrion in indoor and outdoor environments. J Forensic Sci. 2011 Jan;56(1):136–42.

100. Sabucedo AJ, Furton KG. Estimation of postmortem interval using the protein marker cardiac Troponin I. Forensic Sci Int. 2003 Jun 24;134(1):11–6.

101. Hunter MC, Pozhitkov AE, Noble PA. Accurate predictions of postmortem interval using linear regression analyses of gene meter expression data. Forensic Sci Int. 2017;275:90–101.

102. Pechal JL, Crippen TL, Tarone AM, Lewis AJ, Tomberlin JK, Benbow ME. Microbial community functional change during vertebrate carrion decomposition. PloS One. 2013;8(11):e79035.

103. Johnson HR, Trinidad DD, Guzman S, Khan Z, Parziale JV, DeBruyn JM, Lents NH. A machine learning approach for using the postmortem skin microbiome to estimate the postmortem interval. PLOS ONE. 2016 Dec 22;11(12):e0167370.

THE MICROBIOME OF A NEWLY CONSTRUCTED MEAT PROCESSING FACILITY ESTABLISHES OVER TIME BY ROOM FUNCTION AND MICROBIAL SOURCE

Summary

The microorganisms that reside in food processing facilities can have lasting negative consequences on food safety and quality. The microbiomes can harbor important pathogens such as *Listeria monocytogenes* that can transfer to the food products and lead to disease in consumers. They also contain major food spoilage organisms and can lead to poor product quality and shortened shelf lives when they contaminate the food products. Despite the significant consequences of these environments, there has been little study of how these microbial communities form within the processing spaces. The construction of a new meat processing facility provided an opportunity to address this knowledge gap. A study was designed to answer research questions including (1) Is a stable microbiome established in a meat processing facility? (2) What factors are associated with the facility microbial composition? (3) What are the major sources of microbes present in the facility microbiome? Samples of the microbial communities were collected from drains and door handles in the facility approximately monthly spanning the first 18 months of operation. The microbiomes were investigated using 16S rRNA gene sequencing following Earth Microbiome Project protocols. Data were analyzed using QIIME2 and visualizations were constructed in R.

Results indicate that stable microbial communities begin to form throughout the processing facility within the first eight to nine months of consistent production. However, these communities appear subject to perturbation when major conditions in the facility change, such as a large shift in production volume. Additionally, different communities form within spaces, selected for by microbial source, room temperature, general use, and nutrient availability. Interestingly, it also appears that physical barriers within the facility prevent specific organisms from being transmitted between spaces. Overall, this study demonstrates the importance of deliberate facility design and regular cleaning and sanitation practices to control the microbial communities in the food processing space.

Introduction

The growing field of built environment microbiome studies has allowed researchers to focus on the unique relationship between humans and the environments they occupy. Generally, the spaces investigated in these studies are facilities in which humans spend a majority of their time, and in which humans are the major occupant; for example, homes [1–4], school and university buildings [5–7], hospitals [8], and athletic facilities [9,10]. In nearly every case, the microbial composition of the built environment has been shown to reflect that of the primary occupants, even in cases with consistent cleaning and sanitation practices. Not only this, but the transition of the microbial community to reflect the occupants occurs very rapidly, often in under a day [4,8]. However, humans are not the primary occupant of many under-studied built environments, though they can be negatively impacted by the microbial communities found in them. Specifically, the microbial communities of food and beverage production facilities may have important implications on the safety and quality of the commercial food products.

Microorganisms are generally considered the enemies of wholesome food production systems. Many microbes that enter a production facility, especially in products of animal origin, are pathogens that can cause illness in cases of human consumption. Notably, *Listeria monocytogenes* in facilities results in a massive food safety risk as it can transfer to products considered ready-to-eat, which will not be cooked prior to consumption, and can grow under refrigerated conditions. To try to reduce risk of contamination from these organisms, food processing facilities are required to have testing and control plans [11]. However, the majority of organisms present in the production environment are not likely to cause human illness, but instead impact the quality of the product by their involvement in spoilage, especially organisms such as *Pseudomonas*, *Moraxellaceae*, and Lactic Acid Bacteria. Moreover, there is evidence that these organisms can be transferred from the environment to the food products, demonstrating the critical importance of managing the built environment microbiome [12,13]. As a result, advances have been made by food production industries in an effort to reduce the presence of microbes in their facilities, such as the introduction of rigorous cleaning and sanitation regimes and the use of facility design to

prevent cross-contamination between processing steps. Even industries that rely on the presence of microbes to generate their product, such as brewing and cheesemaking, strive to reduce the presence of "wild microbes" [13,14]. Despite these efforts, resident microbial communities have been identified in brewing [13], cheesemaking [14], fruit processing [15], and meat processing [12,16,17] facilities. Though a general picture of these communities is forming through the published literature, there is still a major knowledge gap surrounding the origins of these microbes and how the communities assemble within the facility.

A unique opportunity to address these knowledge gaps recently arose at Colorado State University when construction began on a new meat production facility housed in the Animal Sciences department. The convenient location and collaborations allowed access to the facility beginning prior to any animal products entering the facility, which presented the opportunity to investigate the composition of a meat processing facility microbial community before it is established in the environment. To capitalize on this opportunity, a research project was devised to address several guiding questions: (1) Is a stable microbiome established in a meat processing facility? (2) What factors are associated with the facility microbial composition? (3) What are the major sources of microbes present in the facility microbiome?

Results and Discussion

Sequencing results

To investigate the changes in the microbial communities within a newly constructed meat processing facility, the Global Food Innovation Center (GFIC; Fort Collins, CO), microbiome samples were collected monthly from drains and door handles throughout the facility from January 2019 until August 2020. This timeframe spanned from post-construction cleaning (pre-opening) through 18 months of operation. The microbiome was evaluated using sequencing of the V4 region of the 16S rRNA gene following Earth Microbiome Project protocols. In total, 1,009 samples were sequenced for this study, including 39 negative and no-template controls and 4 mock communities. Sequencing resulted in a total

of 34,332,385 paired-end reads. After denoising, quality filtering, read joining, and chimera removal with the DADA2 plugin, the dataset contained 31,676 distinct amplicon sequence variants (ASVs) in a total frequency of 25,110,424 ASVs (range: 1 to 152,682 ASV/sample, mean: 24,886 ASV/sample). These samples were filtered to remove ASVs that assigned to chloroplasts and mitochondria after taxonomic analysis, resulting in 29,485 ASVs.

Negative controls were evaluated based on number of reads present, and were all determined to be low abundance, indicating that data could be considered uncontaminated. Additionally, the rarefaction level used in diversity analysis for this study was well above the threshold of the highest negative control, giving us confidence in our biological samples. Thirteen mock communities were sequenced for inclusion as positive controls. The taxonomic profiles of these communities were compared with the expected composition based on manufacturer reports. The mock communities resulted in the expected community with no unexpected taxa, indicating expected sequencing quality and no major contamination. All negative and positive control samples were removed from the dataset before further analysis.

Establishment of a Stable Microbial Community

The microbial community that developed within facility drains appears to become consistent over time after the start of consistent production, while communities associated with door handles are highly variable. The microbial diversity within facility drains stabilizes rapidly after the start of production in the facility (**Figure 2.1A**). The mean microbial diversity within drains was unexpectedly high at the first sampling timepoint immediately following the post-construction clean (richness = 286, Shannon's = 5.42, Faith's = 87.9), perhaps indicating the sanitation event was less effective than expected or that sampling selected for dirtier areas. However, the diversity did decrease after the start of production, measured in the second sampling timepoint ($P < 0.05$; richness = 95.3, Shannon's = 2.99, Faith's = 35.0). After this, there were no significant changes in microbial richness or Shannon's diversity between subsequent timepoints ($P > 0.05$), though there was still numerical fluctuation. There was, however, a difference ($P < 0.05$) in Faith's phylogenetic diversity between timepoints two and three and three and four, after which there was

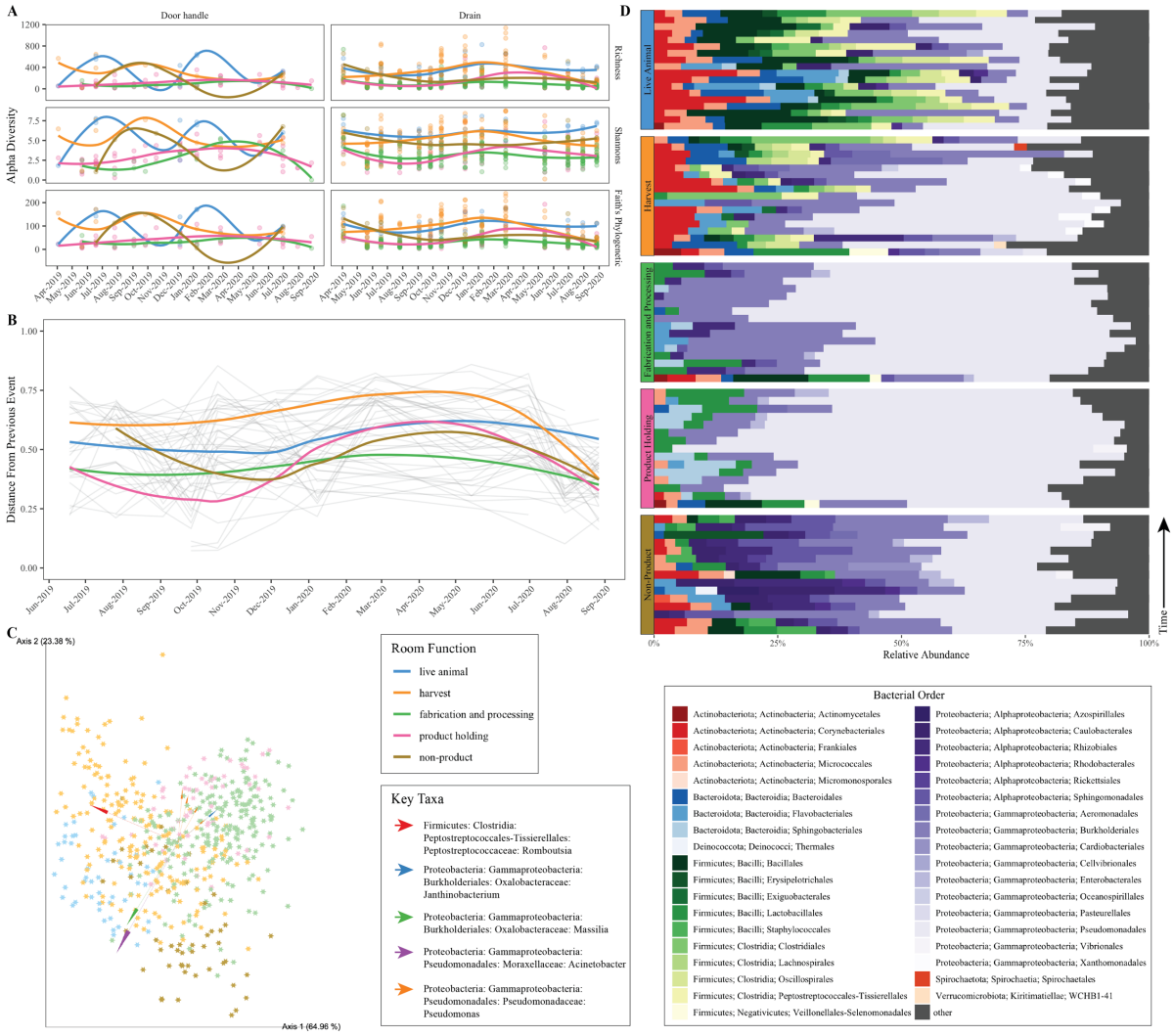

Figure 2.1. The microbial communities associated with the meat processing facility. **A)** Alpha diversity changes over time by facility room function. **B)** The change in similarity between microbial communities sampled from the same facility drain over time. Each point represents the change in diversity between that timepoint and the previous timepoint. A downward slope represents a trend toward a stable community, while a distance of 0 would indicate no changes in a community between sample timepoints. **C)** Biplot of the beta diversity calculated by Robust Aitchison PCA. **D)** Taxonomy of samples collected from the facility, averaged by room function and sampling event.

no further change. The early fluctuation followed by stabilization suggests a trend towards a stable microbial community within the facility drains. The observation of a consistent alpha diversity agrees with other longitudinal studies of the built environment, suggesting that the diversity of indoor microbial communities is stable once microorganisms have been introduced [7,8]. Conversely, microbial samples collected from door handles had a more variable alpha diversity that fluctuated across the entire

experimental period (**Figure 2.1A**). Door handles have more direct contact with personnel in the facility and may be cleaned less consistently than the floors, which may prevent a consistent community from establishing. This is similar to results reported by Ross and Neufeld in a study of the microbiomes of door handles on a college campus, where they demonstrated that individual door handles had distinct microbiomes, that door handle microbial profiles were temporary, and that the diversity directly correlated to debris present on the handle [6]. In the current study there was rarely visible debris on the door handles sampled, but that does not exclude the possibility of the presence of contaminants. Moreover, there was variation in the types of door handles throughout the facility, even within a single room function (i.e., push bars, levers, swinging doors), which may contribute to the variable diversity similar to the "microbial islands" observed by Ross and Neufeld [6].

The microbial community within a drain establishes itself over time with consistent facility use. The microbial diversity within each drain was compared longitudinally to identify whether the communities become more similar across timepoints (**Figure 2.1B**). This calculation was performed such that a decrease in the differences (a negative slope) between samples indicated a trend toward stability of a community. Interestingly, the communities approached stability at two timepoints: November to December of 2019 and September of 2020. The first stability timepoint occurred after approximately eight to nine months of production, at which point the routine within the facility was established and the facility was used consistently, though there was a low volume of product being produced. After these points the drain communities became more dissimilar over time. This is likely due to the occurrence of winter break at the university, when most facility employees took vacation and production decreased. Moreover, a major perturbation to the system occurred in spring of 2020, when the facility closed due to the COVID-19 pandemic and production ceased. In June of 2020, a commercial meat processing company began using the GFIC facility for their harvest and fabrication activities. This company represented a very high production volume with weekly use; this is the most consistent use within the GFIC facility. Almost immediately following the beginning of this new production schedule the microbial communities again approached stability. Notably, the two stable communities presented did not cluster

together in a principal coordinate analysis. This is similar to a study of the establishment of hospital microbiomes by Lax *et al*., in which microbial similarity between samples in a room increased over time with a single patient, but the change in occupant quickly altered the system [8]. Overall, it is likely that a microbial community established in drains during the first year of consistent production at a facility, but major perturbations to the system significantly altered this stable state.

Microbial Communities are Shaped by Room Conditions

The microbial communities within the food processing facility are similar within the function of the room they were collected from. The communities clearly cluster by function of the room in a principal components biplot analysis and have similar taxonomic profiles within a function group (**Figures 2.1C, 2.1D**). The live animal holding spaces and harvest spaces contained very similar, highly diverse communities (**Figure 2.1A, 2.1C**) with a high relative abundance of *Firmicutes*, likely derived from soils and feces deposited by the animals present in the facility. The clustering of samples from these spaces was driven by *Clostridia, Moraxellaceae,* and *Janthinobacterium* (**Figure 2.1C**). *Moraxellaceae* specifically has been previously reported as highly abundant in fruit processing facilities, where there is repeated introduction of outside microbes on the products [15]. Fabrication and processing spaces were consistently dominated by *Pseudomonas*. Indeed, the clustering of these groups is driven by three sequences associated with *Pseudomonas* species. Finally, non-product spaces that are only occupied by humans (hallways, storage rooms) are associated with an abundance of *Alphaproteobacteria*. These organisms, specifically orders *Rhizobiales*, *Rickettsiales*, and *Sphingomonadales*, have been previously reported on surfaces in food processing environments [15,16].

The environmental conditions, especially temperature, may be the driving factor for the differences in communities across room function. Rooms are kept at different temperatures based on their primary function, with the product holding spaces kept the coldest (below -18 °C or below 4 °C), the fabrication and processing spaces also kept cold (below 10 °C), and live animal, harvest, and non-product spaces not temperature controlled. These uncontrolled spaces are generally room temperature or slightly

colder due to cooler activity in adjacent rooms, but during activity may become quite warm due to body heat and hot water use. Microbial communities in built environments are strongly influenced by temperature, so this likely plays a role in the drain community assembly [1,2,8,18]. Specifically, the communities in cold areas (fabrication and processing, product holding) were dominated by *Pseudomonas*, a group of psychrotrophic organisms that could thrive and out-compete other organisms in these spaces. Similarly, the dominant organisms in the warm rooms tend to thrive at higher temperatures. In fact, some, such as *Clostridia*, would not even enter a vegetative state until the temperatures are sufficiently high. These associations make it highly likely that the temperature of the spaces, controlled due to the function of the space, influences the assembly of the community.

The frequency of cleaning and sanitation within the facility also influences the ability of microorganisms to form resident communities, as it results in a low nutritional availability, disrupts the formation of biofilms, and may force the organisms to remain the lag growth phase, slowing overall growth of organisms. However, these conditions are impacted by the function of the space. The live animal and harvest rooms, though regularly cleaned and sanitized, are still subjected to the high-volume input of potential nutrients through dirty livestock being introduced such as fecal material, blood, and viscera. Conversely, the fabrication and processing spaces generally only contain already sanitized meat products and regularly cleaned equipment, so the introduction of nutrients is less frequent. This further elucidates the competitive advantage of organisms such as *Pseudomonas* in these spaces, as these organisms have a high tolerance for low nutrients and sanitizers [19].

It is well-established in the literature that the occupants of a space in the built environment have a strong influence on the microbial community [3,4,7,8,20]. However, in food processing environments the room occupants are not just the human residents, but also the ingredients and raw materials used in processing. Samples from the feces, hide, and carcasses of livestock, soil near the entrances, and human employees in the facility were collected to evaluate the impact of various sources on the facility microbiome. As expected, the livestock-associated samples clustered with samples collected from live animal and harvest spaces and human hand swabs associated with non-product spaces (**Figure 2.2A**).

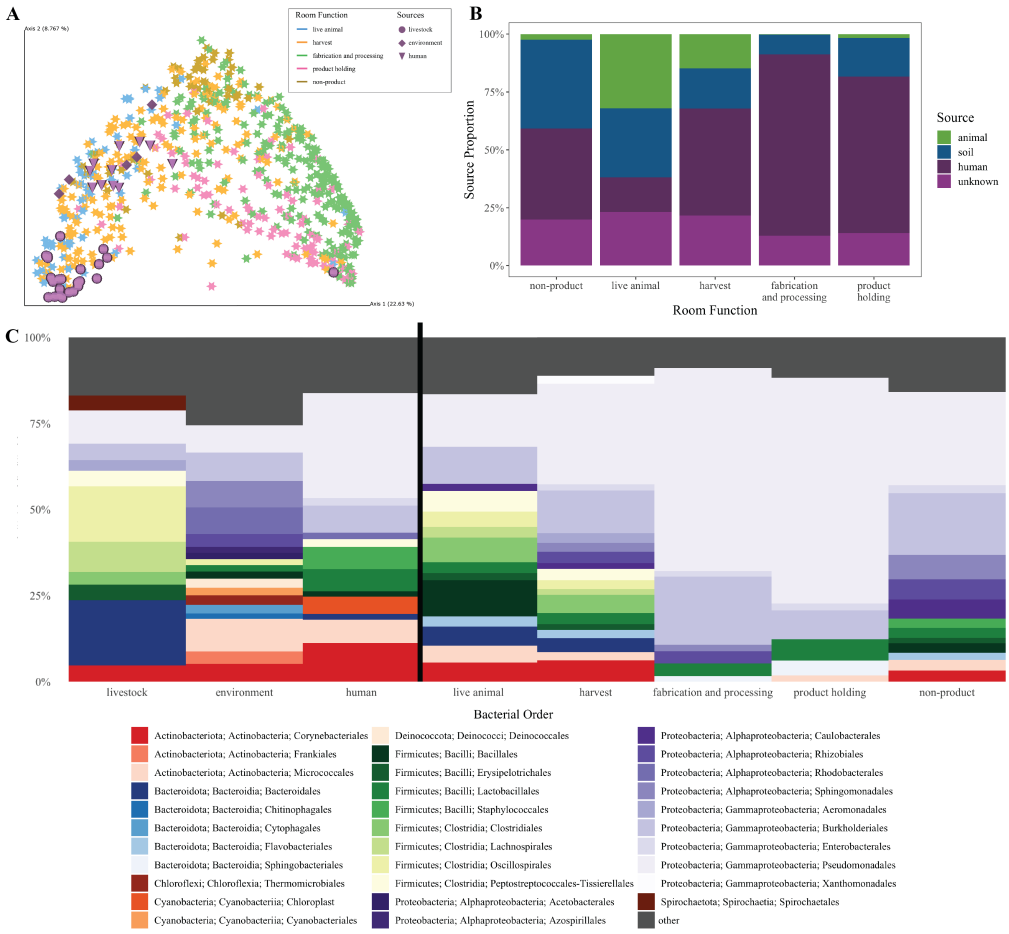

Figure 2.2. An analysis of sources of microorganisms in the GFIC facility. **A)** Principal coordinates plot built with the generalized Unifrac metric at a weight of 50%. The processing room spaces are included as stars and the potential sources are in purple. **B)** Proportions of the room microbiome contributed by different sources of microorganisms.

To confirm these observations, a source tracking analysis was conducted to identify the proportion of the drain microbiota that were contributed from each source (**Figure 2.2B**). This analysis suggests that the livestock and external facility soils are the primary source of the microorganisms that establish in the live animal and harvest, while human-associated microbiota are the primary source of microorganisms in fabrication and processing and product holding spaces. A taxonomic analysis was used to hypothesize which organisms were likely contributed from each source (**Figure 2.2C**). *Actinobacteria*, *Bacteriodota*, and *Firmicutes* that were enriched in live animal and harvest spaces were likely contributed by the livestock sources, and both the human and environmental communities could be the source of the *Pseudomonadales* that drove the separation of fabrication and processing spaces, though as the employees

This resource was prepared by the author(s) using Federal funds provided by the U.S. Department of Justice. Opinions or points of view expressed are those of the author(s) and do not necessarily reflect the official position or policies of the U.S. Department of Justice.

change shoes and wear protective clothing it is unlikely that outside soil was transferred in sufficient quantities to these spaces. Another study has also reported that the input materials were the primary source of microbes in a food processing facility [13]. The formation of distinct microbial communities within different functional spaces of the facility is clearly demonstrated by the results of these studies. However, the drivers of these associations are less obvious. It is likely that the initial microbial community is driven by the source, and then the environmental conditions, especially room temperature, selects for specific organisms.

Spatial Movement of Microbes Through the Facility

The physical layout of the GFIC facility impacts the distribution of microbes through the spaces. Guidelines for the construction of meat processing facilities recommend physical separation of product types to prevent cross-contamination. This is especially focused on separating cooked products (ready-to-eat) from raw products, but the concept could extend to all spaces in the facility. In the GFIC, each functional space is physically separated by wall, even within a functional category. For example, the dirty (hide on) versus clean (hide off) harvest areas are partially separated, with an open area connecting them to allows carcass passage. This structure provides an opportunity to demonstrate how physical barriers can impact the movement of microbes thorough the facility. The relative abundance of microbes that are biologically important to the industry or statistically important after compositional analysis were spatially plotted to track their movement through the facility (**Figure 2.3**). *Clostridiales*, which differentiated samples collected from livestock holding and harvest areas in principal components analysis, appear in high relative abundance early in the livestock holding space, then could be transferred into the harvest spaces. After the June 2019 sampling timepoint these spaces were consistently colonized by *Clostridiales*. This order appears in low relative abundance in other spaces, notably in some product holding and human only spaces, where it might be physically tracked from the live animal and harvest spaces. But the segregation of these live animal and harvest spaces from other locations limits the spread of this organism within the facility.

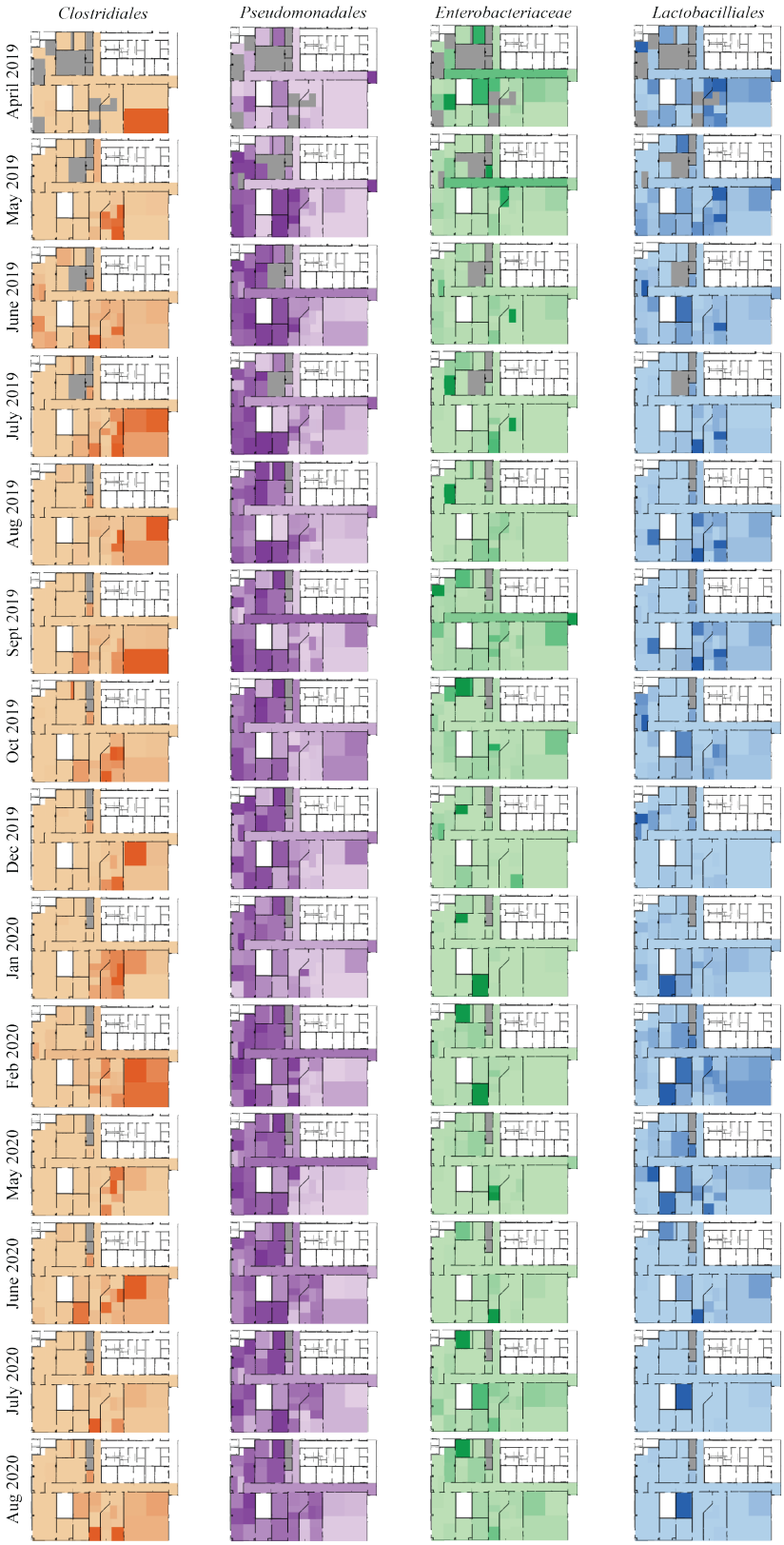

Figure 2.3. The spatial movement of microorganisms through drains in the meat processing facility. Darker colors represent a higher relative abundance of the given organism in the drain associated with that position in the facility.

Pseudomonadales, the group of organisms associated with aerobic food spoilage, is found in high relative abundance in fabrication and processing spaces. These organisms are found in these spaces without first being documented in the previous rooms (i.e. harvest, carcass coolers), which suggests that they may be brought into this space through human contact rather than following the processing pipeline. Alternatively, fabrication and processing spaces may select for *Pseudomonadales*. Moreover, after these organisms establish in the space they remain in high relative abundance for the rest of the experimental period. These organisms are found beyond these spaces, likely due to the ability to outcompete other organisms in spaces kept at colder temperatures and in spaces where the microbial biomass is lower due to infrequent inoculation events. Bokulich *et al.* reported similar findings in a study of the brewery environment, where the dominant microorganisms were clustered near the sites of introduction and were not frequently found in other areas [13].

The *Enterobacteriaceae* family contains many organisms generally associated with the gut, including many of the important pathogens identified in raw meats. These organisms appear sporadically throughout the facility, but do not tend to remain in high abundance in any given sample site across consecutive sampling timepoints. The most frequent site of these organisms was the cooked meats room, where raw products are placed before entering the smokehouses. Perhaps the longer dwell time in a given space, as opposed to the pace at which products move through processing, allows more of these organisms to transfer to the space. This is also a very small space relative to most others evaluated in this study, which could cause these organisms to be concentrated in a single sampling site. Also, this room tends to maintain higher temperatures due to the proximity with the smokehouses. Still, the *Enterobacteriaceae* do not appear to be in high relative abundance in the stable microbial community in the facility. This contradicts previous reports that indicate *Enterobacteriaceae* as a highly abundant organism in food processing environments, however these generally focus on direct contact surfaces, where these organisms may be transferred more frequently than drains [19]. *Enterobacteriaceae* are also used as indicators of good manufacturing practices in the industry, so the low relative abundance of these organisms in most production spaces indicated effective cleaning and sanitation within the facility

[21,22]. Similarly, the *Lactobacilliales* do not appear confined to a single processing space. Previous studies have reported that these organisms were among the most widespread in meat processing facilities [23], though they suggest that these organisms were introduced from ingredients that may not be consistent with those used in the GFIC facility. Indeed, another study of cold-tolerant organisms in meat processing facilities reported that *Lactobacilliales* were found in low abundance more consistent with the findings presented here [24]. Here, these organisms are likely introduced in the harvest spaces and may move from these into the carcass coolers. But they are not found in abundance consistently, which suggests that the physical separation in the facility is sufficient to prevent these organisms from becoming detectable? in processing and packaging spaces. This is beneficial, as these organisms are the primary spoiler of vacuum-packaged meats, so preventing cross-contamination into the final products can improve overall product quality. Overall, the microbes that make up the meat processing communities may be variable over time but tend to be restricted from moving into other spaces by physical and environmental barriers within the facility.

Conclusions

The objectives of this study were to identify, if present, the stable microbiome that persists in meat processing environments and to elucidate the factors that shape the formation of this microbial community. To address this, the microbial communities of drains and door handles in a meat processing facility were monitored for the first approximately 18 months of operation. From these observations it became clear that consistent microbial communities do form within approximately nine months of consistent facility use, but these communities can be disrupted with perturbations to the system. Moreover, the microbial communities assemble differentially based on the function of the room, a variable which serves as a proxy for room temperature, nutrient introduction, and potential sources of the microbes. The microbes are not likely to be found in environments other than those in which they are introduced, likely due to physical and environmental barriers in the spaces. This has major implications

for the meat processing industry, as it demonstrates the importance of rigorous sanitation and monitoring protocols and deliberate facility design.

Materials and Methods

The Global Food Innovation Center

The Global Food Innovation Center (GFIC) is a state-of-the-art-food processing and research center associated with the Department of Animal Sciences at Colorado State University (Fort Collins, Colorado). The facility is 36,000 square feet, with 20,000 square feet allocated directly to meat laboratory spaces. Spaces include live animal handling and overnighting holding facilities, harvest spaces, fabrication (the breakdown of carcasses to primals and cuts), processing rooms, smokehouses, ready-to-eat spaces separated from previous rooms by the pass-through smokehouses, and several carcass coolers and product holding rooms (see facility map in **Figure 2.4**). During normal production, live animals are introduced in the livestock holding space. Then, animals are harvested and converted to carcasses in the clean and dirty harvest rooms. The carcass chill cooler is used to rapidly reduce temperatures immediately after harvest, then the carcass holding cooler is used to store carcasses until fabrication. The carcasses are converted to saleable products in the fabrication and processing spaces. If a product is to be sold fresh, it is moved to the product cooler or freezer immediately after fabrication. If it is further processed, it is cooked in the smokehouses between cooked meats and the in-process cooler, then finished in the cooked meats packaging room before being stored in the product cooler or freezer.

Figure 2.4. The GFIC facility layout and experimental design. Rooms within the facility are categorized by the general function. The sampling sites are identified by their location within the facility by either circles (drains) or triangles (door handles). The general flow through the facility is indicated by arrows and icons representing the product held in the spaces.

Room temperatures are carefully managed to maintain the cold chain during production. Carcass and product coolers (carcass chill cooler, carcass holding, product cooler, in-process cooler) are kept below 4 °C, the product freezer is kept below -18 °C, and processing rooms (fabrication, processing, cooked meats packaging) are kept below 10 °C. Temperatures of other spaces are not precisely controlled as they do not contain products susceptible to spoilage or contamination. Construction of the facility began in December of 2017 and was completed in January of 2019. Production began in the facility on January 12, 2019. Production was paused from February to May 2020 as a consequence of covid-19 restrictions. Additionally, beginning in June of 2020 a commercial meat processing company began to operate in the GFIC facility due to loss of the company facilities, which increased and altered the production rates and personnel present in the facility during this period.

Experimental Design and Sample Collection

A nested longitudinal study design was used to capture the origins and changes in microbial communities in a newly constructed meat processing facility. Samples were collected from drains and door handles from production, storage, and human-only spaces in the GFIC facility approximately

This resource was prepared by the author(s) using Federal funds provided by the U.S. Department of Justice. Opinions or points of view expressed are those of the author(s) and do not necessarily reflect the official position or policies of the U.S. Department of Justice.

monthly. The first sampling event occurred immediately after the post-construction clean but before production began within the facility. This point was staggered as construction completed at different times for different spaces (January – April 2019). Following the final initial sampling event, samples throughout the facility were collected approximately monthly until August 2020, with a short cessation from February 2020 to May 2020 when the facility was closed due to COVID-19 regulations, as described above. The personnel performing the sample collection wore recommended personal protective equipment (disposable coats, disposable boot covers, hair nets, hard hats, gloves) and moved from "clean" (ready-to-eat, fabrication) to "dirty" (harvest, livestock holding) spaces in order to reduce the amount of contamination transferred through the facility and to follow facility regulations.

Sample were collected from drains and door handles throughout the GFIC facility (**Figure 4**). At each sampling point a sterile double headed SWUBE swab (BD; Franklin Lakes, NJ) was used to collect a sample for microbiome analysis. Drain samples were collected by swabbing both the top and bottom of the drain cover and the opening to the drainpipe. The facility contains several types of door handles that had to be swabbed differently; but, in general, the samples were collected by swabbing the part of the handle with human hand contact and the surface an employee would push to open the door. If a sampling point had two doors, the right-side door handle was chosen to be swabbed. The smokehouse doors had two handles, one to open the door and one to open a viewing window, and at the site, both of these handles were swabbed as one sample. After collection, swabs were immediately placed on ice, then frozen at -4 °C after completion of a sampling event to be stored until sequencing.

To identify potential sources of microbes found within the facility, samples were taken from employee skin, animals being introduced to the facility, and surrounding environment using a double headed SWUBE swab (BD, Franklin Lakes, NJ). Human skin samples were taken by providing the employee with a swab and instructing them to vigorously swab their dominant hand. Animal samples were collected at the time of harvest using the sterile SWUBE swabs. Skin or hide swabs were collected from the left shoulder of the animal immediately after sticking, fecal samples were collected from the rectum before bunging, a pre-wash carcass sample was collected from the left shoulder after evisceration

but before final trim, and the post-chill carcass sample was collected from the left shoulder after the carcass had undergone 24 hours of chilling. Environmental samples were collected from roads and sidewalks leading into the main facility doors.

DNA Extraction and Sequencing

Microbial communities were characterized using paired-end 16S rRNA gene sequencing. DNA was extracted from the sampling swabs using the Qiagen PowerSoil Kit (Qiagen; Hilden, Germany) following the manufacturer recommendations. In order to collect adequate DNA for sequencing from the door handle samples, DNA was extracted from both heads of the swab, while only one head was used for the drain samples. Extraction was conducted using 96-well plates, with 7 negative controls and one mock community positive control (Zymo; Irving, CA) per plate.

After extraction, DNA was amplified and sequenced following the Earth Microbiome Project Protocols using the 515f/806r primers (EMP; www.earthmicrobiome.org) [25]. PCR primers included error correcting Golay barcodes to allow for multiplexing. PCR products were quantified using the Picogreen Quant-iT (Invitrogen, Life Technologies; Grand Island, NY) and then pooled at equimolar concentrations for sequencing. Pools were sequenced using a 500-cycle kit on the Illumina miSeq sequencing platform (Illumina; San Diego, CA). Due to the high number of samples and the long time period across which samples were collected, samples were sequenced across four sequencing lanes, with samples randomized across plates so no one run contained samples from all sampling events, room, or sample type to prevent confounding by technical artifacts.

Microbial Community Analysis

After sequencing, data were demultiplexed and denoised with DADA2 using QIIME2 version 2020.8 software [26,27]. Taxonomy was classified using the SILVA 138 99% database with the QIIME2 feature-classifier plugin, which classifies the reads using a pre-trained machine learning classifier [28,29].

The taxonomy was used to filter out reads that were classified as chloroplast and mitochondria as these sequences were not considered part of the true microbiome. Additional filtering steps were used to remove sequences that appeared in less than 10% of samples.

To conduct phylogenetic diversity analyses, a phylogenetic insertion tree was constructed using the SEPP program with the SILVA 128 tree as a backbone [30]. Then, data were rarefied to 9,204 and a phylogenetic diversity analysis was conducted using the core metrics pipeline in QIIME2 [26]. Alpha diversity statistical comparisons were made using a Kruskal-Wallis test with a Benjamini-Hockberg multiple testing correction [31]. Beta diversity was analyzed using a generalized Unifrac test with a weight of 50% and statistical comparisons were made using a PERMANOVA test with multiple testing correction [32]. Additionally, community differences were visualized using the DEICODE pipeline to generate a Robust Aitchison Principal Components Analysis [33]. Changes in community diversity over time were analyzed using the QIIME2 longitudinal plugin [34]. The first distances method with the generalized Unifrac metric was used to calculate the differences in beta diversity between each sampling event to demonstrate the movement of a microbial community within a single drain towards a stable community over time. This calculation was visualized using a volatility plot with changes summarized across room function and evaluated statistically using a linear mixed effects model, with the first distance as the dependent variable, room function and time as fixed effects, and drain id as a random effect. A negative slope was used to indicate a trend towards stability in the community.

Taxonomy changes across time and space in the facility were also evaluated. Organisms that changed significantly within a room function group over time were identified using an Analysis of Composition of Microbiomes analysis [35]. Organisms with a large, statistically significant change from this analysis and biological significance based on prior knowledge of food processing microbiota were further investigated using a spatial relative abundance map generated with the SitePainter tool [36]. Microbial sources were analyzed using SourceTracker2 software (github.com/biota/sourcetracker2). The analysis was conducted using the developer version of the software and following developer instructions. Samples taken from facility drains were used as the sinks and samples collected from livestock feces and

hides, employee hands, and soils outside the facility were used as sources. Throughout the study, all statistical analysis was conducted with an alpha of 0.05.

REFERENCES

1. Dai D, Prussin AJ, Marr LC, Vikesland PJ, Edwards MA, Pruden A. Factors shaping the human exposome in the built environment: opportunities for engineering control. Environ Sci Technol. 2017 Jul 18;51(14):7759–74.

2. Kembel SW, Jones E, Kline J, Northcutt D, Stenson J, Womack AM, Bohannan BJ, Brown GZ, Green JL. Architectural design influences the diversity and structure of the built environment microbiome. ISME J. 2012 Aug;6(8):1469–79.

3. Lax S, Smith DP, Hampton-Marcell J, Owens SM, Handley KM, Scott NM, Gibbons SM, Larsen P, Shogan BD, Weiss S, Metcalf JL, Ursell LK, Vázquez-Baeza Y, Van Treuren W, Hasan NA, Gibson MK, Colwell R, Dantas G, Knight R, Gilbert JA. Longitudinal analysis of microbial interaction between humans and the indoor environment. Science. 2014 Aug 29;345(6200):1048–52.

4. McCall L-I, Callewaert C, Zhu Q, Song SJ, Bouslimani A, Minich JJ, Ernst M, Ruiz-Calderon JF, Cavallin H, Pereira HS, Novoselac A, Hernandez J, Rios R, Branch OH, Blaser MJ, Paulino LC, Dorrestein PC, Knight R, Dominguez-Bello MG. Home chemical and microbial transitions across urbanization. Nat Microbiol. 2020 Jan;5(1):108–15.

5. Nygaard AB, Charnock C. Longitudinal development of the dust microbiome in a newly opened Norwegian kindergarten. Microbiome. 2018 Sep 15;6(1):159.

6. Ross AA, Neufeld JD. Microbial biogeography of a university campus. Microbiome. 2015 Dec 1;3(1):66.

7. Sharma A, Richardson M, Cralle L, Stamper CE, Maestre JP, Stearns-Yoder KA, Postolache TT, Bates KL, Kinney KA, Brenner LA, Lowry CA, Gilbert JA, Hoisington AJ. Longitudinal

homogenization of the microbiome between both occupants and the built environment in a cohort of United States Air Force Cadets. Microbiome. 2019 May 2;7(1):70.

8. Lax S, Sangwan N, Smith D, Larsen P, Handley KM, Richardson M, Guyton K, Krezalek M, Shogan BD, Defazio J, Flemming I, Shakhsheer B, Weber S, Landon E, Garcia-Houchins S, Siegel J, Alverdy J, Knight R, Stephens B, Gilbert JA. Bacterial colonization and succession in a newly opened hospital. Sci Transl Med. 2017 May 24;9(391).

9. Wood M, Gibbons SM, Lax S, Eshoo-Anton TW, Owens SM, Kennedy S, Gilbert JA, Hampton-Marcell JT. Athletic equipment microbiota are shaped by interactions with human skin. Microbiome. 2015 Jun 19;3(1):25.

10. Bräuer SL, Vuono D, Carmichael MJ, Pepe-Ranney C, Strom A, Rabinowitz E, Buckley DH, Zinder SH. Microbial sequencing analyses suggest the presence of a fecal veneer on indoor climbing wall holds. Curr Microbiol. 2014 Nov 1;69(5):681–9.

11. Food and Drug Administration. Current Good Manufacturing Practice, Hazard Analysis, and Risk-Based Preventative Controls for Human Food. Code of Federal Regulations.

12. Zwirzitz B, Wetzels SU, Dixon ED, Stessl B, Zaiser A, Rabanser I, Thalguter S, Pinior B, Roch F-F, Strachan C, Zanghellini J, Dzieciol M, Wagner M, Selberherr E. The sources and transmission routes of microbial populations throughout a meat processing facility. Npj Biofilms Microbiomes. 2020 Jul 10;6(1):1–12.

13. Bokulich NA, Bergsveinson J, Ziola B, Mills DA. Mapping microbial ecosystems and spoilage-gene flow in breweries highlights patterns of contamination and resistance. Kolter R, editor. eLife. 2015 Mar 10;4:e04634.

14. Bokulich NA, Mills DA. Facility-specific "ouse" microbiome drives microbial landscapes of artisan cheesemaking plants. Appl Environ Microbiol. 2013 Sep 1;79(17):5214–23.

15. Tan X, Chung T, Chen Y, Macarisin D, LaBorde L, Kovac J. The occurrence of Listeria monocytogenes is associated with built environment microbiota in three tree fruit processing facilities. Microbiome. 2019 Aug 21;7(1):115.

16. Fagerlund A, Møretrø T, Heir E, Briandet R, Langsrud S. Cleaning and Disinfection of Biofilms Composed of Listeria monocytogenes and Background Microbiota from Meat Processing Surfaces. Appl Environ Microbiol. 2017 Sep 1;83(17).

17. Zhao T, Doyle MP, Zhao P. Control of Listeria monocytogenes in a biofilm by competitive-exclusion microorganisms. Appl Environ Microbiol. 2004 Jul;70(7):3996–4003.

18. Gilbert JA, Stephens B. Microbiology of the built environment. Nat Rev Microbiol. 2018 Nov;16(11):661–70.

19. Møretrø T, Langsrud S. Residential bacteria on surfaces in the food industry and their implications for food safety and quality. Compr Rev Food Sci Food Saf. 2017;16(5):1022–41.

20. Richardson M, Gottel N, Gilbert JA, Lax S. Microbial similarity between students in a common dormitory environment reveals the forensic potential of individual microbial signatures. mBio. 2019 Aug 27;10(4).

21. Baylis C, Uyttendaele M, Joosten H, Davies A. The Enterobacteriaceae and their significance to the food industry. Enterobact Their Significance Food Ind. 2011;

22. van Schothorst M, Oosterom J. Enterobacteriaceae as indicators of good manufacturing practices in rendering plants. Antonie Van Leeuwenhoek. 1984;50(1):1–6.

23. Pothakos V, Stellato G, Ercolini D, Devlieghere F. Processing environment and ingredients are both sources of Leuconostoc gelidum, which emerges as a major spoiler in Ready-To-Eat meals. Appl Environ Microbiol. 2015 May 15;81(10):3529–41.

24. Hultman J, Rahkila R, Ali J, Rousu J, Björkroth KJ. Meat processing plant microbiome and contamination patterns of cold-tolerant bacteria causing food safety and spoilage risks in the manufacture of vacuum-packaged cooked sausages. Appl Environ Microbiol. 2015 Oct 15;81(20):7088–97.

25. Thompson LR, Sanders JG, McDonald D, Amir A, Ladau J, Locey KJ, Prill RJ, Tripathi A, Gibbons SM, Ackermann G, Navas-Molina JA, Janssen S, Kopylova E, Vázquez-Baeza Y, González A, Morton JT, Mirarab S, Zech Xu Z, Jiang L, Haroon MF, Kanbar J, Zhu Q, Jin Song S, Kosciolek T, Bokulich NA, Lefler J, Brislawn CJ, Humphrey G, Owens SM, Hampton-Marcell J, Berg-Lyons D, McKenzie V, Fierer N, Fuhrman JA, Clauset A, Stevens RL, Shade A, Pollard KS, Goodwin KD, Jansson JK, Gilbert JA, Knight R, Earth Microbiome Project Consortium. A communal catalogue reveals Earth's multiscale microbial diversity. Nature. 2017 Nov 23;551(7681):457–63.

26. Bolyen E, Rideout JR, Dillon MR, Bokulich NA, Abnet CC, Al-Ghalith GA, Alexander H, Alm EJ, Arumugam M, Asnicar F, Bai Y, Bisanz JE, Bittinger K, Brejnrod A, Brislawn CJ, Brown CT, Callahan BJ, Caraballo-Rodríguez AM, Chase J, Cope EK, Da Silva R, Diener C, Dorrestein PC, Douglas GM, Durall DM, Duvallet C, Edwardson CF, Ernst M, Estaki M, Fouquier J, Gauglitz JM, Gibbons SM, Gibson DL, Gonzalez A, Gorlick K, Guo J, Hillmann B, Holmes S, Holste H, Huttenhower C, Huttley GA, Janssen S, Jarmusch AK, Jiang L, Kaehler BD, Kang KB, Keefe CR, Keim P, Kelley ST, Knights D, Koester I, Kosciolek T, Kreps J, Langille MGI, Lee J, Ley R, Liu Y-X, Loftfield E, Lozupone C, Maher M, Marotz C, Martin BD, McDonald D, McIver LJ, Melnik AV, Metcalf JL, Morgan SC, Morton JT, Naimey AT, Navas-Molina JA, Nothias LF, Orchanian SB, Pearson T, Peoples SL, Petras D, Preuss ML, Pruesse E, Rasmussen LB, Rivers A, Robeson MS, Rosenthal P, Segata N, Shaffer M, Shiffer A, Sinha R, Song SJ, Spear JR, Swafford AD, Thompson LR, Torres PJ, Trinh P, Tripathi A, Turnbaugh PJ, Ul-Hasan S, van der Hooft JJJ, Vargas F, Vázquez-Baeza Y, Vogtmann E, von Hippel M, Walters W, Wan Y, Wang M, Warren J, Weber

KC, Williamson CHD, Willis AD, Xu ZZ, Zaneveld JR, Zhang Y, Zhu Q, Knight R, Caporaso JG. Reproducible, interactive, scalable and extensible microbiome data science using QIIME 2. Nat Biotechnol. 2019 Aug;37(8):852–7.

27. Callahan BJ, McMurdie PJ, Rosen MJ, Han AW, Johnson AJA, Holmes SP. DADA2: High-resolution sample inference from Illumina amplicon data. Nat Methods. 2016 Jul;13(7):581–3.

28. Quast C, Pruesse E, Yilmaz P, Gerken J, Schweer T, Yarza P, Peplies J, Glöckner FO. The SILVA ribosomal RNA gene database project: improved data processing and web-based tools. Nucleic Acids Res. 2013 Jan;41(Database issue):D590–6.

29. Pedregosa F, Varoquaux G, Gramfort A, Michel V, Thirion B, Grisel O, Blondel M, Prettenhofer P, Weiss R, Dubourg V, Vanderplas J, Passos A, Cournapeau D, Brucher M, Perrot M, Duchesnay É. Scikit-learn: Machine Learning in Python. J Mach Learn Res. 2011;12(85):2825–30.

30. Janssen S, McDonald D, Gonzalez A, Navas-Molina JA, Jiang L, Xu ZZ, Winker K, Kado DM, Orwoll E, Manary M, Mirarab S, Knight R. Phylogenetic placement of exact amplicon sequences improves associations with clinical information. mSystems. 2018 Jun 26;3(3).

31. Kruskal WH, Wallis WA. Use of ranks in one-criterion variance analysis. J Am Stat Assoc. 1952;47(260):583–621.

32. Anderson MJ. A new method for non-parametric multivariate analysis of variance. Austral Ecol. 2001;26(1):32–46.

33. Martino C, Morton JT, Marotz CA, Thompson LR, Tripathi A, Knight R, Zengler K. A novel sparse compositional technique reveals microbial perturbations. mSystems. 2019 Feb;4(1).

34. Bokulich NA, Dillon MR, Zhang Y, Rideout JR, Bolyen E, Li H, Albert PS, Caporaso JG. q2-longitudinal: longitudinal and paired-sample analyses of microbiome data. mSystems. 2018 Dec 26;3(6).

35. Mandal S, Van Treuren W, White RA, Eggesbø M, Knight R, Peddada SD. Analysis of composition of microbiomes: a novel method for studying microbial composition. Microb Ecol Health Dis. 2015;26(1):27663.

36. Gonzalez A, Stombaugh J, Lauber CL, Fierer N, Knight R. SitePainter: a tool for exploring biogeographical patterns. Bioinformatics. 2012 Feb 1;28(3):436–8.

AIR VERSUS WATER CHILLING OF CHICKEN: A PILOT STUDY OF QUALITY, SHELF-LIFE, MICROBIAL ECOLOGY, AND ECONOMICS[1]

Summary

The United States' large-scale poultry meat industry is energy and water intensive, and opportunities may exist to improve sustainability during the broiler chilling process. By USDA regulation, after harvest the internal temperature of the chicken must be reduced to 40 °F or less within 16 hours to inhibit bacterial growth that would otherwise compromise the safety of the product. This step is accomplished most commonly by water immersion chilling in the United States, while air chilling methods dominate other global markets. A comprehensive understanding of the differences between these chilling methods is lacking. Therefore, we assessed the meat quality, shelf-life, microbial ecology, and techno-economic impacts of chilling methods on chicken broilers in a university meat laboratory setting. We discovered that air-chilling methods resulted in superior chicken odor and shelf-life, especially prior to 14 days of dark storage. Moreover, we demonstrated that air chilling resulted in a more diverse microbiome that we hypothesize may delay the dominance of the spoilage organism *Pseudomonas*. Finally, a techno-economic analysis highlighted potential economic advantages to air chilling when compared to water-chilling in facility locations where water costs are a more significant factor than energy costs.

As the poultry industry works to become more sustainable and to reduce the volume of food waste it is critical to consider points in the processing system that can be altered to make the process more efficient. In this study, we demonstrate that the method used during chilling (air vs water chilling) influences the final product microbial community, quality, and physiochemistry. Notably, the use of air chilling appears to delay the bloom of *Pseudomonas* spp that are the primary spoilers in packaged meat products. By using air chilling to reduce carcass temperatures instead of water chilling producers may

[1] This work has been previously published: Belk AD, Duarte T, Quinn C, Coil DA, Belk KE, Eisen JA, Quinn JC, Martin JN, Yang X, Metcalf JL. 2021. Air versus water chilling of chicken: a pilot study of quality, shelf-life, microbial ecology, and economics. mSystems 6:e00912-20. https://doi.org/10.1128/mSystems.00912-20.

extend the time until spoilage of the products and, depending on costs of water in the area, may have economic and sustainability advantages. As a next step, a similar experiment should be done in an industrial setting to confirm these results generated in a small-scale university lab facility.

Introduction

Currently, the United States is the largest producer and second-largest exporter of poultry meat worldwide [1]. The poultry industry in the United States has seen a five-fold production increase in the last 40 years and currently produces more than 50 million pounds of live birds annually [2]. As a result of increased production, the poultry industry has also seen a tremendous rise in energy expenditures and water depletion [1]. As demands for poultry meat continue to rise [3], novel approaches for reducing the environmental impact of poultry production, while not sacrificing poultry quality, need to be considered.

Temperature control during production and processing is a critical point in ensuring the safety and quality of poultry products. Thus, it is common for broiler production systems to reduce the internal temperature of chicken meat from 40 °C to 4 °C within one to two hours following harvest. This step, though critical to maintaining the safety of the product, is time-consuming and requires significant investments in energy and water, depending on the chilling method utilized [4]. Water immersion chilling (WC) and air chilling (AC) are the two most common chilling methods globally. Water immersion chilling is the most widely used chilling method in the United States, while AC is predominant in Europe, Brazil and Canada [5,6]. During WC, eviscerated chicken carcasses are submerged in cold water that is often supplemented with antimicrobials intended to inhibit microbial growth. The application of these antimicrobials, combined with a continuous clean water system, results in notable reductions to the total bacterial population. However, cross-contamination, retained water on the carcass, consumer perception, water consumption, and wastewater management issues are a few challenges associated with WC [7–9]. As mentioned, AC is widely utilized across Europe, Brazil, and Canada involves the chilling of poultry carcasses by forced air in a cold room. Some studies have shown enhanced microbial quality and less exudative packaging in AC broilers when compared to WC systems [7,10]. However, these microbial

investigations were limited to culture-dependent techniques that focused on just a few microbes and investigations with more robust sampling methods are warranted.

The rapid reduction in carcass temperature during poultry processing provides a unique thermodynamic challenge that requires significant energy inputs. Although AC results in a carcass with a slightly reduced yield (due to evaporative water loss), it has been estimated to require almost 50 times less gross energy than water chilling systems, when entire energy expenditures are considered [11,12]. In that regard, although WC methods are the most commonly utilized in the U.S., the opportunity for significantly reducing water use and energy expenditures by converting to AC systems exists. However, before this transition can be made, it is imperative to assess how the conversion will affect the quality of the final product in addition to the economic viability of the production processing line.

To address meat quality, shelf-life, microbial, and techno-economic impacts of chilling methods, we conducted an experiment at the University of California, Davis (UC Davis) Meat Science Laboratory, in which chickens were either chilled via AC or WC. Novel to this experiment was the assessment of the impacts each chilling system had on the microbiome of poultry products, and how that may relate to the quality of products from each system. This experiment yielded results that enhance the current knowledge regarding not only the quality of broiler meat produced using either chilling method, but also the important techno-economics, which may guide industry investment or utilization in either system.

Results

Experimental Results

In this experiment, 256 chicken carcasses were subjected to either air chilling (AC) or water chilling (WC), then fabricated into either bone-in or boneless breasts before being placed under dark storage for either 7 or 14 days. At each step in the process, 10 carcasses or breasts per treatment were removed to collect physicochemical, microbial count, and microbiome data. These data were then further analyzed to determine the impact that the distinct processing methods had on the quality, shelf-life, and microbial ecology of chicken products.

The chilling method significantly impacted the carcass weight changes during the chilling process. On average, carcasses chilled using the WC system gained 5% of the pre-chilled weight, whereas carcasses chilled using the AC system lost 1.6% of the pre-chilled weight ($P < 0.05$; **Table S1**). This difference in weight change is similar to what has been reported in other studies [12]. There was no difference in pH between AC and WC chicken breasts ($P > 0.05$; data not presented).

Quality and shelf-life implications of chilling strategy

The shelf-life, or period until spoilage, was identified using the aerobic bacterial populations. Microbes were removed from the product surface using a rinseate, which was then serially diluted and plated on Petrifilm aerobic count plates (3M Microbiology, St. Paul, MN). Petrifilms were then incubated at 7°C and 35°C to obtain counts of psychrotrophic and mesophilic aerobic organisms, respectively. The WC chicken had fewer ($P < 0.05$) psychrotrophic bacteria, organisms capable of growing at low temperatures, (1.05 log Colony Forming Units/g; CFU/g) prior to fabrication than the AC chicken (2.12 log CFU/g). However, no difference in mesophilic bacteria, organisms that grow best at moderate temperatures, was observed between the two treatments for pre-fabrication samples (**Table S3.2**). On day 7, an approximately 1-log difference in psychrotrophic bacteria was observed between AC (5.56 log CFU/g) and WC (6.59 log CFU/g) breasts, regardless of fabrication type (**Table 3.1**). WC and AC boneless breasts had lower total microbial counts throughout storage and display than the bone-in samples. Regardless, by day 14 of storage, chicken breasts from both chilling methods (WC and AC) and fabrication types (bone-in and boneless) had mesophilic aerobic bacteria populations greater than 7 log CFU/g, a threshold commonly associated with the end of shelf-life [13].

Instrument assessments of color were taken using a portable spectrophotometer (MiniScan EZ; Hunter Association Laboratory Inc., Reston, VA). These results demonstrated that the International Commission on Illumination (CIE) a^* (redness) and b^* (yellowness) values were greater ($P < 0.05$) for AC breast than WC breasts throughout the display period, indicative of more desirable red and yellow tones within the muscle of AC breasts (**Figure 3.1A**). Similarly, panelist evaluations indicated the

boneless chicken breasts were more desirable than bone-in breasts during the 3-day display period following 7 days dark storage. Although there were notable differences in instrument color between chilling method, the difference was not observed in consumer preference. During the 3-day display following 14 days dark storage, panelists considered the color and odor of all samples unacceptable regardless of the chilling method or fabrication type (**Figure 3.1B**). Chilling method and fabrication type did not have an impact on texture selection ($P > 0.05$). Additionally, trained sensory panelists detected no differences in flavor or texture attributes between chilling methods ($P > 0.05$) (**Table S3.3**).

Table 3.1. Psychrotrophic bacterial counts for bone-in and boneless chicken breast cooled by either air chilling or water chilling at different time points

	Psychrotrophic bacterial count (log CFU/g)[b]			
	Bone-in		Boneless	
Time	Air chilled	Water chilled	Air chilled	Water chilled
Prefabrication	2.12 BY (0.15)	1.05 AX (0.15)	2.12 BY (0.16)	1.05 AX (0.16)
Postfabrication	1.90 BY (0.16)	1.81 BY (0.15)	0.61 AX (0.16)	0.68 AX (0.16)
7-day storage (day 7)	5.86 CX (0.15)	6.96 DY (0.16)	5.26 CX (0.16)	6.22 DY (0.16)
End of display (day 10)	7.00 DY (0.15)	6.92 DY (0.15)	6.44 DY (0.16)	6.42 DY (0.16)
14-day storage (day 14)	8.71 EY (0.15)	9.00 EY (0.15)	8.51 EY (0.16)	8.67 EY (0.16)
End of display (day 17)	9.11 EY (0.15)	9.41 EY (0.16)	8.63 EY (0.16)	9.24 EY (0.16)

As expected, lipid oxidation increased as the time after chilling progressed (**Figure 3.1C**). Lipid oxidation levels, as indicated by measurement of thiobarbituric acid reactive substances, were similar across chilling method and fabrication type on the initial day of processing, 7d of dark storage, 14 days of dark storage, and 7 days of dark storage with 3 days of retail display ($P > 0.05$), though there were differences when comparing sampling groups across these days. The greatest differences between treatments were seen on the samples collected after 14 days of dark storage with a 3-day retail display. Among samples from this time point, the boneless WC breasts had a higher degree of lipid oxidation when compared with the boneless AC breasts ($P < 0.05$).

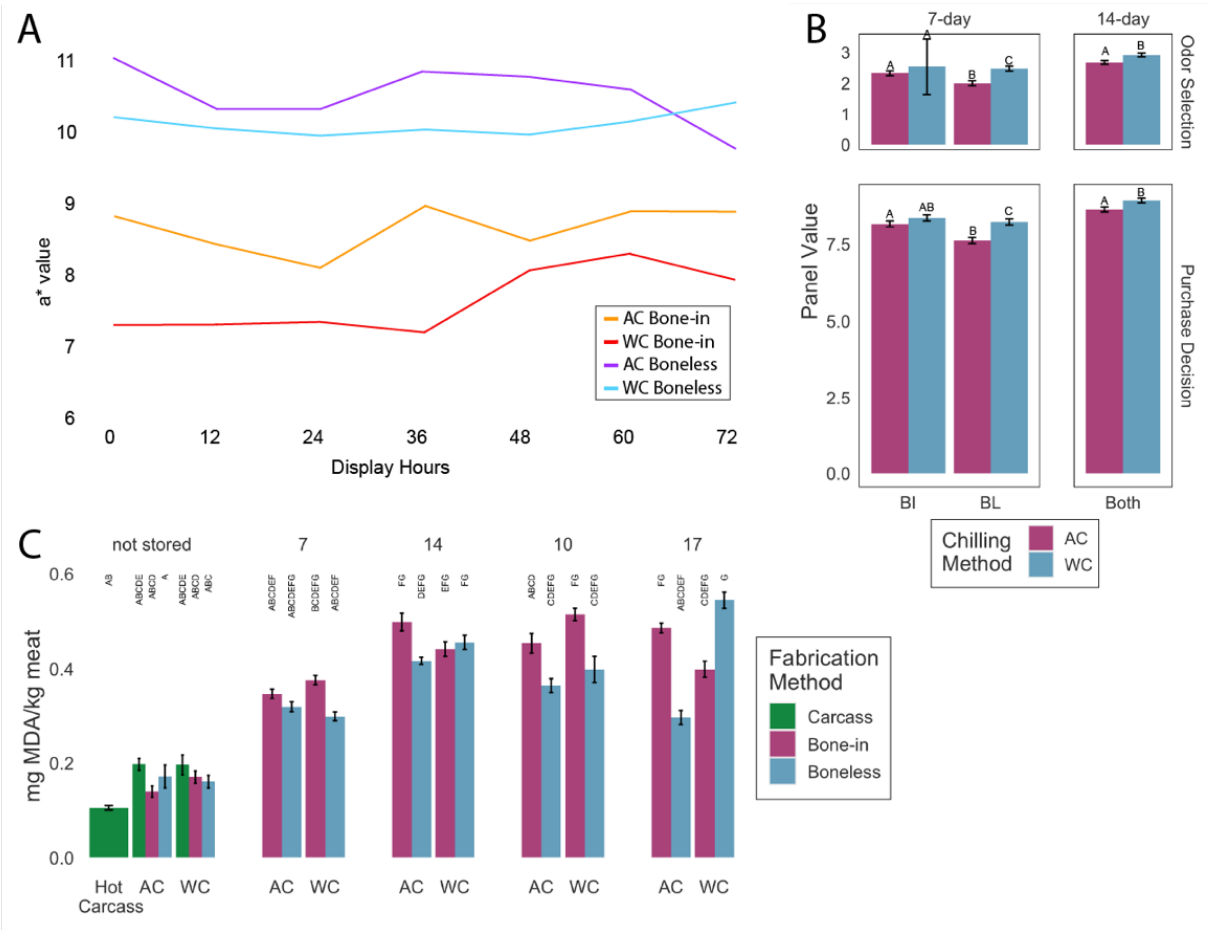

Figure 3.1. Changes in chicken quality over time. **A)** Least square means of *a** values for bone-in and boneless chicken breast chilled by either AC or WC following 7 days dark storage, during 3d retail display. CIE a* represents the favorable redness of breasts. Chilling methods are represented by AC; air chilling and WC; water-chilling. Fabrication methods are denoted as BI; bone-in and BL; boneless. **B)** Least square means of consumer odor and purchase decision selection after dark storage and 3-day retail display. Breasts were placed in dark storage for either 7 or 14 days, then immediately placed in retail display. After 7 days dark storage an interactive effect was observed for both odor selection ($P = 0.0132$) and purchase decision ($P = 0.0017$). After 14 days only the main effect of chilling methods was detected ($P < 0.001$). A hedonic 3-point scale was used for the consumer odor selection (1 = Desirable, 2 = Acceptable, 3 = Unacceptable) and purchase decision (7 = will buy, 8 = will buy with discount, 9 = will not buy). Bars in the same box with the same letter were not significantly different ($P > 0.05$). **C)** The average lipid oxidation levels within a treatment group as measured by thiobarbituric acid reactive substances (TBARS) assay. Bars along the x-axis refer to the chilling method and different colors represent the fabrication methods. As only chicken breasts were placed under dark storage, there were only carcass samples on the initial day of sample collection (not stored). Bars with the same letter were not statistically different ($P > 0.05$)

Nutritional content was very similar between chicken breasts regardless of chilling method (**Table S3.4**). Dry matter measurements ranged from 26.7% to 28.3%, with an overall mean of 26.13%. Within this narrow range, the only difference between treatment groups was between bone-in and

This resource was prepared by the author(s) using Federal funds provided by the U.S. Department of Justice. Opinions or points of view expressed are those of the author(s) and do not necessarily reflect the official position or policies of the U.S. Department of Justice.

boneless breasts collected on the initial day of experimentation. Chilling method, dark storage, and retail display did not impact dry matter content of the chicken breasts ($P > 0.05$). The same pattern was detected in moisture, as moisture and dry matter are inversely related. Measurements of ash and crude protein revealed a few differences between treatment groups, but these did not reveal significant patterns (**Table S3.4**). Crude fat values were, overall, low for all chicken products, ranging from 0.35% to 1.43% with a mean of 0.86%. Differences in these values were detected between fabrication types within a chilling method and sampling day ($P < 0.05$); carcass samples and bone-in breasts had higher crude fat content within almost all chilling methods and sampling days ($P < 0.05$; **Table S3.4**). However, no differences were observed between WC and AC ($P > 0.05$). Following this trend, the relative abundance of fatty acids was not grossly different between chilling methods on any sampling day. However, among fatty acids with less than 10% relative abundance, linoleate methyl ester (C18 and C18:9c12c) were more abundant in WC than AC breasts after 7 days dark storage with 3 days retail display (**Figure S3.1**).

Microbial ecology of chilled, fabricated, and packaged chicken

The microbial ecology of the chicken products was investigated using 16S rRNA gene sequencing. Microbes were removed from the surface of the products using a sterile rinseate, from which DNA was extracted and sequenced following the Earth Microbiome Project protocols (www.earthmicrobiome.org/protocols-and-standards/16s/). Sequencing a total of 286 samples and controls resulted in a total of 3,837,564 demultiplexed reads. After denoising, quality filtering, read joining, and chimera removal via the DADA2 pipeline, 3,262,269 sequence reads (ranging from 1-54,662 sequences per sample with a mean of 13,418 sequences) were assigned to 774 amplicon sequence variants (ASVs). Subsequently, we filtered out ASVs that were taxonomically identified as representing mitochondria and chloroplasts, resulting in 3,261,944 sequence reads and 752 ASVs. The commercial positive control sample (Zymo; Irvine, CA) resulted in the expected community of five microbes with no unexpected taxa, indicating no major contamination (**Figure S3.2)**. There were 24 negative/mock DNA extraction controls included in this sequencing run, which resulted in an average of 113 reads per negative

control (range 1 - 1,086) compared to 15,195 sequences per sample for DNA recovered from chicken rinsate (range 3 - 51,660). This was considered an acceptable level for quality control. Additionally, samples were rarefied at 6,152 sequences for diversity analysis, which was well above the highest negative control level. After rarefaction, all samples below this threshold were excluded from the diversity analysis, retaining 202 out of 259 rinsate samples. Before further analysis, negative and positive control samples were excluded from the experimental dataset.

The alpha (within sample) bacterial diversity of chicken products was reduced during chilling and processing (**Figure 3.2A**). The hot carcass microbiome contained the highest mean alpha diversity (Shannon's = 2.29, Faith's = 9.96, observed ASVs = 50.6). During the chilling process, the mean Shannon's diversity and observed ASVs were reduced, significantly ($P < 0.05$) in AC. After fabrication, or the cutting of the chicken carcasses into breasts, the alpha diversity increased, though not to the original levels. The high microbial diversity on chicken carcasses before product storage was associated with microbial communities dominated by organisms in the family *Enterobacteriaceae*. These communities also included bacteria at lower relative abundance from families *Clostridiaceae*, *Bacillaceae*, and *Pseudomonadaceae* (**Figure 3.2B**). There were no significant differences in diversity between pre-storage products (samples collected on the day of harvest that did not undergo a dark storage period) based on the chilling or fabrication methods.

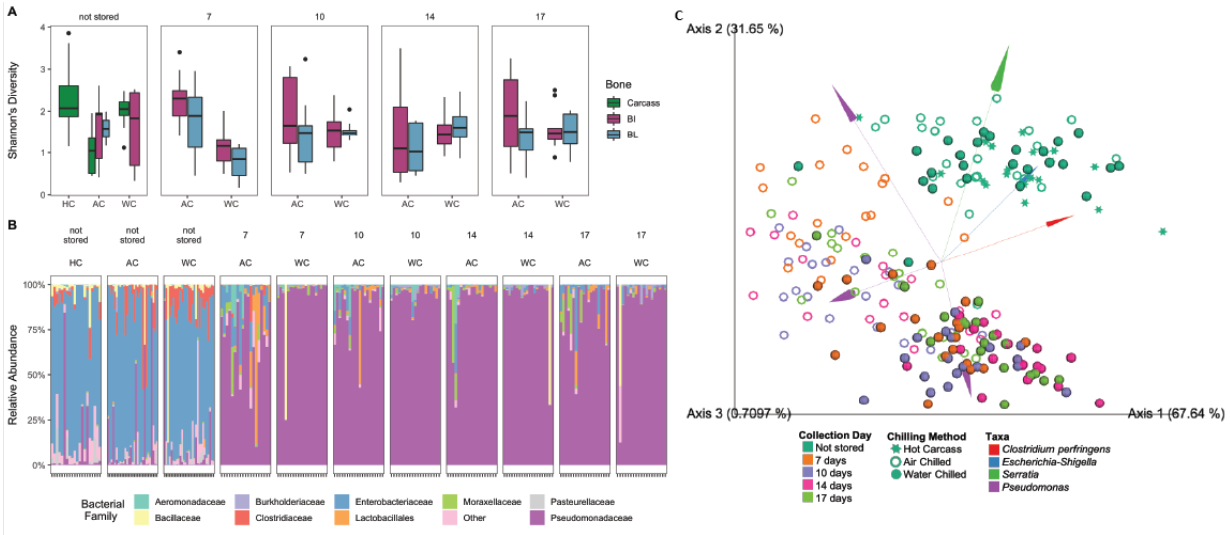

Figure 3.2. A) Shannon's diversity of the bacterial microbiome of chicken product samples, arranged by sampling day (7 and 14 days of storage plus 3 days retail display) and chilling method (Hot carcass, AC, WC) and colored by fabrication method (carcass, bone-in, boneless). The WC-boneless samples were too low biomass, resulting in few DNA sequences, and therefore the samples were excluded after rarefying. **B)** Taxonomy of the bacterial microbiome of chicken products based on analysis with the SILVA database, segmented by sampling day and chilling method. Within a facet, samples are organized as carcass, bone-in and boneless. **C)** A biplot constructed using Robust Aitchison PCA that demonstrates separation in beta diversity between samples. Points are colored by the day samples were collected, including samples collected before dark storage (not stored), after 7 and 14 days of dark storage, and after 3 additional d of retail display (10 day and 17 day). The shape represents the chilling method, including hot carcass (pre-chill), air chilled, and water chilled. The lines show ASVs that are important to the direction of the biplot and are colored by the taxon associated with the specific ASV.

During storage and display, the alpha diversity of samples remained similar between treatment groups while the beta diversity showed clusters separated by chilling method. The greatest difference was seen between AC and WC samples collected after removal from dark storage on day 7. At this time point, the diversity of the WC samples was lower ($P < 0.05$) than the diversity of AC bone-in samples and AC boneless samples. After the 7-day time point, mean diversities were similar (Shannon's = 1.06 - 1.87, Faith's = 1.58 - 3.02, observed ASVs = 10.00 - 19.30). During these post-storage and post-display sampling points, *Pseudomonas* bacteria became the dominant group. For the chicken that was stored for 7 days, followed by 3 days of retail display, communities from WC chicken became dominated by *Pseudomonas* before AC chicken. When the beta diversity was calculated and visualized using Robust Aitchison Principal Components Analysis, samples separate initially by sampling day - all products that were stored, regardless of storage or display time, separated from samples that were not stored (**Figure 3.2C**). Then, within the stored product, the samples clustered by chilling method. When the ASV vectors that explain these separations are overlayed and evaluated, it is clear that the main ASVs that separate the stored microbiome are *Pseudomonas*-associated (**Figure 3.2C**). Moreover, the separation between the chilling methods was primarily associated with distinct *Pseudomonas* ASVs. The patterns of changes in the microbial communities were predictive of spoilage and quality outcomes **(Figure S3.3**). Using a Random Forest Classifier, the microbiome could predict microbial spoilage, as defined by a psychrotrophic bacteria count of greater than 7 log CFU/mL, with an overall accuracy of 75%.

This resource was prepared by the author(s) using Federal funds provided by the U.S. Department of Justice. Opinions or points of view expressed are those of the author(s) and do not necessarily reflect the official position or policies of the U.S. Department of Justice.

Phylogeny, diversity, and spoilage potential of Pseudomonas

Pseudomonas ASVs (n = 33) come to dominate the microbial community during storage and display (**Figure 3.3**), and due to the importance of these ASVs we examined them in more detail. When placed into a phylogenetic tree containing 16S rRNA gene sequences from all *Pseudomonas* type strains, we reveal significant variation of branches associated with sequences from this genus. These ASVs are distributed throughout the phylogenetic tree and most likely represent multiple *Pseudomonas* species (**Figure S3.4**). We also calculated the average percentage of reads in each sample that belonged to a *Pseudomonas* ASV (**Table S3.5**).

In order to focus on particular ASVs, we performed an analysis of the composition of microbiomes (ANCOM) analysis at each sampling point (Days 0, 7, 14, 17) comparing the two chilling methods (pooling fabrication method). Prior to storage, none of the ASVs that were differentially abundant were ASVs assigned to *Pseudomonas*. At day 7, there was one *Pseudomonas* ASV which differed (ASV7: WC=.21%, AC=14.6%), At day 10 (7 days with 3-day retail display) there also one (ASV10: WC=16.45%, AC=1.8%), at Day 14 there were three (ASV7, ASV10, ASV20), and at day 17 (14 days with 3-day retail display) there were two (ASV7, ASV20).

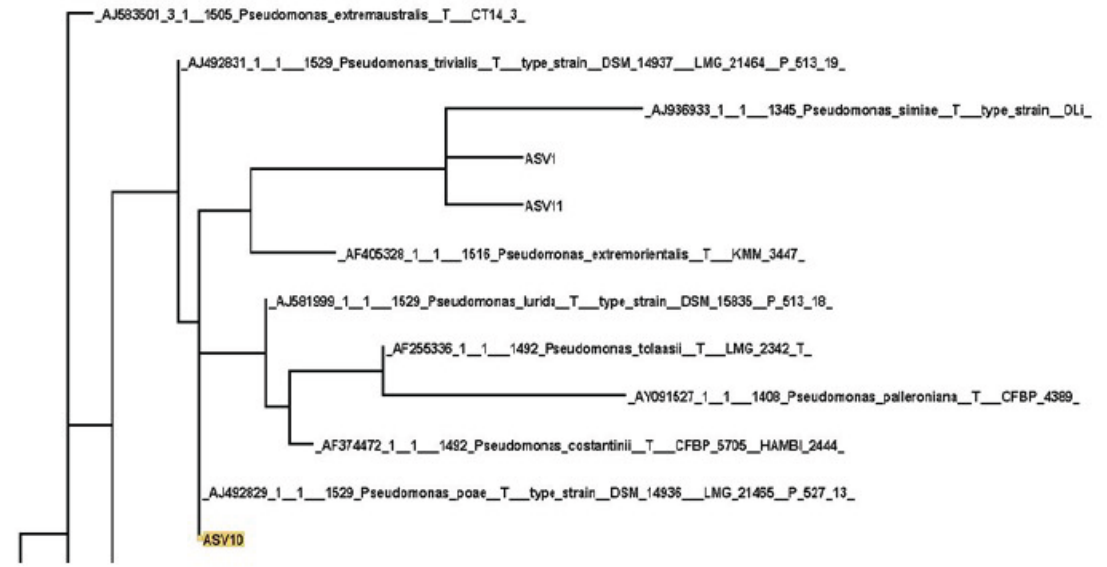

Figure 3.3. A portion of the detailed phylogenetic tree constructed from ASVs that assigned to *Pseudomonas*. The larger tree is included in the supplementary materials as Figure S2.

This resource was prepared by the author(s) using Federal funds provided by the U.S. Department of Justice. Opinions or points of view expressed are those of the author(s) and do not necessarily reflect the official position or policies of the U.S. Department of Justice.

Chilling system techno-economic analysis

Economic viability is a critical aspect of technology adoption. The levelized chilling cost ($/tonne) for the baseline AC and WC models are shown in **Figure 3.4** with the total cost subdivided by capital cost, operational cost, and income tax. The costs for AC and WC are relatively similar, $15.45 per tonne and $14.15 per tonne, respectively. The operational costs dominate the total chilling cost for both the AC and WC systems. While the AC system has a higher capital cost than the WC system, the AC operational costs are less than the WC system. The primary difference between the two systems are the costs associated with electricity and water. The WC systems can use up to 10x more water than the AC system, but the electrical costs of the AC system are only 2x that of the WC system. Sensitivity analyses (**Figure S5**) show there are scenarios where AC has the potential to be superior economically than WC, in particular for regions that might have lower electricity rates and high-water purchase and treatment costs.

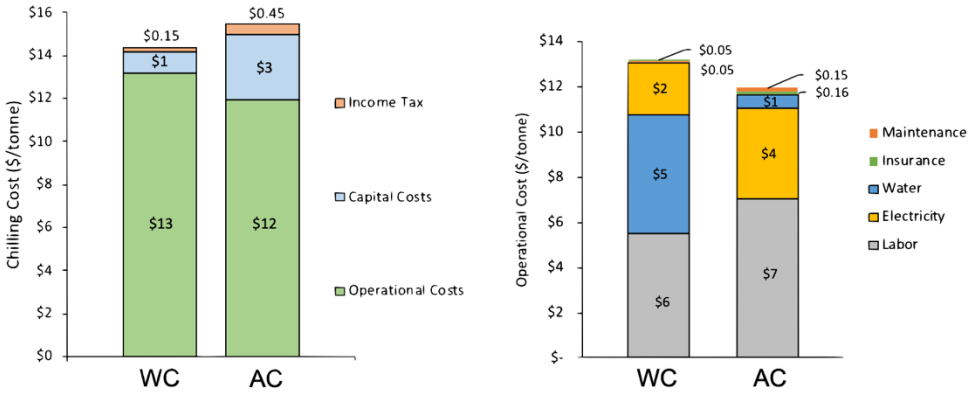

Figure 3.4. The levelized chilling cost ($/tonne) for the baseline AC and WC models is shown in the left panel. The contributions of the capital costs, operational costs, and income tax to the total levelized chilling cost are displayed and demonstrate how the operational costs dominate the total chilling cost in both systems. The operational costs include the labor, electrical, water, maintenance, and insurance costs and are shown in the right panel for both the AC and WC systems.

Discussion

This study demonstrates that the method of chilling poultry carcasses not only influences the shelf-life and quality of chicken breasts, but also has important implications for energy and water usage. Overall, in this study, chicken breasts from carcasses chilled using air-chilling (AC) methods had superior

This resource was prepared by the author(s) using Federal funds provided by the U.S. Department of Justice. Opinions or points of view expressed are those of the author(s) and do not necessarily reflect the official position or policies of the U.S. Department of Justice.

odor and shelf-life (as assessed by psychrotrophic bacterial counts, consumer color and odor panels, and lipid oxidation patterns). Moreover, the microbial communities associated with AC products maintained diversity post-chilling, and therefore may be more favorable by slowing the growth of spoilage organisms such as *Pseudomonas*. Finally, our techno-economic analysis highlighted potential economic advantages to AC when compared to water-chilling (WC) with advantages in areas of limited water and low-cost electricity.

Throughout dark storage and retail display, quality and shelf-life attributes were impacted by the chilling method. While all product was spoiled after 14 days of dark storage, notable quality and physical differences were observed among chicken treated with different chilling methods after 7 days of dark storage and 3 days of retail display. In this time period (7 days of dark storage to retail display), chicken chilled using AC demonstrated more desirable quality attributes, including more yellow tones based and a lower abundance of spoilage-associated fatty acids including linoleate methyl esters. These fatty acids have been associated with odor, color, and shelf-life challenges in previous studies [14–16]. Differences in color and consumer appeal were similar to those reported in Jeong *et al* [17], who demonstrated that, while WC may reduce temperature more quickly, the use of AC resulted in superior color and juiciness. The color difference could be due to evaporative moisture loss drying the surface of the chicken, allowing for the breast muscle under the skin to become more visible [9]. However, they differ from other studies that showed no difference in color between AC and WC breasts [18,19]. The spoilage patterns observed over time were similar to those previously reported by Katiyo *et al* [20]. Taken together, the color and fatty acid differences suggest that WC breasts may reach a spoilage state more rapidly than AC breasts. We did not detect a significant impact on texture, flavor attributes or nutritive composition by chicken chilling method. Previous studies have shown mixed impacts of chilling method on flavor and sensory attributes. For example, Hale *et al* [21] suggested a flavor advantage in AC chicken compared to WC chicken, although their products were fried. Conversely, Ristic [22] suggested that WC can lead to flavor and texture advantages. The lack of consistent impacts on sensory and nutritive variables, combined with

the similarities observed in our study suggest that consumer eating satisfaction and nutrient composition would not be influenced by chilling method selection.

Our results suggest that the physical properties of water versus air may result in distinct initial chicken carcass microbial ecologies. Immediately after chilling we found lower psychrotrophic plate counts in WC than AC carcasses, which suggests that WC is physically washing more cells from the carcass than AC. Previously, Chen *et al.* demonstrated that water chilling alone reduced total viable counts while air chilling did not, which further supports this hypothesis [23]. The difference in bacterial counts did not correspond to a difference in microbial diversity at this time point, similar to findings that demonstrated no difference in the presence of specific microorganisms between chilling methods [6,24]. These initial post-chilling microbial communities were dominated by the families *Enterobacteriaceae*, *Clostridiaceae*, and *Bacillaceae*, in agreement with findings by Handley *et al* [25]. There were more obvious differences in the microbial assemblage patterns following 7 days of dark storage. At this point, there was no difference in psychrotrophic counts between AC and WC, but AC had a lower mesophilic count. These results are similar to those reported by Tuncer and Sireli [26], who concluded that the AC was superior to WC in terms of pathogen growth, though they did not specifically investigate the spoilage bacteria described in the current study. Additionally, after the 7-day dark storage period the AC microbial community was much more diverse than the WC community, which was dominated by *Pseudomonadaceae*. We hypothesize that by removing more bacterial cells during chilling, there is less microbial competition, which in turn allowed *Pseudomonadaceae* to grow more quickly in WC products. Competitive advantages associated with *Pseudomonas* were also found in Katiyo *et al* [20]. Furthermore, we observed more inter-sample diversity in the AC group than the WC. It is likely that, due to the nature of water chilling, there is more opportunity for the microbiomes to become homogeneous, while in air chilling the carcasses were kept separate and therefore microbes were not shared between carcasses. It has been well-documented that water chilling can provide an opportunity for cross-contamination of pathogens, and these results suggest that this trend holds for all bacteria [27–30]. However, there is evidence that this effect can be reduced or eliminated with the addition of antimicrobial compounds to the

chill water, which was not done in this experiment [8]. We hypothesize that the microbial ecology associated with AC delays the Pseudomonas bloom associated with spoilage and may extend the shelf life.

The difference in microbial diversity of chicken breasts under different chilling methods was primarily due to different ASVs that assigned to *Pseudomonas*, further demonstrating that the population of *Pseudomonas* is likely a major driver of the microbial community structure and spoilage outcomes. Our phylogeny of *Pseudomonas* ASVs strongly suggests that the high number of *Pseudomonas* ASVs represents real biological variation. While *Pseudomonas* species, in general, are thought to cause food spoilage [31], they are not often identified to the species level. 16S rRNA sequencing was used in this study to estimate the microbes present in the products, which cannot always define microbial taxonomy at a species level. However, predictions of the *Pseudomonas* species present in chicken products were made by aligning ASV sequences to sequences extracted from the Ribosomal Database Project and maximum likelihood backbones generated using RAxML. These analyses suggest a variety of distinct *Pseudomonas* sequences are present in the chicken carcass microbiome. *P. lundensis* and *P. fragi* are known to cause food spoilage in both dairy and meat [32–34] and were found in a clade with two of our ASVs (ASV24, ASV27), but these ASV were seen at similar abundance in both WC and AC samples (data not shown). Two other species of *Pseudomonas* known to be involved in spoilage, *P. fluorescens* and *P. putida* [32,34], were not found in clades with any of the ASVs in this study. Furthermore, ASV7 (higher abundance in AC at d 7, 14, and 17), ASV21 (no difference), and ASV29 (no difference) were found in a clade with *P. argentinensis, P. straminea, and P. punonensis* which to our knowledge have not been previously shown to be involved in food spoilage. ASV10 (higher abundance in WC at d 10 and 14), ASV1 (no difference), and ASV11 (no difference) were found in a clade containing *P. lurida, P. poae, P. trivialis, P. palleronia, P. tolaasii, P. costantinii, P. extremorientalis*, and *P. simiae.* ASV20 (higher abundance in WC at d 14 and 17) and ASV14 (no difference) were found in a clade with *P. veronii*. While none of these latter Pseudomonas species has been directly shown to be involved in food spoilage, we hypothesize based on these data that at least some of them likely play a role in chicken spoilage.

Although our research suggests that AC may have shelf-life and quality advantages over WC, techno-economics are more nuanced. The WC systems can use up to 10 times more water than the AC system, but the electrical costs of the AC system are two times that of the WC system. Our baseline models do not support the claims by two other studies that AC systems require almost 50 times less gross energy than WC systems, when entire energy expenditures are considered [11,12]. Rather, our results agree with the conclusions of Northcutt *et al.*, specifically, that WC and AC systems have similar total chilling costs [35]. However, Northcutt *et al.* also claimed that the large water requirements, which have been steadily increasing in the United States as a result of USDA regulations, can start to tip the balance for AC over WC systems especially if one considers the potential for changes in water purchase and treatment costs. Therefore, AC may have an economic advantage over WC depending on the local price and availability of water resources.

This experiment was designed to be a laboratory-based, pilot-sized representation of the larger process of chicken chilling, fabrication, storage, and retail display. We made efforts to represent industry conditions as accurately as possible in a small laboratory setting, however there were a few conditions we were unable to replicate. We were unable to reproduce an antimicrobial application, either in the WC chill water or sprayed on the AC carcasses, which could modify some of the microbiological results. Therefore, our experiment represents a worse-case scenario. Moreover, all chicken carcasses used in this experiment were obtained from the same production lot in order to start all chilling processes at the same time. This may have led to a more homogenous outcome than a more randomized selection. Future experiments should confirm the current findings using real industry conditions.

Conclusion

The overarching goal of this study was to combine multi-disciplinary approaches to determine the impact of chilling method on the overall system efficiency and sustainability of chicken production. We were able to conclude that AC methods had an advantage in quality, spoilage, and consumer appeal prior to 14 days of dark storage, that AC appeared to result in a more favorable, diverse microbial community,

and that AC requires less gross energy and, depending on the local price of water, may be the more economically favorable system.

Materials and Methods

Experimental design

The experiment was conducted using a 2 x 2 x 2 factorial design to evaluate three factors: chilling method (air chilling; AC vs. water immersion chilling; WC), fabrication method (bone-in vs boneless) and dark storage period (7 days vs. 14 days). Eviscerated, hot chicken carcasses (n = 256) were obtained from a commercial processing facility in California and transported to the USDA-inspected Meat Science Laboratory at the University of California, Davis (UCD; Davis, CA) within two hours of harvest. Carcasses were transported in sterile 150-quart coolers (MaxCold Cooler; Igloo Products Corp., Katy, Texas) at a mean temperature of 30.25 °C. Upon arrival at UCD, carcasses were divided into sampling groups following the scheme in **Figure 1**. Sixteen carcasses were identified for a taste panel and placed four each in the treatment groups that were placed under 7-day dark storage (AC-bone-in, AC-boneless, WC-bone-in, WC-boneless). Of the other carcasses, 20 were sampled immediately for hot carcass samples and the remainder were randomly and evenly assigned into either AC or WC (n = 110 birds/chilling method). Following chilling (described below), 10 carcasses from each AC and WC treatment group were sampled, and the remaining were evenly assigned to fabrication pathways (n = 50 birds/fabrication) yielding either bone-in or boneless chicken breasts (n = 20 breasts/fabrication pathway). Immediately following fabrication, 10 chicken breasts from each group were sampled, and the remaining breasts were placed on expanded polystyrene trays and overwrapped with polyvinyl chloride film (40-gauge, Berry AEP1504310). Overwrapped trays were placed in rigid cardboard boxes (n = 8 trays/box) and stored at 4 °C (3-6°C) for either 7 or 14 days, a timeframe which reflects industry standards. At each storage interval (7 or 14 days), individual packages of chicken breasts (bone-in and boneless) were removed from dark storage. Ten breasts from each group were sampled immediately after removal from

storage, and the remaining packaged breasts were placed in a retail display case (Barker, Keosauqua, IA, average light intensity 1061 LUX) maintained at 4°C (3-6°C) for 3 days.

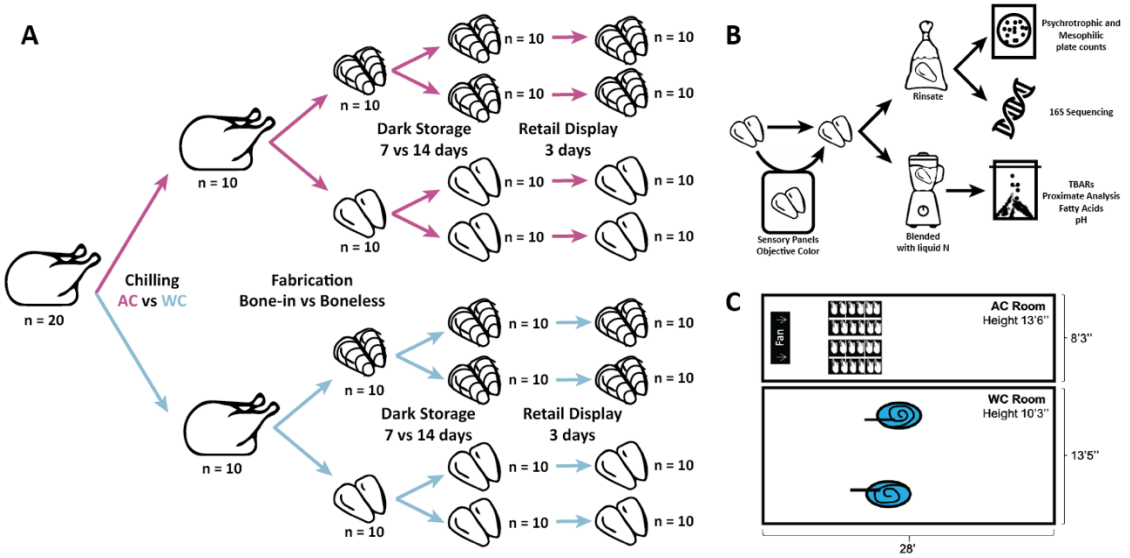

Figure 5. Representation of the experimental design. **A)** The processing scheme with time points for sampling during the experiment. **B)** The sampling process after the chicken product had been collected. The product was either sampled immediately or used for sensory panels. Microbial samples were taken via rinsate, which was then used for microbiological and microbiome analysis. The product was then flash-frozen in liquid nitrogen and powdered, then used for physicochemical analyses including pH, thiobarbituric acid assay (TBARs), proximate analysis, and fatty acid profiling. **C)** Representation of the two rooms used for carcass chilling.

Chicken processing

Procurement of Chicken Carcasses. A commercial chicken processing facility in California was utilized to procure hot chicken carcasses for this research. Live birds were subjected to standard poultry harvest protocols as implemented by the commercial processing facility. Carcasses used for this experiment were obtained following defeathering, evisceration, and application of an initial post-harvest antimicrobial carcass spray. Prior to chilling, the carcasses (n = 256) were removed from the processing line, placed in sterile plastic bags (n = 30-32 carcasses/bag), and bags placed in sealed sterile coolers for transportation to the Meat Science Laboratory at UC-Davis (Davis, CA). Additionally, temperature

This resource was prepared by the author(s) using Federal funds provided by the U.S. Department of Justice. Opinions or points of view expressed are those of the author(s) and do not necessarily reflect the official position or policies of the U.S. Department of Justice.

recorders (LogTag Tred30-16r; LogTag, Auckland, NZ) were placed in the coolers to monitor temperature during transportation.

Processing and Chilling of Chicken Carcasses. It should be noted that this process, while designed to mimic industrial systems, was performed on a much smaller scale. Upon arrival at the UC Davis Meat Science Laboratory, 20 chicken carcasses were randomly selected for initial evaluations (described below), while the remaining carcasses were randomly and evenly assigned to one of two chilling methods (AC or WC; **Fig. 5A l**). Weights (g) of individual carcasses were obtained prior to chilling for comparison with weights obtained following chilling (described below). Sixteen carcasses were reserved for taste evaluation (described below) after seven days of storage and three days of retail display. This subset of carcasses was subjected to both chilling methods and fabrication methods (described below), leaving 240 carcasses for laboratory analyses. Carcasses designated for WC were submerged in one of two simulated water chill tanks (**Fig. 5C**). Simulated water chill tanks were constructed from commercial water tanks (Structural Form Stock Tanks, 150 gal, Rubbermaid), and a slurry of water and ice was formulated using potable water and commercial ice. Water temperature was monitored throughout chilling and birds were agitated while submerged using a paddle. Carcass temperature was monitored regularly using a thermometer (Multitrip Data Logger, Temprecord, New Zealand) probe inserted into the thickest portion of the chicken breast. When the average internal carcass temperature reached 4 °C, the chicken carcasses were removed from the water chilling system and placed on sterile wire racks for 10 minutes. Post-chilling weight and temperature were obtained after the 10-minute holding period. Additionally, five carcasses were randomly selected for analyses (described below).

To simulate air chilling, an isolated cold room in the UC-Davis Meat Science Laboratory was outfitted with a high-velocity fan (Model # BF60BDORGPRO, Maxx Air; 60’ fan with 19000 CFM, providing an airflow of 1.23 m/s.) as shown in **Figure 3.5C**. Chicken carcasses were placed on sterile wire racks located approximately six m from the commercial fan. The wire racks were rotated throughout the chilling process to assure equitable exposure to the chilling conditions. Carcass temperature was

monitored throughout by inserting a thermometer probe into the thickest portion of the breast, and once the average internal temperature reached 4 °C, the carcasses were removed from the AC room. A post-chilling weight and internal temperature were obtained from individual carcasses. Additionally, 10 carcasses from each method were randomly selected for analyses (described below).

Fabrication of Chicken Carcasses, Packaging of Chicken Breasts, and Dark Storage. Immediately following chilling, carcasses within each chilling method (AC and WC) were randomly and evenly assigned to one of two fabrication methods (n = 50/ fabrication method) for the generation of bone-in and boneless chicken breasts. Carcasses were fabricated, meaning cut from carcasses into individual parts, by trained personnel in the UC Davis Meat Science Laboratory using sterile instruments and WC and AC carcasses were fabricated separately. Bone-in chicken breasts contained the ribs and part of the spine, while boneless breasts had these bones further removed. Immediately following fabrication, 10 chicken breasts from each group were sampled, and the remaining breasts were placed on expanded polystyrene trays and overwrapped with polyvinyl chloride film (40-gauge, Berry AEP1504310). Overwrapped trays were placed in rigid cardboard boxes (n = 4 trays/box) and stored at 4 °C (3-6 °C) for either 7 or 14 days.

Retail display. At each storage interval (7 or 14 days), individual packages of chicken breasts (bone-in and boneless) were removed from dark storage. Ten breasts from each group were sampled immediately after removal from storage, and the remaining packaged breasts were placed in a retail display case (Barker, Keosauqua, IA, average light intensity 1061 LUX) maintained at 4 °C (3 °C - 6 °C). Packages remained in the retail display case for three days. Instrumental meat color, measured via evaluating the lean color of the boneless samples and skin color of the bone-in samples, was taken using a portable spectrophotometer (MiniScan EZ; Hunter Association Laboratory Inc., Reston, VA) that was standardized before each use. A total of three readings of the International Commission on Illumination (CIE) L* (lightness), a* (redness) and b* (yellowness) values were taken using an illuminant A/10° observer for each breast. Measurements were taken through the packaging material at three separate

locations on the chicken breast and were averaged prior to analyses. Packages were rotated in the display case every 12 h to assure equitable temperature and light exposure.

Microbial sample collection/processing

At each sampling point, the microbial communities of the chicken products were collected using a rinsate method. At pre-fabrication timepoints, the entire chicken carcass was placed in a sterile collection bag (Whirl-Pak; Nasco, Fort Atkinson, WI) with 200 ml of phosphate-buffered saline (PBS; National Diagnostics, Atlanta, GA) and agitated for 60 seconds to dislodge surface bacteria. After this, the carcass was removed from the rinsate and saved for physicochemical analysis. At the post-fabrication timepoints, each chicken breast was divided in half. One half was placed in a sterile collection bag (Whirl-Pak; Nasco, Fort Atkinson, WI) with 50 mL of PBS and agitated for 60 seconds. The second half was reserved for physicochemical analysis. At all timepoints, the rinsate was collected from the sampling bag into 50 mL falcon tubes (Corning Science, Mexico) for analysis. A 10 mL aliquot of each sample was separated to be used for aerobic bacteria population analysis and the remainder was frozen to -80 °C and transported to Colorado State University (Fort Collins, CO) PI Metcalf Laboratory for microbial ecology analysis.

The rinsate sample collected for microbiome analysis was further divided into 30 mL aliquot before DNA extraction. Cells within the rinsate were concentrated into a pellet by centrifugation at 4,600 g for 15 minutes in a swing bucket rotor (Sorvall Legend X1R; Thermo Scientific, Waltham, MA)). The supernatant was poured off and a portion of the pellet equivalent to approximately 600 uL was used for analysis. DNA was extracted from the pellet following standard protocols utilizing the Qiagen PowerSoil DNA 96 well extraction kit (Qiagen, Hilden, Germany) following manufacturers protocol for low biomass samples, which included the additional step of allowing the EB solution to be heated to 65°C before adding to the DNA plate wells for five minutes before eluting. DNA was eluted in two steps. Initially, 60 µL was eluted and considered our more concentrated DNA extraction. Next, an additional 80 µL of DNA was eluted. Each 96-well plate included 8 mock extractions (no sample added) and 1 positive

control (ZymoBIOMICS D6300). The 16S rRNA gene (V4 region) was amplified using primers 515F and 806R universal primers with the forward primer barcoded to allow for multiplexing during sequencing, following the Earth Microbiome Project protocols (www.earthmicrobiome.org/protocols-and-standards/16s/). The forward primer 515F included the unique sample barcode following Parada *et al.* [36], and both primers included degeneracies as described in Parada *et al*. and Apprill *et al*. [36,37]. Two PCR reactions using Invitrogen Platinum Hot Start PCR 2x Mastermix (Invitrogen, Carlsbad, CA) with 1 µL of DNA and a final concentration of 0.2 µM primer were run for each sample and combined to a total of 75µL. The PCR product was quantified using a Pico Assay read by a Fluorskan plate reader (ThermoFisher Scientific, Waltham MA) and then pooled into a single pool in equimolar concentrations with the exception of samples that did not meet a minimum concentration, in which case 25 µL were added (this allowed the inclusion of mock extraction controls in the sequencing run). The resulting pool was cleaned using a Minelute PCR purification kit (Qiagen) and sequenced with a Miseq reagent v2 500 cycle kit at the CSU Next Generation Sequencing Core on the Illumina Miseq platform.

After sequencing, microbiome data were analyzed using QIIME2 [38] and R software version 3.5.1. Sequences were demultiplexed and quality-filtered in QIIME2 using error-correcting Golay barcodes that prevent misassignment. Reads were trimmed to 250 bp, then amplicon sequence variants (ASVs) were inferred using DADA2 [39]. Taxonomy was then assigned using the QIIME2 feature-classifier plugin [40] against the SILVA-132 99% database [41]. Non-microbial sequences that assigned to mitochondria and chloroplasts were filtered from the dataset. Samples were rarefied to 6,152 sequences, retaining 38.10% of features in 71.63% of samples, and diversity metrics were calculated using the QIIME2 core metrics pipeline. Statistical comparisons for alpha diversity were made using the Kruskal-Wallis test with an alpha of 0.05 and statistical comparisons for beta diversity were made using PERMANOVA with multiple testing correction and an alpha level of 0.05. The composition of the microbiomes was compared by testing the differential abundance of taxa using the ANCOM plugin in QIIME2 [42]. The ability of microbial communities to predict quality and spoilage outcomes was assessed using the QIIME2 sample-classifier classify-samples plugin [43,44]. Models were trained and tested using *k*-fold cross-validation

and the Random Forest classifier with hyperparameter tuning. Visualizations were generated using QIIME2 and R software with ggplot2 [38,44]. 16S rRNA gene sequencing data is available in the EBI-ENA database, accession number PRJEB41700, and in QIITA, study 12193. Analysis details can be accessed at https://github.com/Metcalf-Lab/Air-versus-water-chilling-of-chicken.

Phylogenetic trees

All *Pseudomonas* ASV sequences were extracted from the feature table by filtering based on assigned taxonomy. An alignment of all type strain 16S rRNA gene sequences for this genus was downloaded from the Ribosomal Database Project [45], along with an appropriate outgroup. A maximum likelihood backbone tree was generated using RAxML 8.2.12 [46] using the GTRGAMMA substitution matrix and 100 rapid bootstraps on the RDP alignment. An information file was then generated to be used in SATé-Enabled Phylogenetic Placement (SEPP) which was modified to fit the parsing parameters from pplacer v1.1.alpha13-0-g1ec7786 (removed 1 line according to documentation on the SEPP website https://github.com/smirarab/sepp/issues/40) [47]. SEPP 4.3.10 was then run with the following parameters (-P=33 -A 10) to optimize the alignment breakdown using the ASVs file, the RAxML tree, the RAxML info file and the reference alignment as input.

Quality measurements

Aerobic Bacteria Populations. Aerobic bacterial populations are strong indicators of the end of shelf-life. Thus, quantifying the aerobic populations present--in addition to the characterization of the microbiome--will provide insight into the shelf-life impacts of the microbial population. At each sampling interval, the carcass of one sample from each chicken was rinsed using 200 ml PBS for the carcass and 50 ml for the breast. One milliliter of the rinsate was serially diluted in 0.1% buffered peptone water (BPW; Becton, Dickinson and Company, Sparks, MD) and plated in duplicate onto Petrifilm aerobic count plates (3M Microbiology, St. Paul, MN). Plates were then incubated at 7 °C for 10 days and 35 °C for 48 hours.

Physicochemical Analysis. Numerous biochemical and physicochemical changes that affect shelf-life occur in post-harvest meat products [48]. Thus, an assessment of these changes during processing was conducted to obtain information regarding product quality. At each sampling point, after the rinsate was collected, the sample was fabricated to a boneless breast if it was not already, though the skin was left on for carcass and bone-in samples. Then, the breast was flash-frozen in liquid nitrogen and homogenized using a blender (Magic Bullet; Capital Brands, Los Angeles, CA). To evaluate the carcass samples and bone-in breasts, the breast meat was removed from the bone at the time of sampling. The frozen homogenate was then transported to the Colorado State University Center for Meat Safety and Quality (Fort Collins, CO) for physicochemical and compositional analyses.

Fatty Acid Composition. Fatty acid composition was obtained using gas chromatography following methods described by Engle et al. and Kang and Wang [49,50]. First, fat was extracted using the Folch method [51]. One gram of the frozen homogenate was combined with 20 mL of 2:1 chloroform:methanol mixture and homogenized, then filtered using Whatman No. 1 filter paper (Fisher Scientific; Waltham, MA). Then, 4 mL of 0.9% NaCl solution was added per 20 mL chloroform:methanol and the solution was incubated at 4 °C overnight. During this time the solvent separated into two phases; the lower phase contained the lipid extract, which was separated and dried in a dry matter oven at 100 °C for 16 h. After this extraction, the lipid extract was methylated by adding 1 mL of 0.5 N KOH in MeOH and heated in a water bath. Samples were then prepared for gas chromatography by mixing with 2 mL HPLC-grade hexane and 2mL saturated NaCl, which was then back-extracted and reconstituted to concentrate the fatty acids. The reconstituted lipid was measured by gas chromatography (Agilent 6890 plus; Agilent, Wilmington, DE) with standard fatty acid methyl ester mixtures and SUPELCO FAME standard (Millipore Sigma, Darmstadt, Germany) to calibrate. Fatty acids were identified by matching relative peak retention times to those of the standards, calculated as normalized area percentages of fatty acids.

Lipid Oxidation. Lipid oxidation was measured using the thiobarbituric acid assay (TBARs), as described in Yin *et al*. [52]. Briefly, 5 g of the frozen homogenate was mixed with trichloroacetic acid,

homogenized using a standing homogenizer, and filtered using Whatman No.1 filter paper (Fisher Scientific; Waltham, MA). A 1mL aliquot of the filtrate was mixed with 1 mL of 10 mM thiobarbituric acid and incubated at 25 °C for 20 h, after which the absorbance at 532 nm was measured using a spectrophotometer (UV-2401, Shimadzu Inc., Columbia, MD).

Proximate Analysis. Nutrient composition analysis (proximate analysis) was conducted to determine the dry matter, moisture, ash, crude fat, and crude protein composition within each sample. Dry matter and moisture were measured using the AOAC oven drying method, 950.46 and 934.01[53]. Two grams of frozen homogenate were weighed and placed in a standard laboratory convection oven for 24 h at 60 °C, then re-weighed. Percent moisture was calculated using the formula: % moisture content = [[(wet weight - dry weight) / wet weight] * 100]. Percent dry matter was calculated as 100 - moisture content. Ash content was determined using the ash oven method as described in the AOAC 923.03 and 920.153 [54]. Approximately 1 g of the frozen homogenate was placed into a dry crucible, then inserted into a Thermolyne box furnace at 600 °C for 18 h. Percent ash was calculated using the formula: % ash = (ash weight / wet weight) * 100. Crude fat was measured using the Folch method, as described above. Finally, crude protein was measured following AOAC method 992.15 [55], which used a TrueSpec CN nitrogen determinator (LECO, St. Joseph, MI). Percent protein was calculated using the formula: % protein = total % N * 6.25. Results were represented on a dry matter basis. Statistical analyses on all physiochemical tests were conducted using ANOVA and the emmeans package [56] with a 2 x 2 x 2 factorial design with an alpha level was 0.05.

Sensory Analysis. Eight untrained participants were asked to evaluate the acceptability of three sensory attributes (color, odor, texture) during retail display using a three-point sensory scale described by Lytou *et al.* [57]. In addition, subjective color (desirable, acceptable, unacceptable) and willingness to purchase (would purchase, would not purchase, would purchase at a discounted price) was evaluated by these untrained panelists every 12 h during retail display. At the end of each three-day retail display period (10 day and 17 day) the same participants were then asked to evaluate subjective odor, texture and purchase selection using the same approach. Evaluation scores were analyzed as continuous data using

mixed procedures of SAS (version 9.4; SAS Inst. Inc., Cary, NC). Participants were treated as random variables and the alpha level was defined as 0.05.

In addition to evaluation of chicken breast color, odor, and texture, trained taste panelists were asked to evaluate various palatability attributes (chicken flavor intensity, off-flavor intensity, springiness, cohesiveness of mass, and moistness) of bone-in and boneless chicken breasts representing both chilling methods following 7 days of dark storage. Panelists consisted of graduate students from the CSU Center for Meat Safety and Quality and were trained to recognize the aforementioned attributes using methods and references described by Solo [58]. Samples for evaluation were randomized and panels were conducted over two days to avoid sensory fatigue. Chicken breasts were cooked to an internal temperature of 76 °C and cut into 2.54 x 2.54-cm cubes before being served to panelists under red lights. Panelists then ranked each breast portion for each of the above attributes on a 100-point scale. Data were analyzed using an ANOVA and the emmeans package in R [56] with an alpha level of 0.05.

Chilling system techno-economic analysis

An economic evaluation of each chilling system, AC and WC, was also performed. The work included the development of baseline models of each system that allowed for a direct comparison on the metric of economics. The baseline models used the same system boundaries that limited this techno-economic assessment to the chilling process and used harmonized model inputs when possible for consistency. Some facilities include maturation as an extension of the chilling process; however, these baseline models don't include anything outside the chilling process. The models used standard n^{th} plant economic assumptions from literature and assumed 10% internal rate of return (IRR), 20-year facility life, 8% loan interest rate on a 10-year loan with 40% equity, and the 2019 U.S. corporate tax rate of 21% [59–61]. The above economic assumptions were combined with capital costs, operational costs, linear depreciation, and poultry processing rate to perform a 20-year discounted cash flow rate of return (DCFROR) for each poultry chilling system. These models use the IRR as the discount rate to determine the minimum processing cost ($/metric ton) associated with poultry chilling while providing a net present

value (NPV) of zero. This minimum processing cost represents a levelized cost of chilling poultry carcasses that supports a 10% IRR over the 20-year life of the system.

All baseline values were taken from literature or acquired through communication with poultry chilling equipment manufacturers and poultry processing facilities. In particular, the system layout and energy consumptions reported in the literature were found to be antiquated and thus most of these data were acquired through communications with industry. The mutual baseline inputs were plant operation (250 d per year, 16 h per day), poultry processing rate (16.5 tonne/hour), water treatment ($1.5/$m^3$; [9,35,62,63]) and electricity ($0.10/kWh) prices, and fixed annual maintenance cost (5% of total capital cost). While AC and WC fixed and variable labor requirements might vary slightly, the labor requirements were assumed to be equivalent for the baseline cases for both systems. Based on input from chilling equipment suppliers, the AC and WC models reflect the major differences between the two systems (WC, AC); floor space requirements (100 m^2, 500 m^2), water use (3200 L/tonne; 300 L/tonne), and chilling energy costs (20.9 kWh/tonne, 31.4 kWh/tonne). Due to the complexity and high variability in WC and AC system designs and operational characteristics, sensitivity analyses were used to evaluate how system parameters can impact the levelized cost associated with chilling poultry carcasses. The sensitivity analysis varied the following model values by ±50%: capital cost ($/tonne), chilling floorspace (m^2), processing rate (tonne/hour), chilling energy (kWh/tonne), worker capacity (tonne/hour), water use (L/tonne), water price plus water treatment cost ($/L), and electricity cost ($/kWh). The end result is a direct comparison of the two technologies in terms of costs with sensitivity used to highlight high impact variables.

REFERENCES

1. Putman B, Thoma G, Burek J, Matlock M. A retrospective analysis of the United States poultry industry: 1965 compared with 2010. Agricultural Systems. 2017;157(C):107–17.

2. United States Department of Agriculture. National Agricultural Statistics Service - Charts and Maps - Poultry [Internet]. Available from: https://www.nass.usda.gov/Charts_and_Maps/Poultry/index.php

3. Food and Agriculture Organization of the United Nations. Meat Market Review: Overview of global meat market developments in 2019. Rome, Italy; Report No.: CA8819EN/1/04.20.

4. Zhuang H, Bowker BC, Berrang ME, Meinersmann RJ, Buhr RJ. Impact of eliminating the carcass chilling step in the production of pre-cooked chicken breast meat. Journal of Applied Poultry Research. 2017 Sep 1;26(3):431–6.

5. Sams AR, Alvarado CZ, Owens CM. Poultry Meat Processing. Vol. 7. Boca Raton: CRC Press; 2001.

6. Zhang L, Jeong JY, Janardhanan KK, Ryser ET, Kang I. Microbiological quality of water immersion-chilled and air-chilled broilers. J Food Prot. 2011 Sep;74(9):1531–5.

7. Sánchez MX, Fluckey WM, Brashears MM, McKee SR. Microbial profile and antibiotic susceptibility of Campylobacter spp. and Salmonella spp. in broilers processed in air-chilled and immersion-chilled environments. Journal of Food Protection. 2002 Jun 1;65(6):948–56.

8. Smith DP, Cason JA, Berrang ME. Effect of fecal contamination and cross-contamination on numbers of coliform, Escherichia coli, Campylobacter, and Salmonella on immersion-chilled broiler carcasses. Journal of Food Protection. 2005 Jul 1;68(7):1340–5.

9. Huezo R, Smith DP, Northcutt JK, Fletcher DL. Effect of immersion or dry air chilling on broiler carcass moisture tretention and breast fillet functionality. Journal of Applied Poultry Research. 2007 Oct 1;16(3):438–47.

10. Barbut S. The Science of Poultry and Meat Processing. Guelph, CA: Self; 2015.

11. Pederson R. Advantages and disadvantages of various methods for the chilling of poultry. Copenhagen, Denmark: Landbrugsministeriets Slagteri-og Konserveslaboratorium; 1979. Report No.: 189.

12. James C, Vincent C, de Andrade Lima TI, James SJ. The primary chilling of poultry carcasses—a review. International Journal of Refrigeration. 2006 Sep 1;29(6):847–62.

13. Dainty RH, Mackey BM. The relationship between the phenotypic properties of bacteria from chill-stored meat and spoilage processes. Soc Appl Bacteriol Symp Ser. 1992;21:103S-14S.

14. Lorenzo JM, Bedia M, Bañón S. Relationship between flavour deterioration and the volatile compound profile of semi-ripened sausage. Meat Sci. 2013 Mar;93(3):614–20.

15. Rivas-Cañedo A, Juez-Ojeda C, Nuñez M, Fernández-García E. Volatile compounds in ground beef subjected to high pressure processing: A comparison of dynamic headspace and solid-phase microextraction. Food Chemistry. 2011 Feb;124(3):1201–7.

16. Angelo AJS, Vercellotti DJ, Jacks T, Legendre MM. Lipid oxidation in foods. Critical Reviews in Food Science and Nutrition. 1996 Feb 1;36(3):175–224.

17. Jeong JY, Janardhanan KK, Booren AM, Harte JB, Kang I. Breast meat quality and consumer sensory properties of broiler carcasses chilled by water, air, or evaporative air. Poultry Science. 2011 Mar 1;90(3):694–700.

18. Fleming BK, Froning GW, Yang TS. Heme pigment levels in chicken broilers chilled in ice slush and air. Poultry Science. 1991 Oct 1;70(10):2197–200.

19. Zhuang H, Savage EM, Smith DP, Berrang ME. Effect of dry-air chilling on Warner-Bratzler shear force and water-holding capacity of broiler breast meat deboned four hours postmortem. 2008;

20. Katiyo W, de Kock HL, Coorey R, Buys EM. Sensory implications of chicken meat spoilage in relation to microbial and physicochemical characteristics during refrigerated storage. LWT. 2020 Jun 1;128:109468.

21. Hale KK, Stadelman WJ, Bramblett VD. Effect of dry-chilling on the flavor of fried chicken. Poultry Science. 1973 Jan 1;52(1):253–62.

22. Ristic M. Influence of the water cooling of fresh broilers on the shelf life of poultry parts at -15 degrees C and -21 degrees C. LEBENSM-WISS+TECHNOL. 1982;15(2):113–6.

23. Chen SH, Fegan N, Kocharunchitt C, Bowman JP, Duffy LL. Changes of the bacterial community diversity on chicken carcasses through an Australian poultry processing line. Food Microbiology. 2020 Apr 1;86:103350.

24. Berrang ME, Meinersmann RJ, Smith DP, Zhuang H. The effect of chilling in cold air or ice water on the microbiological quality of broiler carcasses and the population of Campylobacter. Poultry Science. 2008 May 1;87(5):992–8.

25. Handley JA, Park SH, Kim SA, Ricke SC. Microbiome profiles of commercial broilers through evisceration and immersion chilling during poultry slaughter and the identification of potential indicator microorganisms. Front Microbiol. 2018;9.

26. Tuncer B, Sireli UT. Microbial growth on broiler carcasses stored at different temperatures after air- or water-chilling. Poultry Science. 2008 Apr 1;87(4):793–9.

27. Mead GC, Hudson WR, Hinton MH. Use of a marker organism in poultry processing to identify sites of cross-contamination and evaluate possible control measures. British Poultry Science. 1994 Jul 1;35(3):345–54.

28. Lillard HS. The impact of commercial processing procedures on the bacterial contamination and cross-contamination of broiler carcasses. Journal of Food Protection. 1990 Mar 1;53(3):202–4.

29. Gumhalter Karolyi L, Medić H, Vidaček S, Petrak T, Botka−Petrak K. Bacterial population in counter flow and parallel flow water chilling of poultry meat. Eur Food Res Technol. 2003 Nov 1;217(5):412–5.

30. Munther D, Sun X, Xiao Y, Tang S, Shimozako H, Wu J, Smith B, Fazil A. Modeling cross-contamination during poultry processing: dynamics in the chiller tank. Food Control. 2016 Jan 1;59:271–81.

31. Raposo A, Pérez E, Faria CT de, Ferrús MA, Carrascosa C. Food Spoilage by Pseudomonas spp.—An Overview. In: Foodborne Pathogens and Antibiotic Resistance. John Wiley & Sons, Ltd; 2016. p. 41–71.

32. Tryfinopoulou P, Tsakalidou E, Nychas G-JE. Characterization of Pseudomonas spp. associated with spoilage of gilt-head sea bream stored under various conditions. Appl Environ Microbiol. 2002 Jan;68(1):65–72.

33. Morales PA, Aguirre JS, Troncoso MR, Figueroa GO. Phenotypic and genotypic characterization of Pseudomonas spp. present in spoiled poultry fillets sold in retail settings. LWT. 2016 Nov 1;73:609–14.

34. Wang G-Y, Wang H-H, Han Y-W, Xing T, Ye K-P, Xu X-L, Zhou G-H. Evaluation of the spoilage potential of bacteria isolated from chilled chicken in vitro and in situ. Food Microbiol. 2017 May;63:139–46.

35. Northcutt J, Smith D. Chillin' Chickens: Which Method Works Best? Agricultural Research [Internet]. 2008 Apr;56(4). Available from: https://agresearchmag.ars.usda.gov/2008/apr/chicken

36. Parada AE, Needham DM, Fuhrman JA. Every base matters: assessing small subunit rRNA primers for marine microbiomes with mock communities, time series and global field samples. Environ Microbiol. 2016 May;18(5):1403–14.

37. Apprill A, McNally S, Parsons R, Weber L. Minor revision to V4 region SSU rRNA 806R gene primer greatly increases detection of SAR11 bacterioplankton. Aquatic Microbial Ecology. 2015;75:129–37.

38. Bolyen E, Rideout JR, Dillon MR, Bokulich NA, Abnet CC, Al-Ghalith GA, Alexander H, Alm EJ, Arumugam M, Asnicar F, Bai Y, Bisanz JE, Bittinger K, Brejnrod A, Brislawn CJ, Brown CT, Callahan BJ, Caraballo-Rodríguez AM, Chase J, Cope EK, Da Silva R, Diener C, Dorrestein PC, Douglas GM, Durall DM, Duvallet C, Edwardson CF, Ernst M, Estaki M, Fouquier J, Gauglitz JM, Gibbons SM, Gibson DL, Gonzalez A, Gorlick K, Guo J, Hillmann B, Holmes S, Holste H, Huttenhower C, Huttley GA, Janssen S, Jarmusch AK, Jiang L, Kaehler BD, Kang KB, Keefe CR, Keim P, Kelley ST, Knights D, Koester I, Kosciolek T, Kreps J, Langille MGI, Lee J, Ley R, Liu Y-X, Loftfield E, Lozupone C, Maher M, Marotz C, Martin BD, McDonald D, McIver LJ, Melnik AV, Metcalf JL, Morgan SC, Morton JT, Naimey AT, Navas-Molina JA, Nothias LF, Orchanian SB, Pearson T, Peoples SL, Petras D, Preuss ML, Pruesse E, Rasmussen LB, Rivers A, Robeson MS, Rosenthal P, Segata N, Shaffer M, Shiffer A, Sinha R, Song SJ, Spear JR, Swafford AD, Thompson LR, Torres PJ, Trinh P, Tripathi A, Turnbaugh PJ, Ul-Hasan S, van der Hooft JJJ, Vargas F, Vázquez-Baeza Y, Vogtmann E, von Hippel M, Walters W, Wan Y, Wang M, Warren J, Weber KC, Williamson CHD, Willis AD, Xu ZZ, Zaneveld JR, Zhang Y, Zhu Q, Knight R, Caporaso JG. Reproducible, interactive, scalable and extensible microbiome data science using QIIME 2. Nature Biotechnology. 2019 Aug;37(8):852–7.

39. Callahan BJ, McMurdie PJ, Rosen MJ, Han AW, Johnson AJA, Holmes SP. DADA2: High-resolution sample inference from Illumina amplicon data. Nature Methods. 2016 Jul;13(7):581–3.

40. Bokulich NA, Kaehler BD, Rideout JR, Dillon M, Bolyen E, Knight R, Huttley GA, Gregory Caporaso J. Optimizing taxonomic classification of marker-gene amplicon sequences with QIIME 2's q2-feature-classifier plugin. Microbiome. 2018 May 17;6(1):90.

41. Quast C, Pruesse E, Yilmaz P, Gerken J, Schweer T, Yarza P, Peplies J, Glöckner FO. The SILVA ribosomal RNA gene database project: improved data processing and web-based tools. Nucleic Acids Res. 2013 Jan;41(Database issue):D590–6.

42. Mandal S, Van Treuren W, White RA, Eggesbø M, Knight R, Peddada SD. Analysis of composition of microbiomes: a novel method for studying microbial composition. Microbial Ecology in Health and Disease. 2015;26(1):27663.

43. Bokulich NA, Dillon MR, Bolyen E, Kaehler BD, Huttley GA, Caporaso JG. q2-sample-classifier: machine-learning tools for microbiome classification and regression. J Open Res Softw. 2018 Oct 23;3(30).

44. Wickham H. ggplot2 - Elegant Graphics for Data Analysis [Internet]. 1st ed. Springer-Verlag New York; 2009. 213 p. (Use R). Available from: https://www.springer.com/gp/book/9780387981413

45. Cole JR, Wang Q, Fish JA, Chai B, McGarrell DM, Sun Y, Brown CT, Porras-Alfaro A, Kuske CR, Tiedje JM. Ribosomal Database Project: data and tools for high throughput rRNA analysis. Nucleic Acids Res. 2014 Jan;42(Database issue):D633-642.

46. Stamatakis A. RAxML-VI-HPC: maximum likelihood-based phylogenetic analyses with thousands of taxa and mixed models. Bioinformatics. 2006 Nov 1;22(21):2688–90.

47. Janssen S, McDonald D, Gonzalez A, Navas-Molina JA, Jiang L, Xu ZZ, Winker K, Kado DM, Orwoll E, Manary M, Mirarab S, Knight R. Phylogenetic placement of exact amplicon sequences improves associations with clinical information. mSystems. 2018 Jun 26;3(3).

48. Giménez A, Ares F, Ares G. Sensory shelf-life estimation: A review of current methodological approaches. Food Research International. 2012 Nov 1;49(1):311–25.

49. Engle TE, Spears JW, Armstrong TA, Wright CL, Odle J. Effects of dietary copper source and concentration on carcass characteristics and lipid and cholesterol metabolism in growing and finishing steers. J Anim Sci. 2000 Apr;78(4):1053–9.

50. Kang JX, Wang J. A simplified method for analysis of polyunsaturated fatty acids. BMC Biochemistry. 2005 Mar 24;6(1):5.

51. Folch J, Lees M, Sloane Stanley GH. A simple method for the isolation and purification of total lipids from animal tissues. J Biol Chem. 1956;226:497–508.

52. Yin MC, Faustman C, Riesen JW, Williams SN. α-Tocopherol and ascorbate delay oxymyoglobin and phospholipid oxidation in vitro. Journal of Food Science. 1993;58(6):1273–6.

53. AOAC Authors. Reference data: Method 934.01; WATER. Official Methods of Analysis Proximate Analysis and Calculations. 2006;

54. AOAC Authors. Official methods of analysis Proximate Analysis and Calculations Ash Determination (Ash) Flour - item 49. Official Methods of Analysis Proximate Analysis and Calculations. 2006;17.

55. AOAC Authors. Official methods of analysis Proximate Analysis and Calculations Crude Protein Meat and Meat Products Including Pet Foods - item 80. Official Methods of Analysis Proximate Analysis and Calculations. 2006;17.

56. Lenth RV, Buerkner P, Herve M, Love J, Riebl H, Singmann H. emmeans: Estimated Marginal Means, aka Least-Squares Means. 2021.

57. Lytou A, Panagou EZ, Nychas G-JE. Development of a predictive model for the growth kinetics of aerobic microbial population on pomegranate marinated chicken breast fillets under isothermal and dynamic temperature conditions. Food Microbiol. 2016 May;55:25–31.

58. Solo J. Meat Quality and Sensory Analysis of Broiler Breast Fillets with Woody Breast Muscle Myopathy [Internet]. [Fayettville, AR]: University of Arkansas; 2016. Available from: https://scholarworks.uark.edu/etd/1603

59. Davis R, Markham J, Kinchin C, Grundl N, Tan ECD, Humbird D. Process Design and Economics for the Production of Algal Biomass: Algal Biomass Production in Open Pond Systems and Processing Through Dewatering for Downstream Conversion. National Renewable Energy Lab. (NREL), Golden, CO (United States); 2016 Feb. Report No.: NREL/TP-5100-64772.

60. Summers HM, Ledbetter RN, McCurdy AT, Morgan MR, Seefeldt LC, Jena U, Hoekman SK, Quinn JC. Techno-economic feasibility and life cycle assessment of dairy effluent to renewable diesel via hydrothermal liquefaction. Bioresour Technol. 2015;196:431–40.

61. Cruce JR, Quinn JC. Economic viability of multiple algal biorefining pathways and the impact of public policies. Applied Energy. 2019;233–234:735–46.

62. Ricke SC. Achieving sustainable production of poultry meat [Internet]. 1st ed. Vol. 1. London: Burleigh Dodds Science Publishing; 2016. 502 p. Available from: https://doi.org/10.4324/9781351114127

63. Northcutt JK, Jones DR. A survey of water use and common industry practices in commercial broiler processing facilities. J Appl Poult Res. 2004;13(1):48–54.

MICROBIOME DATA ACCURATELY PREDICT THE POSTRMORTEM INTERVAL USING RANDOM FOREST REGRESSION MODELS[1]

Summary

Death investigations often include an effort to establish the postmortem interval (PMI) in cases in which the time of death is uncertain. PMI can lead to the identification of the deceased and the validation of witness statements and suspect alibis. Recent research has demonstrated that microbes provide an accurate clock that starts at death and relies on ecological change in the microbial communities that normally inhabit a body and its surrounding environment. Here, we explore how to build the most robust Random Forest regression models for prediction of PMI by testing models built on different sample types (gravesoil, skin of the torso, skin of the head), gene markers (16s rRNA, 18s rRNA, ITS), and taxonomic levels (Sequence Variants, Species, Genus). We also tested whether particular suites of indicator microbes were informative across different datasets. Generally, results indicate that the most accurate models for predicting PMI were built using gravesoil and skin data using the 16s rRNA genetic marker at the taxonomic level of phyla. Additionally, several phyla consistently contributed highly to model accuracy and may be candidate indicators of PMI.

Introduction

Unattended death scenes pose challenges for crime scene investigators because the time of death, also known as the postmortem interval (PMI), is often unknown. However, no death scene is really unattended - microorganisms are ubiquitous, and these tiny witnesses can provide clues about the events surrounding death. For example, communities of microorganisms often have predictable ecologies, which can be leveraged for temporal [1,2] and geographic information [3]. Due to the rapidly decreasing costs of next-generation sequencing, it is feasible and cost-effective to track microbial community change during

[1] This work has been previously published: Belk A, Xu ZZ, Carter DO, Lynne A, Bucheli S, Knight R, Metcalf JL. Microbiome Data Accurately Predicts the Postmortem Interval Using Random Forest Regression Models. Genes. 2018 Feb 16;9(2):104. 10.3390/genes9020104.

decomposition via standard microbiome sequencing protocols [4]. Three taxonomically informative genomic markers - 16S rRNA (archaea and bacteria), 18S rRNA (microbial eukaryotes), and internal transcribed spacer regions (ITS; fungi specifically) - have been widely utilized to characterize microbial community composition and diversity [5–7]. Using these markers, recent research has revealed that tracking microbial community succession associated with mammalian cadaver decomposition can be a useful tool for estimating PMI [8]. This idea is very similar to tools developed in the field of forensic entomology, in which the succession of insects can be informative about the time frame and season of death [9]. Several studies have demonstrated consistent changes in microbial community composition during mammalian decomposition associated with skin [10–12], gastrointestinal/rectal locations [10,11,13,14], oral sites [12], nasal and ear cavities [15], and cadaver-associated soils [10,11,16–18]. These studies have used a variety of model-based statistical approaches for estimating PMI. For example, Pechal et al. [12] utilized an indicator species analysis at the bacterial family taxonomic level over 5 days of decomposition. Furthermore, Hauther et al. [13] utilized an exponential decay model based on declines in relative abundance of particular bacteria such as *Bacteroides*, *Lactobacillus*, and *Bifidobacterium*. However, the most accurate estimates of PMI have employed machine learning approaches [10,11,15], which are ideal for constructing models that utilize changes in relative abundance of all microorganisms in the entire community, as opposed to focusing on a subset of taxa that may not be the most temporally informative.

The reproducibility of microbial community succession during mammalian decomposition indicates that it can be used to predict the PMI. However, there is no single microbial species informative enough for accurate prediction. Machine learning is a powerful tool to discover the patterns in complex data and thus can be applied in this case to predict PMI utilizing a diverse microbial community [19]. Using the quantification of each microbial taxa by a marker gene (16S rRNA, 18S rRNA, or ITS) as a predictive feature, supervised regression models can be trained to learn the implicit relationship between microbiome composition and decomposition time point. The Random Forest regression model is widely used because of its robustness to overfitting, excellent performance, and easy parallelization of computing

[20]. Random Forest is an ensemble machine learning method that fits a set of decision trees on subsamples of the data set, and then combines the results to improve regression accuracy. Like all tree-based regression methods, Random Forest tends to overestimate the PMI of samples at the low end of PMI and underestimate at the high end of PMI. However, this systematic bias in Random Forest model is well known and can be calibrated with additional data sets [21]. In previous reports, Random Forest regression has been shown to achieve accurate PMI prediction in multiple skin and cadaver-associated soil gene marker data sets across decomposition of different host species [10,11].

We identified several knowledge gaps for developing robust machine learning Random Forest regression models for estimating PMI and addressed them using a meta-analysis of four previously published mammalian decomposition time-series data sets [10,11]. We aim to address which sample type(s), gene marker(s), and taxonomic level(s) provide the most accurate microbial model for estimating PMI. Additionally, we investigated whether particular microbes are informative across different sample types and data sets, which provides insights into whether suites of microbes or microbial groups can be used as indicators, or whether the full community provides the most accurate information. We chose four data sets that represented a range of environments and were generated using a standardized set of microbiome protocols (earthmicrobiome.org/protocols), which makes them directly comparable [22]. We focus our investigations on swabs of skin and gravesoils because these sampling locations would minimally impact the cadaver compared to other, more invasive, locations such as the GI tract. Thus, skin and soils are realistic sample types for development into a viable forensic tool. Each data set included 16S rRNA and 18S rRNA data, and three of the data sets also included ITS data. We looked for consistent trends across the datasets to help point researchers in the most fruitful future directions.

Results

Cross-validation error rates: comparison of sample types

The datasets used for this study contained a variety of sampling sites, so those used most consistently were selected for this study to determine the best sampling location for microbiome

prediction. Sample types investigated included cadaver-associated gravesoil, skin of the torso, and skin of the head. Results are summarized in **Table 4.1**. Both mouse model laboratory studies resulted in lower within study errors than the human studies. This is likely because these mouse studies were conducted under controlled laboratory conditions, as opposed to the human studies, which were conducted in the field with no control over environmental factors such as rainfall, temperature, and insect colonization. Overall, there is not a clear trend across the studies or gene markers of which sample type performed best. The lowest mean absolute error was from 16S data in gravesoil samples in a mouse decomposition study (mdc2), in which mice used were of the same breed, age, and were co-housed before being sacrificed for the study [11]. Within the two human studies, skin locations provided the lowest error for 16S rRNA marker, while soils provided the lowest errors for both microbial eukaryotic markers.

Cross-validation error rates: comparisons of genetic markers across taxonomic levels

Three taxonomically informative microbial gene markers (16S rRNA, 18S rRNA, and ITS) were compared at different sequence variant and taxonomic levels across sample types for each experiment (**Figure 4.1**, **Table 4.1**). Overall, the lowest within-study MAE for each experiment was generated using the bacterial and archaeal data (16S rRNA marker). However, all markers performed reasonably well with ITS producing the highest errors, which were as low as +/- 2.6 days over 25 days for mouse decomposition experiment 2 (mdc2). Within experiment, MAEs for each marker type were fairly similar. Furthermore, models consistently performed best at the class and phylum taxonomic levels for 16S rRNA and 18S rRNA, and at the class level for ITS. The sequence variant level (highest resolution possible) had the highest MAEs compared to sequences summarized into lower levels of taxonomy.

Table 4.1. A comparison of Mean Absolute Error (MAE) of models built using data from each gene marker (16S, 18S, ITS) for each sample type (soil, skin_torso, skin_head). Data were collected from four studies (mouse decomposition 1 (mdc1), mouse decomposition 2 (mdc2), SHSU human April (shsu_spring), SHSU human February (shsu_winter)). The ITS marker was not sequenced for mdc1. Models were generated based on data from the first 25 days of decomposition and the model with the best MAE after parameter tuning was selected. The lowest error within each marker for each experiment is highlighted in bold, black text.

Genomic Marker	Study Name	Sample Type	Sequence Variants	Species Level	Genus Level	Family Level	Order Level	Class Level	Phylum Level
16S	mdc1	soil	5.068	4.528	4.439	4.574	4.596	4.308	4.565
		skin_torso	4.602	3.744	3.577	3.353	3.889	4.377	4.070
		skin_head	4.272	3.816	3.816	3.747	3.442	**3.315**	4.672
	mdc2	soil	2.571	1.943	1.955	1.911	2.062	1.971	**1.737**
		skin_torso	3.357	2.926	2.898	2.783	2.826	2.942	2.856
		skin_head	3.001	2.383	2.379	2.340	2.467	2.369	2.405
	shsu spring	soil	5.225	3.594	3x.632	3.660	3.966	3.868	3.877
		skin_torso	4.303	3.830	3.807	4.106	4.343	4.311	4.022
		skin_head	3.890	3.506	3.385	3.577	3.342	**2.940**	3.006
	shsu winter	soil	4.985	3.922	3.980	3.947	3.848	4.026	3.783
		skin_torso	5.237	4.543	4.483	4.385	3.970	3.704	**3.265**
18S	mdc1	soil	4.370	3.125	3.072	3.135	2.813	2.942	2.733
		skin_torso	4.333	3.821	3.447	3.030	3.549	**2.702**	4.521
		skin_head	4.744	4.583	4.138	4.616	4.251	3.775	4.657
	mdc2	soil	3.505	3.237	3.208	3.107	3.221	**3.043**	3.330
		skin_torso	3.907	3.870	3.856	3.676	3.910	3.867	3.704
		skin_head	3.772	3.761	3.575	3.725	3.665	3.819	3.912
	shsu spring	soil	5.486	4.654	4.459	4.283	3.837	3.400	**3.264**
		skin_torso	5.457	4.654	5.196	5.404	5.264	5.754	5.974
		skin_head	4.645	4.571	4.370	5.148	5.028	4.763	5.218
	shsu winter	soil	5.239	4.429	4.442	4.239	4.042	**3.449**	3.504
		skin_torso	5.141	4.880	4.721	4.962	5.028	4.660	4.604
ITS	mdc2	soil	3.497	3.169	3.157	2.957	2.941	2.820	2.797
		skin_torso	3.505	3.237	3.211	3.083	3.023	**2.597**	3.036
		skin_head	3.648	3.561	3.523	3.483	3.509	3.413	3.305
	shsu spring	soil	5.586	4.735	4.836	4.629	4.980	**4.461**	4.713
		skin_torso	4.837	4.671	4.563	4.688	4.786	4.860	5.500
		skin_head	6.080	5.996	6.083	5.803	6.090	5.965	5.416
	shsu winter	soil	4.675	4.114	3.965	3.954	3.933	**3.671**	4.077

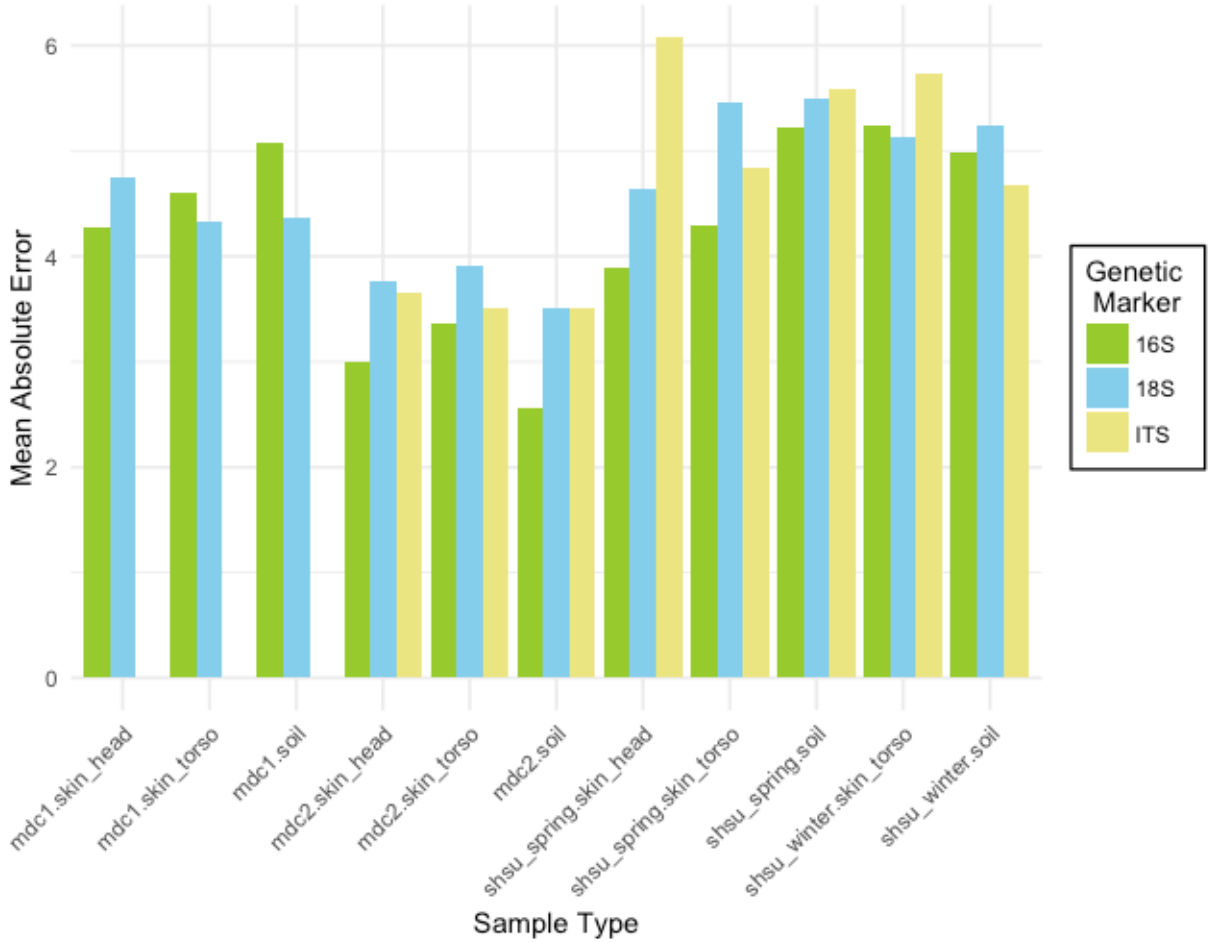

Figure 4.1. The Mean Absolute Error (MAE) rates for Random Forest models trained to predict the postmortem interval. For each marker type (16S bacterial and archaeal rRNA, 18S microbial eukaryote rRNA, ITS fungal gene marker), models were generated for three sample types (skin_head, skin_torso, soil) from four studies (mouse decomposition 1 (mdc1), mouse decomposition 2 (mdc2), SHSU human April (shsu_spring), SHSU human February (shsu_winter)). Skin_head samples were not collected for shsu_winter. Datasets were subset to include only the first 25 sampling days. Though all marker types performed well, the 16S rRNA marker generally resulted in the most accurate PMI prediction models.

Cross-study error rates

Cross-study error rates were generated between the two studies using human cadavers (shsu spring and shsu winter). Models were constructed for two sample types, cadaver-associated gravesoil and skin of the torso (skin), for each experiment, then tested on the same sample type for the other season. The skin of the head samples were excluded from this analysis as only one of the human datasets included this sample location. PMI was represented as 0 °C-base accumulated degree day (ADD) to account for the differences in temperature between the two seasons. Resulting cross study MAE are presented in **Table**

4.2, and plots of observed versus predicted PMI are presented in **supplementary figures S4.4 – S4.10**. For each marker type, the lowest error was generated using a gravesoil data set. The overall lowest cross-experiment error was generated from the model trained on the spring soil data set using bacterial and archaeal data at the phylum level.

Table 4.2. The mean absolute error (MAE) of models used in cross-experiment testing using accumulated degree days (ADD) with a minimum developmental threshold of 0°C. Models were built using 16S rRNA (green text), 18S rRNA (blue text), and ITS (orange text) markers from human cadaver decomposition data from two seasons: spring and winter. Models were built on sequence variant data and family-, genus- and species-level taxonomy. After model construction, the model was tested on the other dataset to evaluate the ability of the model to predict postmortem interval (PMI) beyond the original dataset. The lowest error for each marker within each cross-experiment test is in bold and black font.

Genomic Marker	Training Dataset	Sample Type	Sequence Variants MAE	Species Level MAE	Genus Level MAE	Family Level MAE	Order Level MAE	Class Level MAE	Phylum Level MAE
16S	Spring	soil	88.693	57.929	59.251	57.045	56.936	55.367	**48.686**
		skin	92.598	90.197	90.584	104.770	109.412	117.672	135.749
	Winter	soil	109.482	91.406	91.295	91.857	91.025	88.849	**83.312**
		skin	120.764	129.695	130.763	122.418	124.701	123.043	108.737
18S	Spring	soil	81.013	62.572	62.850	55.648	51.316	51.481	**50.082**
		skin	88.155	93.173	85.754	89.676	91.793	72.846	67.242
	Winter	soil	96.145	82.780	75.628	72.228	67.725	71.757	**63.465**
		skin	111.004	110.772	101.268	101.222	101.524	107.409	105.248
ITS	Spring	soil	111.806	94.797	94.742	93.504	85.282	80.856	**58.359**
		skin	101.852	96.815	99.272	101.086	104.162	106.043	94.468
	Winter	soil	104.775	99.360	96.392	96.604	93.564	87.709	**81.623**
		skin	114.027	110.865	107.026	113.294	117.302	115.937	87.274

Similar to the within-study errors, lower-level taxonomies generally resulted in more accurate models compared to sequence variant-level resolution. In particular, phylum level taxonomy appeared to provide the most accurate models overall in cross-experiment model testing. MAE was lowest at the phylum level for all three markers - 48.686, 50.082, and 58.359 for 16S, 18S, and ITS, respectively, or approximately 5 - 6 chronological days. For models trained on the winter data set, the soil microbial eukaryotic 18S rRNA marker returned the lowest error. ITS data resulted in the highest error in spring-trained data, while 16S data resulted in the highest error in winter-trained data.

Overall, the models built on the spring data were more accurate in predicting the PMI of the winter data. This is likely because the spring data set spans a broader range of ADDs, which results in a more accurate model compared to the winter data set. Models trained on the winter skin samples resulted in the highest error when tested on the spring skin samples.

Important feature taxa

Not all taxa or taxa groups contribute temporal information equally. We assessed how informative each taxon was in the regression model by computing the average decrease of impurity during the tree splitting process in model training as one taxa or taxa group was removed iteratively for 16S rRNA data [20]. We reported the feature importance of phyla for all three sample types (soil, skin of the torso, skin of the head) in the human decomposition data sets (**Figure 4.2)**. The importance of each phylum is highly correlated between sample types within study for both the spring and winter season (**Figure 4.2A**, **Fig S4.2**-winter). The soil and skin of the head samples appear to share the most bacterial phyla compared to the skin of the torso, and are the most highly correlated, with a Spearman correlation coefficient of 0.90 within spring samples. Samples from the skin of the head were not taken during the winter months for comparison, but the correlation between the spring skin of the head and winter soil was lower (0.77), though it is not clear whether the lower correlation was due to the sample type or the difference in season. Furthermore, only a few phyla contribute substantially to the models (**Figure 4.2A**). The most informative phyla for the spring season include Fusobacteria, Actinobacteria, Firmicutes, Verrucomicrobia, Proteobacteria, Acidobacteria, and Planctomycetes (**Figure 4.2B**). Furthermore, phyla important in the model were highly correlated between the spring and winter seasons (**Figure 4.2C**) of human decomposition ($p < 0.01$).

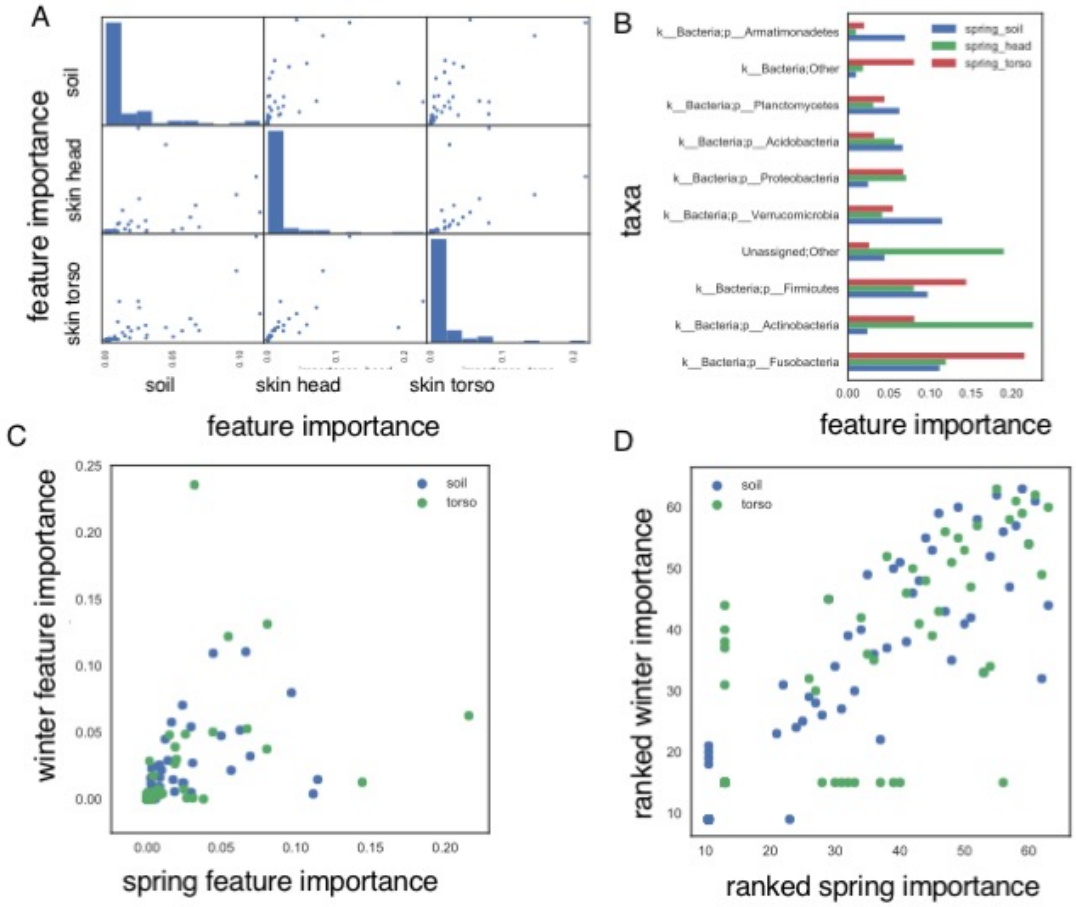

Figure 4.2. The feature importance measures the contribution of each phylum to the PMI regression model (results from SHSU spring study) using the 16S rRNA genetic marker. (A) The feature importance is correlated across 3 sample types. Each scatter plot shows the correlation between feature importances of every pair of models built from each sample type. Each dot represents a phylum and its value on the x- or y-axis represents its feature importance in the 2 models of sample types. The Spearman correlation coefficients are 0.90 (head vs. torso), 0.84 (head vs. soil), and 0.93 (torso vs. soil), with p-values << 0.01. The diagonal histogram plots show that most of phyla do not contribute much to regression models of each sample type; (B) The top ten phyla that are most informative for PMI prediction within each sample type; (C) The importance of the phyla to the regression models are highly correlated across spring and winter seasons. Each dot represents the importance of a phylum in winter season (y-axis) and in spring (x-axis). The correlation coefficients between winter and spring feature importances are 0.78 (soil) and 0.93 (torso), with p-values < 0.01; (D) same plot as C, except axes are feature importance ranks instead of scores.

Discussion

Machine learning methods are powerful tools for utilizing high dimensional datasets for prediction. Machine learning is ideal for finding patterns in complex and diverse microbiome data sets and utilizing these patterns to predict outcomes [19], such as disease states [19,23]. Leveraging biological

information associated with crime scenes is another excellent opportunity for the development of machine learning tools that utilize microbiome datasets. With the goal of developing the most robust model, we assessed how several variables affect within-study and cross-experiment errors for estimating PMI. Results of this meta-analysis indicate that the most robust models predicting PMI utilized cadaver-associated soil or skin data and the 16S rRNA gene marker summarized at class- or phylum-level taxonomies.

In this study, models for estimating PMI were developed using data from the first 25 sample days of each study, as preliminary data indicated the earlier sampling days resulted in more accurate models. Early decomposition may be the most accurate time frame because microbial succession is rapid and diversity is high compared to later stages of decomposition [10,11,16]. However, in the studies incorporated into this analysis the sampling was more frequent during early decomposition, and more frequent sampling has been demonstrated previously to improve model accuracy [11]. Therefore, the lower errors are likely, at least to some extent, an artifact of the change in sampling rate. Further investigation into the accuracy of models across different timeframes is warranted.

Cadaver-associated soils as well as cadaver skin sites both appear to be promising sampling locations for developing microbiome-based PMI estimation tools. A wide diversity of sample sites has been investigated for microbial succession during decomposition, though few employed machine learning to estimate PMI, possibly due to small sample sizes. Soils and skin are both attractive sampling locations because they are easy to access without disturbing the remains. The soil microbiome has been shown to change predictably during mammalian decomposition, a change which is little affected by body mass [16,18] and soil type [11]. The skin, at various sample sites, has been demonstrated to accurately predict PMI using machine learning techniques [12,15,16]. Johnson et al. [15] demonstrated low errors for skin samples collected from the inner ear of human cadavers. Therefore, a comparison of different skin locations within a study would be useful to help identify locations in which microbial succession is the most clock-like. In our meta-analysis, we discovered fairly similar prediction accuracies using soils and skin, which may be because the two sample types are not independent. For example, Cobaugh et al. [16]

demonstrated that the microbiomes associated with the skin of the body may transfer to the soil and persist in the soil microbiome.

Most microbiome studies, including those investigating the PMI, utilized the 16S rRNA gene marker. We have investigated the use of two additional microbial markers: 18S rRNA which amplifies microbial eukaryotes, and ITS, which amplifies fungi specifically. Although 16S rRNA provided the most accurate within-study models, the 18S rRNA marker had similar accuracies, and was more accurate in several cases during the cross-experiment validation. However, larger sample sizes would make these analyses considerably more robust. 18S rRNA has been previously shown to be more stable across seasons than bacteria [17], which may explain why it is robust in our cross-experiment model testing in which models were tested across the winter and spring seasons. Furthermore, for each marker gene, we tested multiple taxa levels and discovered that in all cases lower levels of taxonomy, particularly class and phylum levels, produced more accurate models, which agrees with results reported by Johnson et al. [15] on an independent data set of human cadaver skin samples. Furthermore, these models generally improve on error rates published in the original papers. For example, the mdc2 study originally reported error rates for 16S rRNA of 2.5 days (at the OTU level), and here we report 1.7 days at the Phylum level. However, we note that results reported here are not directly comparable published results because we used a different processing method (e.g. deblur instead of 97% OUT clustering methods). Finally, we discovered that only a subset of phyla was highly informative to models and these important groups of microbes were similar across seasons, at least in one study. Those highly informative phyla are consistent with those reported in other studies [12,15]. This suggests that accurate models of the PMI may be constructed based on a subset of the microbial community, which may open the door for cheaper, targeted assays.

In this study, we focused on utilizing a very powerful tool, Random Forests regressors. Every regression method has caveats. For example, Random Forest does not perform as well at the extreme ends of PMI. Another popular regressor, K-nearest neighbor (KNN e.g. Johnson et al. [15]), is a simple and intuitive model that works well on pattern recognition problems [24]. Linear regression (and its variants, lasso, ridge, elastic net) is also popular in regression analysis. It is interpretable how much every feature

contributes to the model; however, the strong assumption of linearity between outcome and features are often violated. Support Vector Machine (SVM) is also a proved accurate method in many scenarios and handles high dimensional data very well [24]. Although beyond the scope of this current manuscript, a systematic comparison of regression methods will be informative and is planned as part of future research on a forthcoming large data set.

Determining timelines has been described as the Achilles heel of forensic pathology [25]. There are very few tools, and most are only applicable within the initial hours and days following death, and each method is vulnerable to biases [26]. Therefore, developing new tools that leverage independent information for estimating the time since death is critical. There is evidence that gene meter expression data may be used to predict PMI. In a proof of principle study authors demonstrated that gene transcripts could be used to produce linear models of PMI with correlation coefficients of 1 [27]. This method may be an interesting alternative to microbial and entomological prediction methods as analyses are expanded. However, this has yet to be applied to human decomposition for further viability testing, and machine learning techniques were not applied.

Conclusions

The results of the current meta-analysis provide directions for future research on developing microbial-based models for estimating PMI. Currently, the greatest barrier to creating generalizable microbial models for estimating PMI is a lack of human cadaver-associated data sets from different environments and seasons. However, coordinated research is underway to overcome this limitation and generate a comprehensive data set to train, test, and generate robust models with larger sample sizes. Once available, existing and new datasets can be combined to determine the best generalizable model for estimating PMI based on microbes.

Materials and Methods

Amplicon sequencing data processing

Previously published 16S rRNA, 18S rRNA, and ITS data were obtained from the open-source microbiome study management platform, QIITA (https://qiita.ucsd.edu/) under studies 714, 1889, 10141, 10142, and 10143 [10,11]. Briefly, these studies included two laboratory decomposition experiments [10,11], in which mice were decomposed on soils with the exclusion of insects and destructively sampled in replicates of 5 for 8 time points over 2 to 3 months. We also included two experiments in which two human donors were allowed to decompose outdoors in the winter season and in the spring season (a total of four donors) at the Southeast Texas Applied Forensic Science (STAFS) laboratory [11]. For complete details on the data used for this study, see **Table 4.3**. Briefly, for each gene marker in these data sets, the Earth Microbiome Project primer pair and standard protocols were utilized [4]. Amplicons for each gene marker were then sequenced using the Illumina HiSeq 2000 platform (2x100 bp reads), and forward reads for each gene marker were used to create a feature table of sequences. Sequence data, metadata, and feature tables are available and curated on QIITA (qiita.ucsd.edu), where they are periodically re-annotated to be consistent with current best practices utilizing the QIIME pipeline [28]. Therefore, we utilized data processed using the deblur method, which utilizes sequence error profiles to derive putatively true biological sequences, resulting in high quality sequence variant data as opposed to Operational Taxonomic Units (OTUs) in which sequence variation is lost because sequences are collapsed, usually at a sequence identity of 97% [29]. In the original publication of these datasets [10,11], a closed reference OTU-picking method was used to generate OTU tables, which likely resulted in the loss of potentially useful sequence data that did not match the greengenes database [30] within 97% similarity. Therefore, the current meta-analysis provides an opportunity to reanalyze these valuable datasets with more current methods. The 16S rRNA and 18S rRNA amplicon sequence files were trimmed for quality to 90bp reads. For ITS data, 100bp reads were utilized. For 16S, the resulting feature table was further processed by removing sequences that did not match a positive reference database with 80% similarity (reference-hit.biom table downloaded). For 18S and ITS, a positive reference database was

not used (all.biom table downloaded). ITS data were only available for studies 10141, 10142, and 10143. For each data set, we retained common sample types, including those taken from gravesoil near the torso, and from the skin of the left hip, right hip, torso, and head. These were categorized into three sample groups for analysis: cadaver-associated gravesoil, skin of the torso, and skin of the head.

Assigning taxonomy

Each table was individually processed to assign taxonomy and filter out taxa that were not considered part of the microbiome. Taxa were assigned using classifiers specific to each marker: greengenes 13.8 for 16S rRNA [30], SILVA 128 for 18S rRNA [31], and UNITE 7 developer classifier for ITS [32], all at the 99% sequence identity threshold level. Sequences filtered out of the 16S rRNA data set included those assigned to chloroplasts and mitochondria. Sequences filtered out of the 18S rRNA data included those assigned to Archaeplastida, Arthropoda, Chordata, Mollusca, as well as sequences that were not assigned to Eukarya. For ITS, sequences that did not assign to Fungi were filtered out. Following this, filtered tables were combined into a single sequence variant table per marker type to be used in modeling. These tables were then used to generate additional tables summarized at different taxonomic levels, including species (16S rRNA L6; 18S rRNA L12; ITS L6), genus (16S rRNA L5; 18S rRNA L10; ITS L5), family (16S rRNA L4; 18S rRNA L8; ITS L4), order (16S rRNA L3; 18S rRNA L6; ITS L3), class (16S rRNA L3; 18S rRNA L4; ITS L3), and phylum (16S rRNA L2; 18S rRNA L3; ITS L2). We would note that the SILVA taxonomy levels were very uneven across different groups of eukaryotes (e.g. *Amoebozoa*, *Opisthokonta*, and *Alveolata*). Therefore, the levels chosen (L12, 10, 8, 6, 4, and 3) generally represent summaries at progressively higher levels of taxonomy, but are not strictly adhering to species, genus and family level across each major eukaryotic group.

Model testing

PMI prediction models were generated using Random Forest regressors based on sequence variant and taxa abundance data. Data were divided into subsets by sample type and normalized using the Calour library [33]. Using the Calour library, we chose to utilize total-sum scaling normalization, as opposed to rarefaction, to avoid the loss of statistical power by discarding reads and/or samples. Random Forest is insensitive to the methods of normalization used. For human body decomposition, each subset was partitioned based on individual for cross validation so that the samples from the same individuals are either in the training set or testing set, but not both. Training refers to fitting or building the model while testing is equivalent to predicting. The accuracy of the models was measured using the Mean Absolute Error (MAE), calculated as the deviation of the predicted from observed values and representing the average prediction error in the same unit of the original data. Within each dataset of each study, the best Random Forest regression model after hyperparameter tuning through cross validation was selected to represent the final model. We also applied the model trained from one study to predict PMI of another study (i.e. cross-study prediction) to test the generalizability of the model. Each experiment was conducted over a different number of sampling days ranging from a total of 48 to 142 days (**Table 4.3**), so for consistency one model timeframe was selected for inclusion in the model. Preliminary model tests were conducted to determine the timeframe for use in this experiment, results of this analysis are presented in **supplementary figure S4.1**. Overall, the inclusion of all experimental sampling days resulted in the highest MAE, while using only the first 25 days resulted in invariably lower MAEs (**Fig S4.2**). Therefore, data subset to the first 25 days of decomposition were selected for the modeling in this study. The modeling was done with Python machine learning package scikit-learn v19.0 [34]. Data were analyzed and graphics were generated using R software, version 3.4.1, the ggplot2 package, and matplotlib 2.0.0 [35,36].

Table 4.3. A summary of all studies included in the meta-analysis. Studies were obtained from the QIITA open-source study managements platform. All studies were downloaded as deblur processed tables, along with the corresponding metadata information. Different table types and trim lengths were selected based on the data availability and marker type.

QIITA Study Number	QIITA Study Name	Our Study Name	Shorthand Name	Prep Number	Marker	Trim Length	OTU Table Type	Number of Days Sampled
714	A microbial clock provides an accurate estimate of the postmortem interval in a mouse model system	Mouse Decomposition 1	mdc1	769	16S	90bp	reference-hit.biom	48
1889	A microbial clock provides an accurate estimate of the postmortem interval in a mouse model system - 18S	Mouse Decomposition 1	mdc1	1204	18S	90bp	all.biom	48
10141	Metcalf microbial community assembly and metabolic function during mammalian corpse decomposition	Mouse Decomposition 2	mdc2	1265	16S	90bp	reference-hit.biom	70
				1038	18S	90bp	all.biom	70
				345	ITS	100bp	all.biom	70
10142	Metcalf microbial community assembly and metabolic function during mammalian corpse decomposition SHSU winter	SHSU Winter	shsu_winter	333	16S	90bp	reference-hit.biom	132
				1166	18S	90bp	all.biom	132
				335	ITS	100bp	all.biom	132
10143	Metcalf microbial community assembly and metabolic function during mammalian corpse decomposition SHSU April 2012 exp	SHSU Spring	shsu_spring	1107	16S	90bp	reference-hit.biom	82
				1109	18S	90bp	all.biom	82
				1110	ITS	100bp	all.biom	82

REFERENCES

1. McGeachie MJ, Sordillo JE, Gibson T, Weinstock GM, Liu Y-Y, Gold DR, Weiss ST, Litonjua A. Longitudinal prediction of the infant gut microbiome with dynamic Bayesian networks. Sci Rep. 2016 Feb 8;6:20359.

2. Carter DO, Yellowlees D, Tibbett M. Cadaver decomposition in terrestrial ecosystems. Naturwissenschaften. 2007 Jan 1;94(1):12–24.

3. Noronha MF, Lacerda Júnior GV, Gilbert JA, de Oliveira VM. Taxonomic and functional patterns across soil microbial communities of global biomes. Sci Total Environ. 2017 Dec 31;609:1064–74.

4. Thompson LR, Sanders JG, McDonald D, Amir A, Ladau J, Locey KJ, Prill RJ, Tripathi A, Gibbons SM, Ackermann G, Navas-Molina JA, Janssen S, Kopylova E, Vázquez-Baeza Y, González A, Morton JT, Mirarab S, Zech Xu Z, Jiang L, Haroon MF, Kanbar J, Zhu Q, Jin Song S, Kosciolek T, Bokulich NA, Lefler J, Brislawn CJ, Humphrey G, Owens SM, Hampton-Marcell J, Berg-Lyons D, McKenzie V, Fierer N, Fuhrman JA, Clauset A, Stevens RL, Shade A, Pollard KS, Goodwin KD, Jansson JK, Gilbert JA, Knight R, Earth Microbiome Project Consortium. A communal catalogue reveals Earth's multiscale microbial diversity. Nature. 2017 Nov 23;551(7681):457–63.

5. Parfrey LW, Walters WA, Lauber CL, Clemente JC, Berg-Lyons D, Teiling C, Kodira C, Mohiuddin M, Brunelle J, Driscoll M, Fierer N, Gilbert JA, Knight R. Communities of microbial eukaryotes in the mammalian gut within the context of environmental eukaryotic diversity. Front Microbiol. 2014;5:298.

6. Willger SD, Grim SL, Dolben EL, Shipunova A, Hampton TH, Morrison HG, Filkins LM, O'Toole GA, Moulton LA, Ashare A, Sogin ML, Hogan DA. Characterization and quantification of the

fungal microbiome in serial samples from individuals with cystic fibrosis. Microbiome. 2014 Nov 3;2(1):40.

7. Ramirez KS, Leff JW, Barberán A, Bates ST, Betley J, Crowther TW, Kelly EF, Oldfield EE, Shaw EA, Steenbock C, Bradford MA, Wall DH, Fierer N. Biogeographic patterns in below-ground diversity in New York City's Central Park are similar to those observed globally. Proc Biol Sci. 2014 Nov 22;281(1795).

8. Metcalf JL, Xu ZZ, Bouslimani A, Dorrestein P, Carter DO, Knight R. Microbiome tools for forensic science. Trends Biotechnol. 2017 Sep 1;35(9):814–23.

9. Amendt J, Campobasso CP, Gaudry E, Reiter C, LeBlanc HN, Hall MJR, European Association for Forensic Entomology. Best practice in forensic entomology--standards and guidelines. Int J Legal Med. 2007 Mar;121(2):90–104.

10. Metcalf JL, Wegener Parfrey L, Gonzalez A, Lauber CL, Knights D, Ackermann G, Humphrey GC, Gebert MJ, Van Treuren W, Berg-Lyons D, Keepers K, Guo Y, Bullard J, Fierer N, Carter DO, Knight R. A microbial clock provides an accurate estimate of the postmortem interval in a mouse model system. Kolter R, editor. eLife. 2013 Oct 15;2:e01104.

11. Metcalf JL, Xu ZZ, Weiss S, Lax S, Treuren WV, Hyde ER, Song SJ, Amir A, Larsen P, Sangwan N, Haarmann D, Humphrey GC, Ackermann G, Thompson LR, Lauber C, Bibat A, Nicholas C, Gebert MJ, Petrosino JF, Reed SC, Gilbert JA, Lynne AM, Bucheli SR, Carter DO, Knight R. Microbial community assembly and metabolic function during mammalian corpse decomposition. Science. 2016 Jan 8;351(6269):158–62.

12. Pechal JL, Crippen TL, Tarone AM, Lewis AJ, Tomberlin JK, Benbow ME. Microbial community functional change during vertebrate carrion decomposition. PloS One. 2013;8(11):e79035.

13. Hauther KA, Cobaugh KL, Jantz LM, Sparer TE, DeBruyn JM. Estimating time since death from postmortem human gut microbial communities. J Forensic Sci. 2015 Sep;60(5):1234–40.

14. DeBruyn JM, Hauther KA. Postmortem succession of gut microbial communities in deceased human subjects. PeerJ. 2017 Jun 12;5:e3437.

15. Johnson HR, Trinidad DD, Guzman S, Khan Z, Parziale JV, DeBruyn JM, Lents NH. A machine learning approach for using the postmortem skin microbiome to estimate the postmortem interval. PLOS ONE. 2016 Dec 22;11(12):e0167370.

16. Cobaugh KL, Schaeffer SM, DeBruyn JM. Functional and structural succession of soil microbial communities below decomposing human cadavers. PLOS ONE. 2015 Jun 12;10(6):e0130201.

17. Carter DO, Metcalf JL, Bibat A, Knight R. Seasonal variation of postmortem microbial communities. Forensic Sci Med Pathol. 2015 Jun;11(2):202–7.

18. Weiss S, Carter DO, Metcalf JL, Knight R. Carcass mass has little influence on the structure of gravesoil microbial communities. Int J Legal Med. 2016 Jan 1;130(1):253–63.

19. Knights D, Costello EK, Knight R. Supervised classification of human microbiota. FEMS Microbiol Rev. 2011 Mar;35(2):343–59.

20. Breiman L, Friedman J, Stone CJ, Olshen RA. Classification and Regression Trees. 1st ed. Chapman and Hall; 1984. 368 p.

21. Zhang G, Lu Y. Bias-corrected random forests in regression. J Appl Stat. 2012 Jan 1;39(1):151–60.

22. Gilbert JA, Jansson JK, Knight R. Earth Microbiome Project and global systems biology. mSystems. 2018 Jun 26;3(3).

23. Yazdani M, Taylor BC, Debelius JW, Li W, Knight R, Smarr L. Using machine learning to identify major shifts in human gut microbiome protein family abundance in disease. IEEE Int Conf Big Data. 2016 Dec 5;1272–80.

24. Kuhn M, Johnson K. Applied Predictive Modeling [Internet]. New York: Springer-Verlag; 2013 [cited 2021 Jan 28]. Available from: https://www.springer.com/gp/book/9781461468486

25. Byard RW. Timing: the Achilles heel of forensic pathology. Forensic Sci Med Pathol. 2017 Jun;13(2):113–4.

26. Madea B. Methods for determining time of death. Forensic Sci Med Pathol. 2016 Dec;12(4):451–85.

27. Hunter MC, Pozhitkov AE, Noble PA. Accurate predictions of postmortem interval using linear regression analyses of gene meter expression data. Forensic Sci Int. 2017;275:90–101.

28. Bolyen E, Rideout JR, Dillon MR, Bokulich NA, Abnet CC, Al-Ghalith GA, Alexander H, Alm EJ, Arumugam M, Asnicar F, Bai Y, Bisanz JE, Bittinger K, Brejnrod A, Brislawn CJ, Brown CT, Callahan BJ, Caraballo-Rodríguez AM, Chase J, Cope EK, Da Silva R, Diener C, Dorrestein PC, Douglas GM, Durall DM, Duvallet C, Edwardson CF, Ernst M, Estaki M, Fouquier J, Gauglitz JM, Gibbons SM, Gibson DL, Gonzalez A, Gorlick K, Guo J, Hillmann B, Holmes S, Holste H, Huttenhower C, Huttley GA, Janssen S, Jarmusch AK, Jiang L, Kaehler BD, Kang KB, Keefe CR, Keim P, Kelley ST, Knights D, Koester I, Kosciolek T, Kreps J, Langille MGI, Lee J, Ley R, Liu Y-X, Loftfield E, Lozupone C, Maher M, Marotz C, Martin BD, McDonald D, McIver LJ, Melnik AV, Metcalf JL, Morgan SC, Morton JT, Naimey AT, Navas-Molina JA, Nothias LF, Orchanian SB, Pearson T, Peoples SL, Petras D, Preuss ML, Pruesse E, Rasmussen LB, Rivers A, Robeson MS, Rosenthal P, Segata N, Shaffer M, Shiffer A, Sinha R, Song SJ, Spear JR, Swafford AD, Thompson LR, Torres PJ, Trinh P, Tripathi A, Turnbaugh PJ, Ul-Hasan S, van der Hooft JJJ, Vargas F, Vázquez-Baeza Y, Vogtmann E, von Hippel M, Walters W, Wan Y, Wang M, Warren J, Weber KC, Williamson CHD, Willis AD, Xu ZZ, Zaneveld JR, Zhang Y, Zhu Q, Knight R, Caporaso JG. Reproducible, interactive, scalable and extensible microbiome data science using QIIME 2. Nat Biotechnol. 2019 Aug;37(8):852–7.

29. Amir A, McDonald D, Navas-Molina JA, Kopylova E, Morton JT, Zech Xu Z, Kightley EP, Thompson LR, Hyde ER, Gonzalez A, Knight R. Deblur Rapidly Resolves Single-Nucleotide Community Sequence Patterns. mSystems. 2017 Mar 7;2(2).

30. McDonald D, Price MN, Goodrich J, Nawrocki EP, DeSantis TZ, Probst A, Andersen GL, Knight R, Hugenholtz P. An improved Greengenes taxonomy with explicit ranks for ecological and evolutionary analyses of bacteria and archaea. ISME J. 2012 Mar;6(3):610–8.

31. Quast C, Pruesse E, Yilmaz P, Gerken J, Schweer T, Yarza P, Peplies J, Glöckner FO. The SILVA ribosomal RNA gene database project: improved data processing and web-based tools. Nucleic Acids Res. 2013 Jan;41(Database issue):D590–6.

32. Kõljalg U, Nilsson RH, Abarenkov K, Tedersoo L, Taylor AFS, Bahram M, Bates ST, Bruns TD, Bengtsson-Palme J, Callaghan TM, Douglas B, Drenkhan T, Eberhardt U, Dueñas M, Grebenc T, Griffith GW, Hartmann M, Kirk PM, Kohout P, Larsson E, Lindahl BD, Lücking R, Martín MP, Matheny PB, Nguyen NH, Niskanen T, Oja J, Peay KG, Peintner U, Peterson M, Põldmaa K, Saag L, Saar I, Schüßler A, Scott JA, Senés C, Smith ME, Suija A, Taylor DL, Telleria MT, Weiss M, Larsson K-H. Towards a unified paradigm for sequence-based identification of fungi. Mol Ecol. 2013 Nov;22(21):5271–7.

33. Xu ZZ, Amir A, Sanders J, Zhu Q, Morton JT, Bletz MC, Tripathi A, Huang S, McDonald D, Jiang L, Knight R. Calour: an interactive, microbe-centric analysis tool. mSystems. 2019 Feb 26;4(1).

34. Pedregosa F, Varoquaux G, Gramfort A, Michel V, Thirion B, Grisel O, Blondel M, Prettenhofer P, Weiss R, Dubourg V, Vanderplas J, Passos A, Cournapeau D, Brucher M, Perrot M, Duchesnay É. Scikit-learn: Machine Learning in Python. J Mach Learn Res. 2011;12(85):2825–30.

35. Wickham H. ggplot2 - Elegant Graphics for Data Analysis [Internet]. 1st ed. Springer-Verlag New York; 2009. 213 p. (Use R). Available from: https://www.springer.com/gp/book/9780387981413

36. Hunter JD. Matplotlib: a 2D graphics environment. Comput Sci Eng. 2007 May;9(3):90–5.

PATTERNS OF MICROBIAL SUCCESSION IN SKIN AND DECOMPOSITION-ASSOCIATED SOILS ARE PREDICTIVE OF THE POSTMORTEM INTERVAL OF HUMAN REMAINS

Summary

The human microbiome is highly diverse and serves numerous functional purposes during life. However, the loss of functional homeostasis after death leads to decomposition of the human remains, coupled with a shift in the microbial communities due to nutrient availability, temperature changes, and shifts in oxygen availability. As microbial groups take advantage of these changing environmental conditions, it leads to predictable patterns in how the communities assemble. This predictability of microbial taxonomic abundances then can be used to estimate the time since death, or postmortem interval (PMI). This study seeks to improve the understanding of this phenomenon by evaluating the patterns of microbial succession associated with human remains at three geographically distinct locations. The primary objectives were to (1) identify patterns in microbial diversity and taxonomy during human decomposition in skin and decomposition-associated soils across distinct environments and (2) determine the utility of amplicon sequencing-derived microbiome data in predicting the postmortem interval within the first 21 days of decomposition. To achieve these, a total of 36 donated human remains were decomposed across three anthropological research facilities (three per season per facility for four seasons) in distinct climactic regions of the United States. Microbial samples were collected from the skin of the face, skin of the hip, soil near the face, and soil near the hip daily for the first 21 days of decomposition. Samples were then sequenced for the 16S and 18S rRNA genes to evaluate the microbial community composition. Models to estimate PMI were generated using the Random Forest algorithm with nested cross-validation.

Results showed that the microbial diversity of decomposition soils decreased over time, likely due to environmental selection for specific organisms such as *Clostridiales, Pseudomonodales*, and *Xanthamonadales*. The environmental conditions of the anthropological research facilities used in this study led to distinct differences in microbial communities by location, but patterns of succession were

still present. Models constructed to predict PMI from the microbial community were accurate within 49 to 92.33 ADD, which is equivalent to 3 to 5.82 days. Models were more accurate when greater taxonomic resolution was used in training. Overall, these results demonstrate that the patterns of microbial succession are predictive of PMI, even across different environments.

Introduction

During life the vertebrate microbiome is highly diverse and works in symbiosis with the metabolic functions of the body to maintain a functional homeostasis. However, after death the loss of this homeostasis changes the environment; temperatures decrease and the loss of circulation changes oxygen and nutrient availability within and on the body. In outdoor terrestrial settings, the complex process of decomposition proceeds in relatively predictable patterns, as the remains move through stages generally described by their visual condition: early decomposition, active decay, and advanced decay [1]. Each of these stages is accompanied by distinct physiological changes; early decomposition is characterized by skin slippage, hair loss, and fluid purging, active by bloating and rupture, and advanced by tissue loss and partial skeletonization [2,3]. During these physiological changes of the remains, the microbial communities associated with both the remains and the decomposition-associated soils are also shifting as organisms take advantage to the sudden release of high-quality nutrients and changes in temperature and oxygen availability. The patterns in microbial succession observed during the decomposition process are likely highly conserved, as similar microbial functions have been required to breakdown vertebrate remains on evolutionary timescales. As a result, microbial ecology of decomposing vertebrates has been a subject of recent study demonstrating predictable patterns of microbial succession in mice, swine, and small-scale human experiments [4–7]. Recently, researchers have used machine learning algorithms to model these patterns, providing new information about the ecological trends and predicting the time since death of the remains [4,7–9,5]. In addition to increasing our knowledge of the decomposition environment, these advances have the potential to assist in forensic investigations.

In the field of forensic science, the time since death, or postmortem interval (PMI), is a critical metric as it can support the identification of victims or suspects, validate alibis, and aid in the distribution of death certificates. In the first 48 to 72 hours following death there are several tools available to death-scene investigators such as observation of rigor mortis, algor mortis, and livor mortis [10]. After these conditions have lapsed, though, investigators must rely on less accurate estimators such as forensic entomology and visual appraisal. Forensic entomology is one of the most commonly used methods for late-term PMI estimation under current standards; it involves an analysis of the insects, most commonly blowflies, that have colonized the remains and their life stage at the time of discovery [11,12]. These estimates are impacted by the knowledge and ability of an investigator to identify the insects precisely, the impact of environmental conditions such as air temperature and humidity on fly development, and the uncertainty surrounding how quickly the remains are colonized, leading to highly variable PMI predictions [13,14]. Given these limitations, there is a need for more accurate, additional methods to use in conjunction with this commonly applied method. Therefore, we investigate the potential for utilizing microbiome changes over decomposition as a forensic tool. Our objectives included (1) identify patterns in microbial diversity and taxonomy during human decomposition in skin and decomposition soils across distinct environments and (2) determine the utility of amplicon sequencing-derived microbiome data in predicting the postmortem interval within the first 21 days of decomposition.

Results and Discussion

Sequencing results

To evaluate the changes in the microbial community composition during decomposition, a total of 36 donated human remains were placed outdoors to decompose at three anthropological research stations in diverse regions on the United States throughout a year. At each facility, three cadavers were placed to decompose each season (spring, summer, fall, winter) to represent the environmental conditions of an entire year. Remains included in the study were all in the fresh stage of decomposition, had been stored in cooler conditions from the time of death to the time of placement, and had not undergone autopsy.

Beginning on the day of placement, sterile swabs were used to collect microbial samples from the skin of the face, skin of the hip, soil near the face, and soil near the hip of each set of remains, as well as a control soil sample from a site at the facility with no remains. Samples were collected for the first 21 days of decomposition, beginning the day of placement. The microbiome was evaluated using amplicon sequencing of the 16S and 18S rRNA genes following the Earth Microbiome Project protocols on the miSeq and hiSeq platform, respectively. In total, 4,139 samples were sequenced, including 592 negative and no-template controls. Sequencing resulted in a total of 89,288,561 16S rRNA partial gene reads and 1,543,472,127 18S rRNA partial gene reads. After denoising this resulted in 583,683 16S rRNA and 509,301 18S rRNA amplicon sequence variants (ASVs). The 16S rRNA data were filtered to removed sequences that represented chloroplasts and mitochondria, resulting in 518,835 total ASVs. The 18S rRNA data were filtered to remove sequences that represented Bacteria, Archaeplastida, Arthropoda, Chordata, Mollusca, and those that were unassigned, resulting in 105,522 total ASVs. Negative and no-template control samples were analyzed to determine contamination within the samples. Within the 16S rRNA dataset, the number of ASVs present in these samples ranged from 0 to 3,125, with an average of 114.38 ASVs/sample. These values were low abundance and below the threshold used for rarefaction, so the samples were considered uncontaminated. Within the 18S rRNA dataset the number of ASVs ranged from 0 to 14,971 with an average of 1,085.59 ASVs/sample which were generally in low abundance. The few controls that were above the rarefaction threshold clustered separately from samples on PCoA and have low alpha diversities, and so were also considered acceptable. Negative controls were also removed from the dataset for further analysis.

Patterns of microbial succession over time

The microbial communities associated with skin change dramatically during the decomposition period, a pattern primarily associated with the changes in oxygen availability and decomposition state. Bacterial diversity decreased from early to active and advanced decay, while eukaryotic phylogenetic diversity increased from early to active and advanced decay. This is consistent with data previously

reported in other studies that evaluated the postmortem skin microbiome [4,9,15]. The decrease in bacterial diversity can be explained by resource limitation as decomposition progressed and by a shift to more anaerobic organisms. During early decomposition, the microorganisms present in the internal tissues of the remains produce gasses during metabolism that fill the abdomen This environment allows for rapid growth of the anaerobic organisms present. As the soft tissues decay, these organisms are released, at which point they could be detected by the methods used in this experiment. The increase in eukaryotic diversity is likely due to a very low presence of microbial eukaryotes on living human tissue, leaving an open niche for these organisms as they assembled from the gravesoil during decomposition. These trends were further elucidated by the changes in specific organisms observed over time. Within these skin samples, *Bacteroidales* ($W = 216$), several orders within *Firmicutes* ($W = 216$), and *Gammaproteobacteria* ($W > 211$) organisms increased in abundance over time, while *Cardiobacteriales* ($W = 216$) increased in relative abundance during active decay and then decreased during advanced, as demonstrated by an analysis of composition of microbiomes. The skin environment does not become anaerobic during active decay, so many of the anaerobes that grow in the soil are not abundant in the skin communities. However, the increase in other copiotrophic organisms is expected and follows the patterns relating to nutrient presence and are likely migrating from the soil rather than originating from the skin. Therefore, it can be hypothesized that the nutrients and enteric anaerobes contributed by the remains influence the native soil microbes to cause a dynamic community shift that can be indicative of the decomposition timepoint.

The microbial diversity associated with gravesoils decreases over time, likely due to environmental selection for specific organisms. Microbial diversity data are presented in **Figure 5.1** (**A, B**). Initially, the microbial diversity was high, as is expected from environmental soil samples. After placement of the remains and the beginning of decomposition, the bacterial phylogenetic diversity decreased significantly ($P < 0.05$) during each stage of decomposition. Microbial eukaryotes had a lower diversity in initial soil samples, which was maintained throughout early. Then, diversity increased significantly ($P < 0.05$) during active decay before decreasing close to initial levels during advanced

decay. These results agree with those described by Metcalf *et al*. in a similar experiment [4]. It is well-established that soil harbors a diverse microbial community, but the input of concentrated nutrients can quickly alter the composition [16,17]. During vertebrate decomposition, nutrients, including amino acids, phospholipids, and sugars, are deposited into the soil and the release of fluids can create anaerobic micro-environment, altering the microbial growth conditions [18]. This nutrient pulse is the likely driver of the observed shift in diversity as organisms with the ability to metabolize these compounds dominate the community. The increase in eukaryotic diversity may be in response to growth in bacterial populations, as the bacterial cells themselves may provide nutrients to these organisms. Interestingly, the microbial communities of soil samples become more similar over time (**Fig. 5.1 C, D)** even as diversity increased, which suggests that, regardless of the initial microbial community, the postmortem microbiome will move towards a more consistent and conserved state, perhaps due to the consistent appearance of particular decomposition-associated taxa.

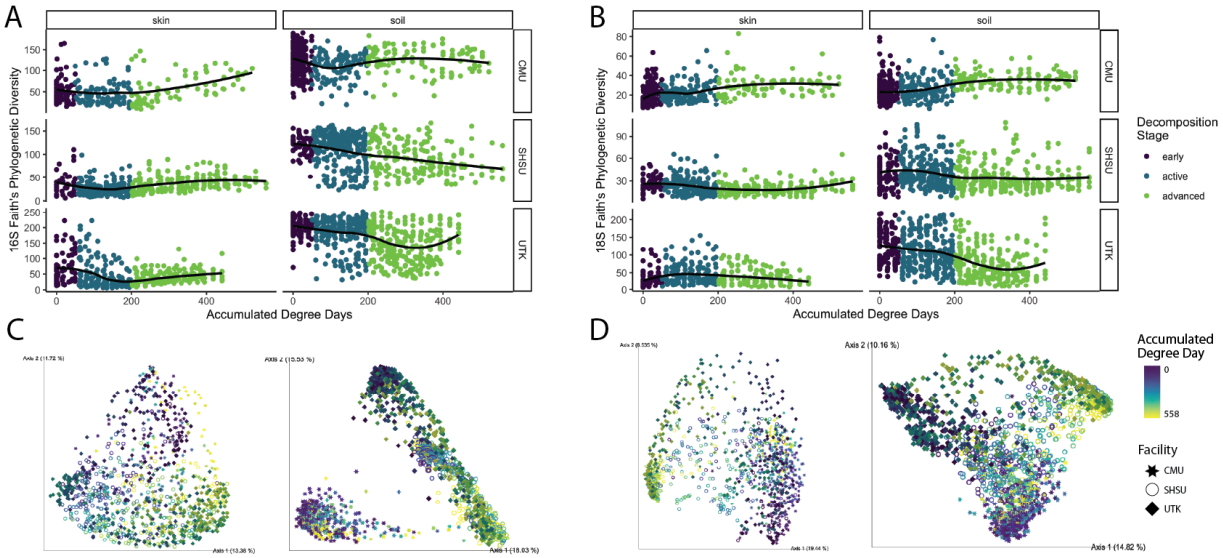

Figure 5.1. Microbial diversity patterns over time and environment. **A)** Phylogenetic alpha diversity changes in bacterial (16S) communities, in skin and soil, within three anthropological research facilities (Colorado Mesa University, CMU; Sam Houston State University, SHSU; University of Tennessee Knoxville, UTK). The horizontal axis uses accumulated degree day as proxy for days of decomposition, and graph is colored to represent distinct stages of decomposition. **B)** The phylogenetic alpha diversity changes in microbial eukaryotic (18S) communities in both skin and soil samples across research facilities. **C)** A principal coordinates analysis of bacterial community dissimilarity calculated using generalized Unifrac with a weight of 0.5 within skin (left) and soil (right) samples. Colors represent accumulated degree day and shapes represent the research facility. **D)** A principal coordinates analysis of microbial eukaryotic community dissimilarity within skin (left) and soil (right) samples.

This resource was prepared by the author(s) using Federal funds provided by the U.S. Department of Justice. Opinions or points of view expressed are those of the author(s) and do not necessarily reflect the official position or policies of the U.S. Department of Justice.

Microbial community assembly patterns were further confirmed with an analysis of deterministic processes. Pairwise comparisons were made between samples within a facility and decomposition stage using the ß-nearest taxon distance metric to demonstrate phylogenetic contributions to the community. These values were compared to null models that represent a phylogenetic community that would form due to chance to calculate the ß-nearest taxon index (ßNTI). Absolute values greater than 2 indicate that the difference between the communities is governed by deterministic processes, and less 2 indicates that the differences are stochastic. In this dataset, changes between samples in early decomposition were generally governed by homogenizing dispersal, which suggests that the environmental conditions (i.e. nutrient availability) drove microbial communities to become more similar than by random chance (**Fig. 5.2**). The observation of these processes during early decomposition further demonstrates the shift to a consistent microbial decomposition community within a facility over time. By advanced decay, the differences between communities were more stochastic, which shows less environmental pressure governing community assembly. Communities within a facility at this point have become similar due to the selective pressure of the decomposition environment, so variation is no longer driven by external conditions.

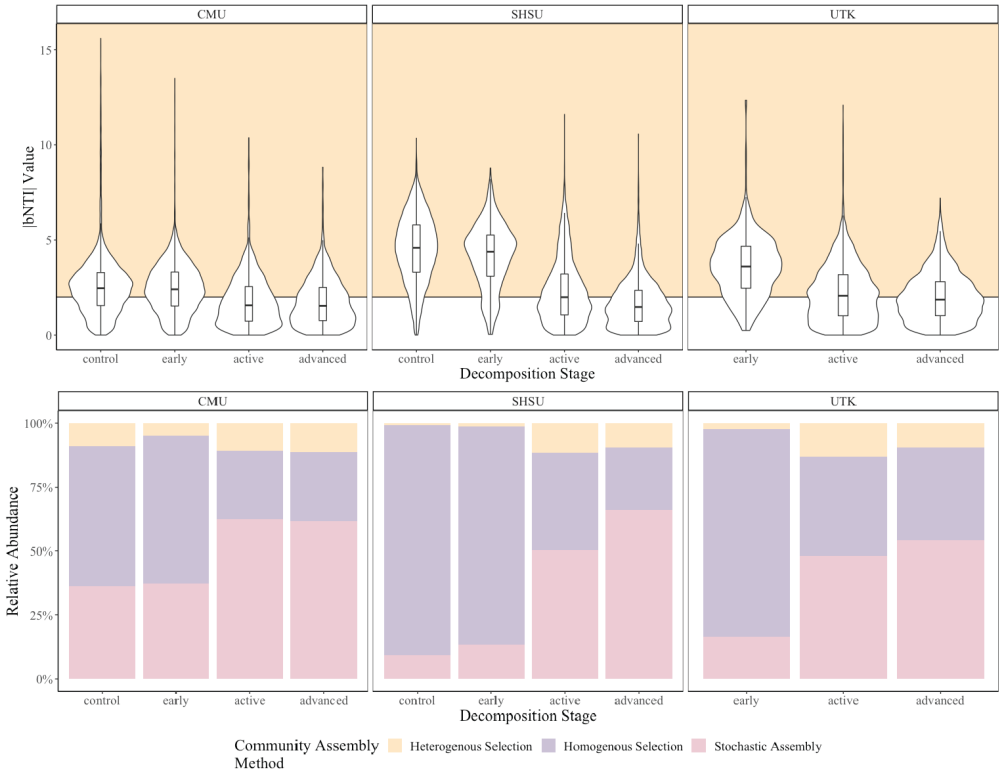

This resource was prepared by the author(s) using Federal funds provided by the U.S. Department of Justice. Opinions or points of view expressed are those of the author(s) and do not necessarily reflect the official position or policies of the U.S. Department of Justice.

Figure 5.2. ßNTI values representing comparison within facility and decomposition timepoints to demonstrate community selection patterns. Values greater than 2 (yellow) represent variable selection and values less than -2 (purple) represent homogenizing selection. Values between -2 and 2 (white) represent stochastic assembly.

The shift in taxonomic composition of the microbial community further demonstrates a microbial response to the input of concentrated nutrients. Moreover, the taxa that changed in abundance over time in the soil samples were very similar to those in the skin samples, indicating a likely transfer of organisms between the two sample types. Beginning after placement, *Clostridiales* ($W = 364$), *Pseudomonadales* ($W = 364$), *Xanthamonadales* ($W = 364$), *Bacteroidiales* ($W = 364$), *Enterobacteriales* ($W = 364$), *Lactobacillales* ($W = 364$), *Fusobacteriales* ($W = 364$), *Trichosporonales* ($W = 351$), and *Nematozoa* ($W = 348$) all increase in relative abundance through all stages, as demonstrated by the analysis of composition of microbiomes (**Fig. 5.3**). *Clostridiales, Pseudomonadales*, and *Xanthamonadales* are soil-associated organisms that are likely in lower relative abundance until nutrients are available; specifically, *Clostridia* are spore-forming organisms that can remain dormant until nutrients are sufficient to support growth, *Pseudomonodales* are important to the decarboxylation of amino acids leading to rapid growth during protein breakdown, and *Xanthamonadales* are slow-responding and will develop best in conditions of nutrient re-introduction [19,20]. *Lactobacillales* and *Fusobacteriales* are human-associated organisms that are likely introduced to the soil after gut rupture and thrive in the anaerobic micro-environment created by the decomposition fluids. Microbial eukaryotes, notably the *Nematozoa*, have previously been shown to alter microbial diversity by creating through predation of the bacteria [21]. The growth of these organisms, therefore, is both supported by and likely necessary for the assembly of the bacterial communities during decomposition. Another bacterial order, *Micrococcales*, decreased in abundance over time ($W = 364$). These oligotrophic organisms grow preferentially in low-nitrogen conditions, so it is likely the high-nitrogen environment created by decomposition of human remains inhibits growth of these organisms [22]. Finally, several microbial groups surged in relative abundance during the active decay stage, including *Cardiobacteriales* ($W = 364$), *Rhodobacterales* ($W = 364$), *Saccharomycetales* ($W = 351$), *Chaetothyriales* ($W = 351$), and *Filobasidiales* ($W = 351$). *Cardiobacteriales* have previously been

associated with high amounts of ammonia, which is likely accumulating in the soil following the metabolism of the organisms mentioned above [23]. These patterns in taxonomic shift agree with those previously reported in decomposition environments [4]. Overall, as microbial diversity decreases, the environment selects for the presence of specific taxa based on nutrient content and oxygen availability. These clear changes demonstrate succession patterns in the soil community composition.

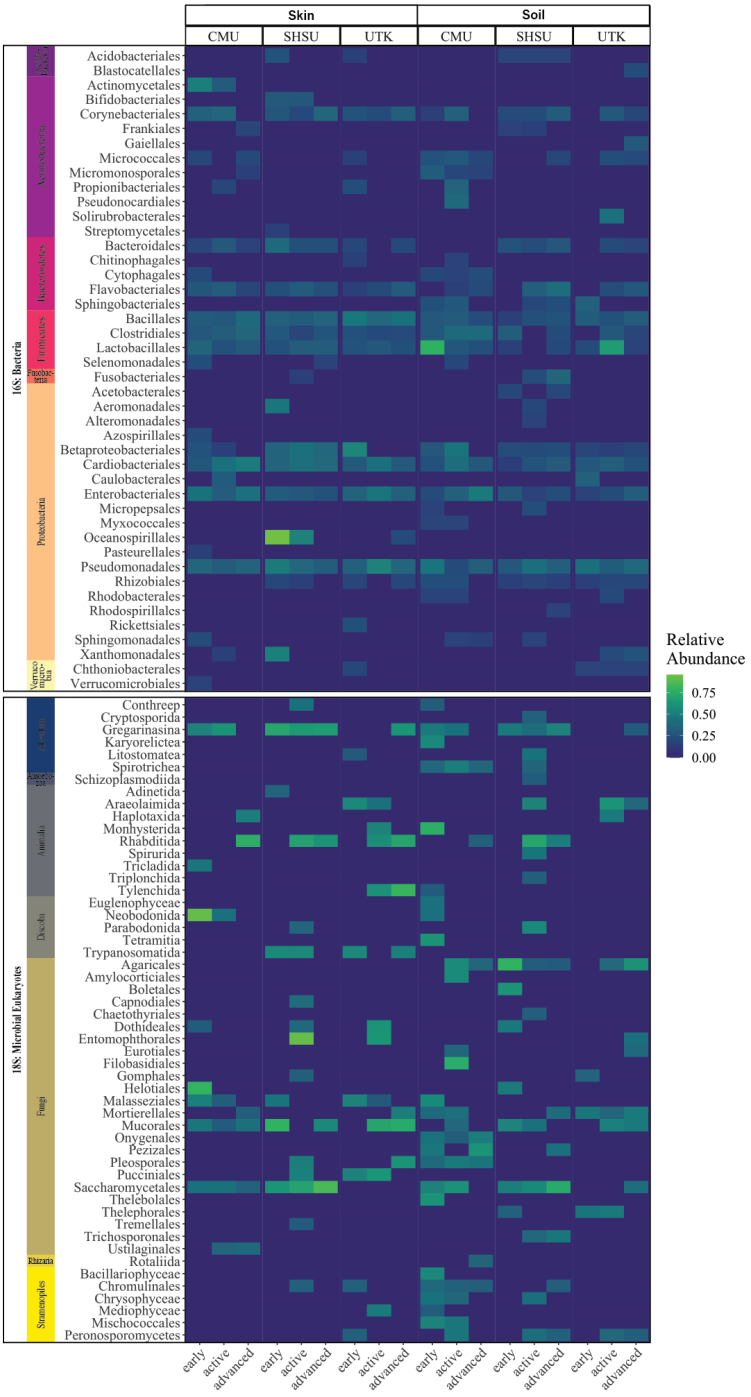

Figure 5.3. Relative abundances of microbial orders within a sample type and facility (Colorado Mesa University, CMU; Sam Houston State University, SHSU, University of Tennessee Knoxville, UTK). Bars on the left represent the microbial phyla. Top: Bacterial orders obtained from 16S rRNA gene sequencing. Bottom: Microbial eukaryotic orders obtained from 18S rRNA gene sequencing. Relative abundances of taxa in individual samples were averaged within a group and decomposition stage

Decomposition microbiomes are differentiated by environment

The environmental conditions of the anthropological research facilities used in this study were associated with distinct difference in microbial communities by location. The Colorado Mesa University Forensic Investigation Research Station (CMU) is located in a high-altitude desert, where the soil is sandy and contains low nutrient quality and sparse plants and the environment is generally low temperature and arid. Conversely both the Sam Houston State University Southeast Applied Forensic Science Facility (SHSU) and the University of Tennessee Knoxville Forensic Anthropology Center (UTK) are located in sub-tropical climates with high temperatures, mild to high humidity, and high-nutrient soils with vegetation and tree cover. This difference in environmental conditions is associate with distinct microbial community compositions between the locations. The beta diversity was calculated using a generalized UniFrac metric with a weight of 50% and visualized using a PCoA analysis (**Fig. 5.1B, 5.1C)**. The skin samples were relatively homogenous regardless of the facility. However, the soil samples clustered distinctly by facility, with the SHSU and UTK samples more similar to each other than to the CMU samples, especially in the 16S analysis. These clusters remain distinct over time, but soil microbiomes do appear to become more similar across facility as the decomposition period increased, which suggests that the differences across facility are likely driven by the initial microbial population, as opposed to distinct microbial succession patterns.

The distinct microbial community found at the CMU facility is more likely driven by the presence of specific organisms rather than overall diversity. To elucidate the inherent differences between facility, an analysis of only soil samples collected on the day of placement of the remains was conducted. An evaluation of the bacterial alpha diversity of these samples revealed that CMU was similar to SHSU based on a phylogenetic metric ($P > 0.05$) but had a significantly lower richness ($P < 0.05$). An analysis

of composition reveals several taxa that are differentially abundant between these facilities. Soils at CMU had a higher abundance of *Azospirillales*, *Deinococcales*, *Nostocales*, *Mitrotrichales*, and *Rhodobacterales*, which are generally oligotrophic organisms that are likely selected for in the low-nutrient soils. Soils at SHSU had a higher abundance of *Micropepsales,* which is associated with plant roots and may be selected for by the vegetation at the facility, *Acidobacteria* which may be associated with needles from the pine trees at the facility*,* and *Acetobacterales*. Both facilities exhibited lower ($P < 0.05$) diversity soil samples than UTK. But the difference in initial soil samples between SHSU and UTK must be quickly overcome, as the communities quickly become similar during decomposition. The alpha diversity of microbial eukaryotes was significantly different between all facilities for both methods ($P < 0.05$). The lowest diversity was at CMU and highest at UTK. The diversity of microbial eukaryotes has been shown to be less correlated to environmental conditions than prokaryotes but can still be influenced by soil pH and moisture, which may be driving this result [24]. It was also possible that the differences in initial soil microbiomes were driven by sampling bias at the facility; it was noted that there were different amounts of residual soil on swabs at different facilities, which could impact the diversity of organisms in the sample. To test whether this changed the outcomes, an analysis of bulk soil samples that were collected from control plots at the facilities during the experiment were sequenced following consistent methods across facility. In this analysis, the diversity of soil from CMU was still lower ($P < 0.05$) than the other facilities, but there was no difference between SHSU and UTK soil diversity ($P > 0.05$). So, while trends remain consistent, perhaps some differences between the two facilities were confounded by sampling bias. Overall, although there is still evidence of microbial succession during the decomposition period within each facility, the differences in microbial community composition driven by location and environment may impact the ability to predict decomposition time.

Predictive models to estimate postmortem interval

To determine the utility of an amplicon sequence model of microbial succession to predict PMI, machine learning models using the Random Forest algorithm were trained on both 16S and 18S data.

This resource was prepared by the author(s) using Federal funds provided by the U.S. Department of Justice. Opinions or points of view expressed are those of the author(s) and do not necessarily reflect the official position or policies of the U.S. Department of Justice.

These models were constructed using nested cross-validation to assess model accuracy and prevent overfitting. Models were trained for each sampling site (skin.face, skin.hip, soil.face, soil.hip) for each amplicon. Results showed that, overall, bacterial data were able to estimate PMI within 49.00 to 92.21 ADD, which is equivalent to approximately 3 to 5.8 days, and microbial eukaryote data were able to estimate PMI within 62.02 to 92.33 ADD, which is equivalent to 3.91 to 5.82 days (**Fig. 5.4**). These results are similar to those obtained in previous studies using machine learning to estimate PMI [4,9]. The bacterial models were generally more accurate than the eukaryotic models, which agrees with previous studies that also reported highly accurate bacterial models and lower accuracy in eukaryotic and fungal models [4,8].

Both bacterial and microbial eukaryotic models accurately predicted PMI at high taxonomic resolution. Models were constructed using taxonomic data at each level (i.e., phylum, class, order, etc.) to determine whether higher resolution improved the model, or whether the patterns were conserved at higher taxonomic orders. The most accurate models to predict PMI using skin bacteria were trained on species-level taxonomy and resulted in errors of 49 and 51.69 ADD for face and skin sites, respectively. The most accurate models to predict PMI using soil bacteria were trained on genus level, with best errors of 57.84 and 60.43 ADD for face and hip sites, respectively. Within microbial eukaryote models, the lowest (most accurate) general errors for each sample site were trained at the species-level taxonomy; 62.02, 67.43, 64.11, and 70.93 ADD for skin.face, skin.hip, soil.face, and soil.hip, respectively. Within all models the accuracy improved consistently with increased taxonomic resolution but remains very similar for genus- and species- level models. These results contradict those published in a recent meta-analysis, but could be explained by more homogenous samples (only human vs human and mice) and updated databases in the current study [8]. However, this pattern in accuracy has been previously reported, suggesting that the results seen here are reasonable [5]. These findings reflect that the accuracy of microbial succession models as a predictive tool is dependent on the quality of the databases.

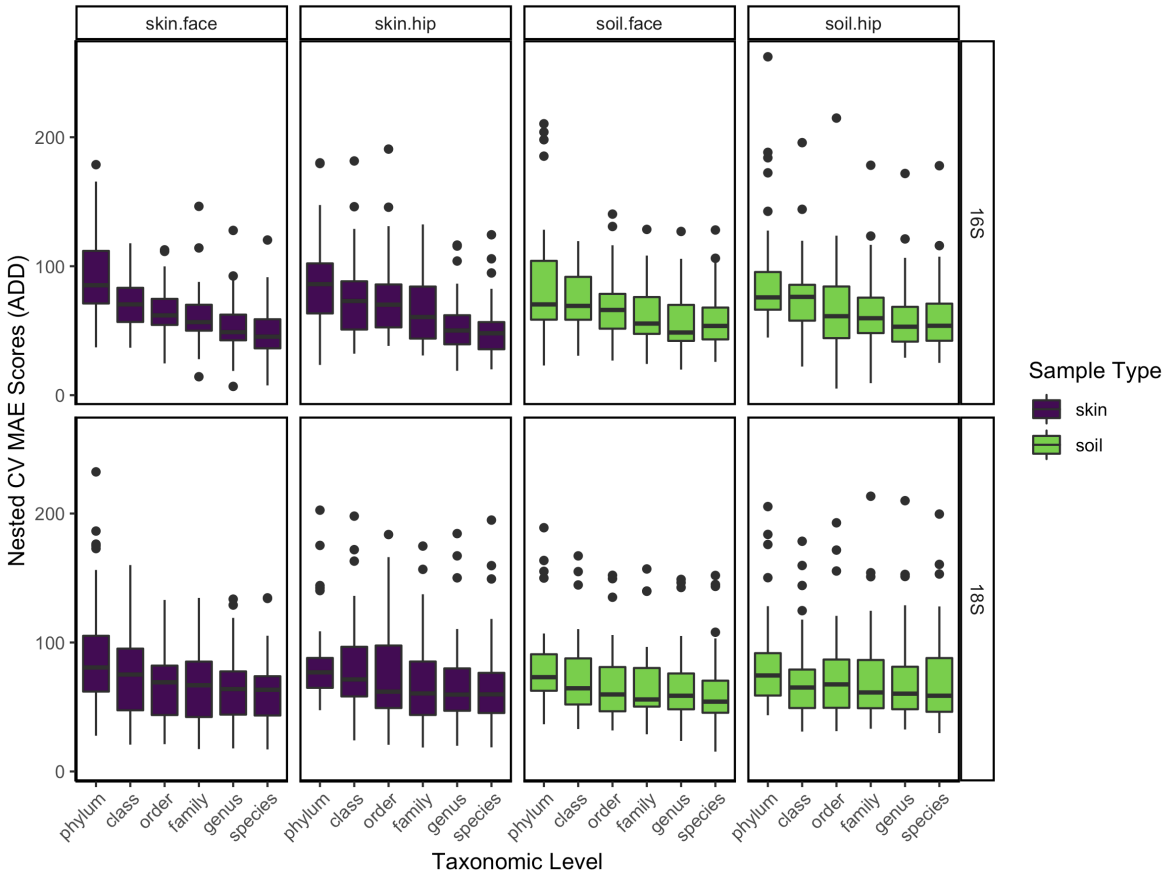

Figure 5.4. Nested cross-validation errors associated with random forest regression machine learning models. Models were trained on microbial abundance data at each taxonomic level to estimate the postmortem interval (PMI). PMI is represented by accumulated degree day as a proxy for days of decomposition.

Models generated from skin and soil samples resulted in similar accuracy, which suggests the patterns in microbial succession is similarly predictive regardless of sample site. The average of general errors for all bacterial models were 67.4 and 69.5 ADD and for all eukaryotic models were 73.4 and 72.4 ADD for skin and soil, respectively. The similar errors reflect the patterns seen in diversity and taxonomy; namely, that different organisms drove the succession patterns, but predictable succession still occurred within each group. Additionally, this further supports the hypothesis that microbes are migrating between skin and soil during the decomposition period, thus creating similar patterns between the two groups. Similarly, the difference between model errors for samples from the face vs hip was negligible, indicating that the same patterns in succession occur regardless of what position on or near the remains is

This resource was prepared by the author(s) using Federal funds provided by the U.S. Department of Justice. Opinions or points of view expressed are those of the author(s) and do not necessarily reflect the official position or policies of the U.S. Department of Justice.

sampled. Previous research has shown that, in living humans, the skin microbiome is distinct at different sampling sites; notable, navel samples clustering separately from forehead and hand samples [25]. If the living microbiome had a strong impact on the decomposition microbiome, therefore, it would be expected that the succession patterns would be different between the face and hip body sites in this experiment. That no major differences were observed suggests that the initial microbiome does not have a major impact on the decomposition environment, at least within a sample type (i.e. skin, soil). This also has implication for the use of these models to estimate PMI in forensic investigations. It will be simpler to instruct crime scene investigators in how to collect the appropriate samples for this analysis if precision is not necessary to achieve an accurate result. Moreover, this method could likely still be applied in situations where taking a sample from on specific point is not possible; for example, if there is no available skin at given location due to scavenger activity or the soil has been disturbed.

Amplicon data compared to metagenomic data to represent microbial succession

Models constructed using amplicon data can be a valuable tool to estimate PMI even when compared to shotgun metagenomics. It has been suggested that metagenomic data may be more useful in constructing accurate models as the data are less limited by the amplicon databases and information. However, metagenomic data are more expensive to produce due to greater sequencing requirements and are more complicated to process. In the same experimental samples used here but presented in a *in prep* study by Burcham *et al*, shallow shotgun sequencing was conducted on all of the skin.hip samples. This allowed for comparisons of diversity, taxonomy, and model accuracy with the 16S sequencing results to determine whether 16S rRNA gene sequencing accurately represents the microbial community. Correlation and Mantel testing was used to determine the similarities in diversity between the 16S and metagenomic data, and found that, overall, results of both methods were highly correlated, and the clustering patterns seen in the principal coordinates analysis were visually similar (**Fig. 5.5**). Moreover, both methods also identified similar microbial taxonomy, though the correlation was reduced as the resolution increased, which does demonstrate the limitations of amplicon sequencing methods. Models

trained using the metagenomic assignments resulted in an accuracy of 64.11, which can be compared to the soil.hip model from the amplicon data (MAE = 60.43). Therefore, despite less distinction in high-resolution taxonomy assignments, amplicon sequencing is a highly accurate measure for PMI from bacterial data.

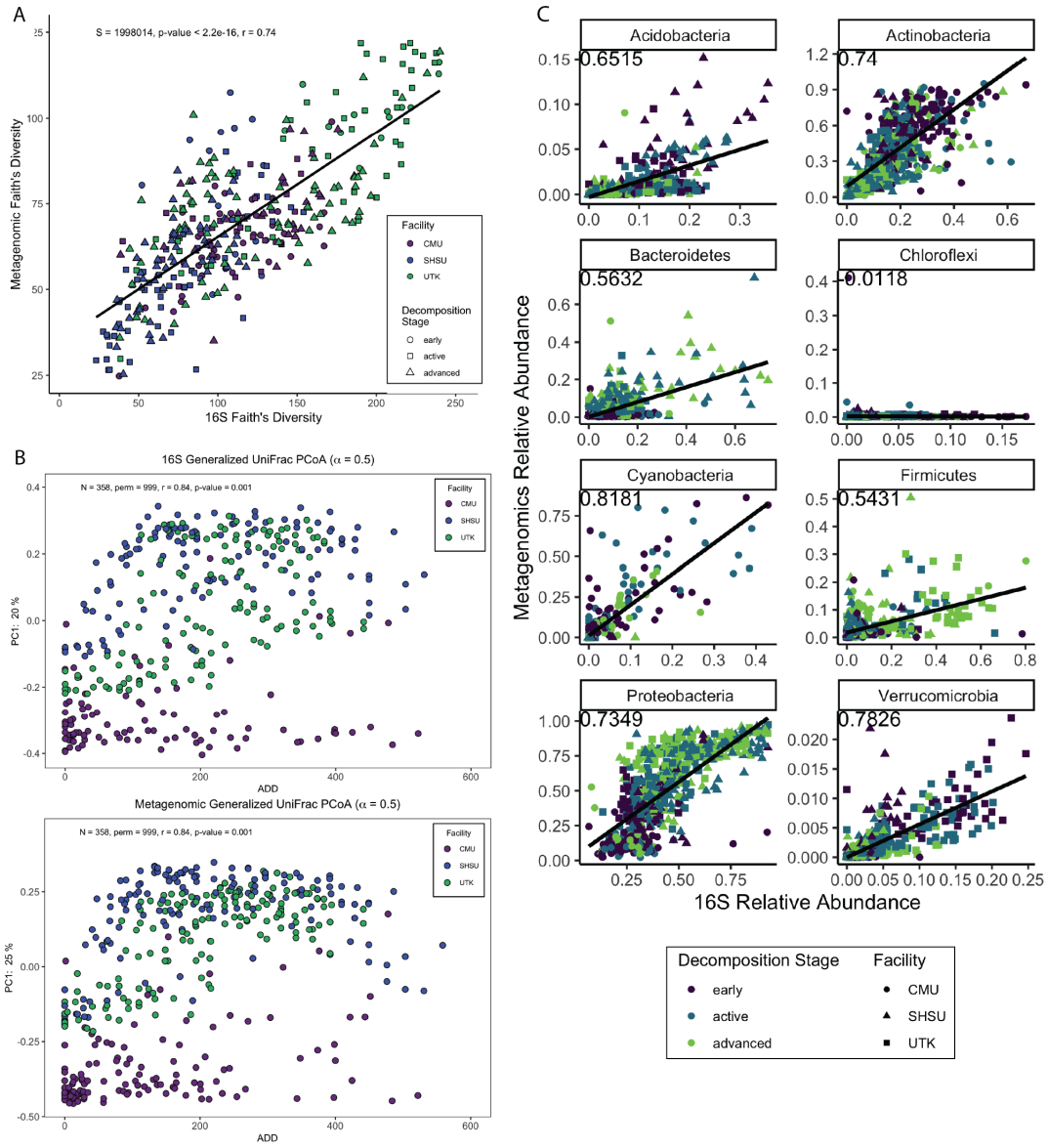

Figure 5.5. Correlations between 16S rRNA gene sequencing and shallow shotgun metagenomic sequencing data. **A)** Phylogenetic alpha diversity comparison using the Faith's diversity metric shows a correlation of 0.74. **B)** Beta diversity principal coordinates analysis measured by generalized Unifrac with a weight of 0.5 of 16S sequencing data (top) and metagenomic sequencing data (bottom) with the x-axis as accumulated degree day (ADD). Correlation between distance matrices was 0.84. **C)** Correlation in relative abundances of bacterial phyla between 16S data and metagenomic data.

Conclusions

This study confirms the existence of a predictable pattern of microbial succession within human decomposition environments. This pattern appears to be driven primarily by the addition of nutrients into the soil, which is followed by a change in the microbial community from primarily oligotrophic organisms to dominated by copiotrophs able to utilize the new metabolites being contributed. In early to active decomposition, deterministic processes drive microbial communities to become more similar within a location, which further confirms the formation of a consistent, predictable decomposition microbiome.

This conclusion is limited, however, by the use of amplicon sequencing data and should be confirmed by metagenomic and metabolomic study. The initial microbial community assembles based on location, with distinct environmental conditions altering the diversity and specific organisms present in a location. However, the process of microbial succession appears to occur regardless of initial microbiome. Models predicting PMI from these succession patterns were highly accurate but may not be easily extrapolated to environments beyond those included in this study. However, the addition of data from novel environments to the model will improve its utility as a forensic tool. Therefore, more study is necessary to establish amplicon sequencing as a universally applicable method for estimating PMI in forensic investigation.

Materials and Methods

Experimental Design and Sample Collection

To assess the patterns in microbial succession during decomposition in different locations, donated human remains were placed at three anthropological research facilities in environmentally distinct regions of the Unites States. The Colorado Mesa University Forensic Investigation Research Station (Grand Junction, CO; CMU) is located in a high-altitude arid environment, the Sam Houston State University Applied Anatomical Research Center (Huntsville, TX; SHSU) is located in a piney woods ecoregion with a humid subtropical climate and sparse forest covering, and the University of Tennessee

Knoxville Forensic Anthropology Center (Knoxville, TN; UTK) is located in a temperate region naturally forested with oak, maple, and hickory trees.

Twelve human remains were placed at each facility, four in each season to represent all climactic conditions within that location (n = 36). All remains were obtained through willed-body donation programs at the facilities, and inclusion criteria required that the remains were in the fresh stage of decomposition and were not be frozen or autopsied prior to placement at the facility. All remains were placed unclothed and prone in the outdoor facilities and allowed to decompose under natural conditions for 21 days, beginning on the day of placement. Samples were collected daily using sterile dual SWUBE swabs (BD; Franklin Lakes, NJ) taken from the skin of the face, skin of the hip, soil associated with the face, and soil associated with the hip, and soil from a control plot with no remains. Swabs were frozen immediately after sampling and were transported to the University of Colorado (Boulder, CO) at the conclusion of the sampling period for analysis. During the sampling period, additional metadata were measured and collected, including environmental data (temperature, humidity, soil temperature) and the condition of the remains (cause of death, initial body condition, Megyesi total body score, maggot presence, scavenging activity). In order to compare remains that were placed on different days and in different locations, accumulated degree day (ADD) was used as a proxy for day of decomposition to describe the postmortem interval (PMI). Accumulated degree day was calculated using a base of 0°C, where: Degree Day (DD) = (average temperature / 2) – base temperature and ADD = (DDx) + (DDx + 1), where x = 24h period.

DNA Extraction and Sequencing

To evaluate the microbial composition during the decomposition period, sampled were subjected to 16S and 18S rRNA gene sequencing, which provide information on bacteria and microbial eukaryote presence, respectively. DNA extraction and next generation sequencing library preparation were conducted at the University of Colorado (Boulder, CO) following Earth Microbiome Project protocols (EMP; www.earthmicrobiome.org/protocols-and-standards) [26]. DNA was extracted in 96-well plates

from one head of the two-headed swab taken at each sample site using the PowerSoil DNA Extraction Kit (Qiagen; Hilden, Germany) following manufacturer instructions. Each 96-well plate included eight negative control samples to evaluate the sequencing quality.

Following extraction, DNA extracts were transported to the Knight Lab at University of California San Diego (La Jolla, CA) for library preparation and sequencing. The total genomic DNA was amplified to target informative amplicons using PCR. For bacterial and archaeal testing, the V4 variable region of 16S rRNA gene was targeted using the EMP bacterial primer set 515f/806r (www.earthmicrobiome.org/protocols-and-standards/16s/). Microbial eukaryote sequences were targeted using the 18S rRNA gene with EMP primers Euk1391f and EukBr with an additional mammal blocking primer (www.earthmicrobiome.org/protocols-and-standards/18s/). For both 16S and 18S sequences, PCR products were quantified using Picogreen Quant-iT (Invitrogen, Life Technologies, Grand Island, NY) and pooled at equimolar concentrations. No-template controls were also included in the pools for each amplicon type. Each amplicon pool was purified using the UltraClean PCR Clean-up Kit (Qiagen; Hilden, Germany). 16S rRNA pools were sequenced using a 300-cycle kit on the Illumina miSeq sequencing platform (Illumina, San Diego, CA) and 18S pools using a 300-cycle kit on the Illumina hiSeq 2500 sequencing platform (Illumina, San Diego, CA).

Data Analysis

Microbial Ecology Analysis

After data generation, sequence data were analyzed in the Metcalf lab at Colorado State University (Fort Collins, CO) using the QIIME2 analysis platform versions 2020.2 and 2020.8 [27]. Sequences were quality-filtered and demultiplexed using error-corrected Golay barcodes to prevent misassignment. Reads were 150bp in length. Sequences were then classified into amplicon sequence variants (ASV) within a sequencing run using the deblur denoising method [28]. Feature tables and representative sequences obtained from denoising each sequencing run were then merged to create complete data for each amplicon method. Taxonomic identifiers were assigned to the ASVs using the

QIIME feature-classifier classify-sklearn [29]. For the 16S rRNA data these assignments were made using the SILVA 132 99% classifier for the 515f/806r gene sequence. ASVs that assigned to chloroplast or mitochondria were filtered out of the dataset before continuing analysis. For 18S rRNA data the RESCRIPt plugin to extract the full 14-level taxonomy from sequences matching the primers used in sequencing from the SILVA 138 99% database, dereplicate the extracted sequences, and train a classifier to assign labels to ASVs in the feature table [30]. This taxonomy was used to filter out ASVs that assigned to *Archaeplastida*, *Arthropoda*, *Chordata*, *Mollusca*, *Bacteria*, or were unassigned.

Microbial diversity metrics were generated for both amplicon types using the QIIME phylogenetic diversity plugin. The phylogenetic trees were constructed for each amplicon using the fragment-insertion sepp method [31] against the SILVA 128 99% reference tree. Alpha diversity metrics were calculated using the observed features and Faith's phylogenetic diversity formulas and statistical comparisons were made using the Kruskal-Wallis pairwise test with a Benjamini-Hockberg multiple-testing correction at an alpha of 0.05 [32]. To evaluate beta diversity, the generalized Unifrac method with a weight of 0.50 was used to calculate dissimilarity and statistical comparisons were made using PERMANOVA with multiple testing correction and an alpha level of 0.05 [33]. Taxonomy and alpha diversity visualizations were created using ggplot2 and the viridis package in R [34]. Beta diversity principal coordinate plots were constructed using the Emperor tool in QIIME2 [35]. Differential abundance testing was completed using the Analysis of Composition of Microbiomes function in QIIME2 [36].

To compare the detection of microbial succession patterns between amplicon and metagenomic data, metagenomic sequencing was conducted on the samples taken from soil near the hip during the same experiment. Metagenomic data and analyses are part of Burcham *et al*. (in prep). Correlations for alpha diversity metrics and taxonomy relative abundance information with the 16S rRNA gene sequencing outcomes were constructed using the cor.test() function in R and visualized using ggplot2 [34,37]. Correlations of dissimilarity matrices between shotgun sequencing data and 16S rRNA gene sequencing data were made using the Mantel test function in QIIME2 [38].

To determine whether microbial community assembly was governed by stochastic or deterministic processes, a pipeline developed by Danczak *et al.*, originally described in Stegen *et al.*, was used [39,40]. First, the ß-mean-nearest taxon distance (ßMNTD) was calculated to quantify the phylogenetic distance between each ASV in the community and its closest relative in a second community. Then, a randomization method shuffled ASV sequence and abundance across the tips of a phylogenetic tree and the ßMNTD was recalculated to give a null distribution. The difference between the observed ßMNTD and the null, referred to as the ß-nearest taxon index (ßNTI) was measured in units of standard deviation. A ßNTI value of <-2 indicates homogenous selection is occurring and a ßNTI value of >2 indicates variable selection, both of which are forms of deterministic structuring. Other values indicate stochastic processes are occurring in the community assembly.

Machine Learning Model Construction

To determine whether the microbial community composition could predict PMI, informative models were constructed using the machine learning algorithm Random Forest Regression. In construction of these models, the microbial data in biom format was used as the predictor and ADD was used as the response variable. Data were rarefied and imported into python using the Calour library [41].

Models were constructed with the Random Forest Regression algorithm with a nested k-fold cross-validation with hyperparameter tuning. Models were constructed with grouping so all data from each individual host (remains) was placed in a validation fold together. An outer validation with 36 folds was created using a leave-one-out method to estimate a general error. The inner validation was conducted by creating training and testing sets within the 35 remaining folds. The accuracy of these models was assessed during cross-validation and measured using the mean absolute error (MAE), calculated as the deviation of the predicted from observed values and represented in the same unit as the original data (ADD). The models with the lowest error after hyperparameter tuning were considered the most accurate. This method was applied to subsets of the data as was necessary to answer specific research questions.

Within the amplicon dataset, models were generated for each sampling site (skin.face, skin.hip, soil.face, soil.hip). These models were constructed using microbiome data at several levels of taxonomic resolution (ASV, species, genus, family, order, class, phylum) to determine which resolution resulted in the most accurate model. Facility was also included as a predictor feature in these models to adjust for distinct microbial signatures in different locations. Recursive feature elimination was used to determine which features contributed to the most accurate final model. All modeling was conducted using the python machine learning package scikit-learn v19.0 [42]. Results were visualized using ggplot2 in R [34].

REFERENCES

1. Goff ML. Early post-mortem changes and stages of decomposition in exposed cadavers. Exp Appl Acarol. 2009 Oct 1;49(1):21–36.

2. Carter DO, Yellowlees D, Tibbett M. Cadaver decomposition in terrestrial ecosystems. Naturwissenschaften. 2007 Jan 1;94(1):12–24.

3. Megyesi MS, Nawrocki SP, Haskell NH. Using accumulated degree-days to estimate the postmortem interval from decomposed human remains. J Forensic Sci. 2005 May;50(3):618–26.

4. Metcalf JL, Wegener Parfrey L, Gonzalez A, Lauber CL, Knights D, Ackermann G, Humphrey GC, Gebert MJ, Van Treuren W, Berg-Lyons D, Keepers K, Guo Y, Bullard J, Fierer N, Carter DO, Knight R. A microbial clock provides an accurate estimate of the postmortem interval in a mouse model system. Kolter R, editor. eLife. 2013 Oct 15;2:e01104.

5. Pechal JL, Crippen TL, Benbow ME, Tarone AM, Dowd S, Tomberlin JK. The potential use of bacterial community succession in forensics as described by high throughput metagenomic sequencing. Int J Legal Med. 2014 Jan;128(1):193–205.

6. Hyde ER, Haarmann DP, Petrosino JF, Lynne AM, Bucheli SR. Initial insights into bacterial succession during human decomposition. Int J Legal Med. 2015 May;129(3):661–71.

7. Metcalf JL, Xu ZZ, Weiss S, Lax S, Treuren WV, Hyde ER, Song SJ, Amir A, Larsen P, Sangwan N, Haarmann D, Humphrey GC, Ackermann G, Thompson LR, Lauber C, Bibat A, Nicholas C, Gebert MJ, Petrosino JF, Reed SC, Gilbert JA, Lynne AM, Bucheli SR, Carter DO, Knight R. Microbial community assembly and metabolic function during mammalian corpse decomposition. Science. 2016 Jan 8;351(6269):158–62.

8. Belk AD, Xu ZZ, Carter DO, Lynne A, Bucheli S, Knight R, Metcalf JL. Microbiome data accurately predicts the postmortem interval using random forest regression models. Genes. 2018 Feb;9(2):104.

9. Johnson HR, Trinidad DD, Guzman S, Khan Z, Parziale JV, DeBruyn JM, Lents NH. A machine learning approach for using the postmortem skin microbiome to estimate the postmortem interval. PLOS ONE. 2016 Dec 22;11(12):e0167370.

10. Shrestha R, Kanchan T, Krishan K. Methods Of Estimation Of Time Since Death. In: StatPearls. Treasure Island (FL): StatPearls Publishing; 2020.

11. Amendt J, Campobasso CP, Gaudry E, Reiter C, LeBlanc HN, Hall MJR, European Association for Forensic Entomology. Best practice in forensic entomology--standards and guidelines. Int J Legal Med. 2007 Mar;121(2):90–104.

12. Joseph I, Mathew DG, Sathyan P, Vargheese G. The use of insects in forensic investigations: An overview on the scope of forensic entomology. J Forensic Dent Sci. 2011;3(2):89–91.

13. Wells J, LaMotte L. The role of a PMI-prediction model in evaluating forensic entomology experimental design, the importance of covariates, and the utility of response variables for estimating time since death. Insects. 2017 May 1;8(2).

14. Sharma R, Kumar Garg R, Gaur JR. Various methods for the estimation of the post mortem interval from Calliphoridae: A review. Egypt J Forensic Sci. 2015 Mar 1;5(1):1–12.

15. Pechal JL, Schmidt CJ, Jordan HR, Benbow ME. A large-scale survey of the postmortem human microbiome, and its potential to provide insight into the living health condition. Sci Rep. 2018 Apr 10;8(1):5724.

16. Marschner P, Kandeler E, Marschner B. Structure and function of the soil microbial community in a long-term fertilizer experiment. Soil Biol Biochem. 2003 Mar 1;35(3):453–61.

17. Sradnick A, Murugan R, Oltmanns M, Raupp J, Joergensen RG. Changes in functional diversity of the soil microbial community in a heterogeneous sandy soil after long-term fertilization with cattle manure and mineral fertilizer. Appl Soil Ecol. 2013 Jan 1;63:23–8.

18. Quaggiotto M-M, Evans MJ, Higgins A, Strong C, Barton PS. Dynamic soil nutrient and moisture changes under decomposing vertebrate carcasses. Biogeochemistry. 2019 Nov 1;146(1):71–82.

19. Putten WH van der, Bradford MA, Brinkman EP, Voorde TFJ van de, Veen GF. Where, when and how plant–soil feedback matters in a changing world. Funct Ecol. 2016;30(7):1109–21.

20. Palmer JS, Hough RL, West HM, Avery LM. A review of the abundance, behaviour and detection of clostridial pathogens in agricultural soils. Eur J Soil Sci. 2019;70(4):911–29.

21. Jiang Y, Liu M, Zhang J, Chen Y, Chen X, Chen L, Li H, Zhang X-X, Sun B. Nematode grazing promotes bacterial community dynamics in soil at the aggregate level. ISME J. 2017 Dec;11(12):2705–17.

22. Cui Y, Fang L, Guo X, Wang X, Wang Y, Li P, Zhang Y, Zhang X. Responses of soil microbial communities to nutrient limitation in the desert-grassland ecological transition zone. Sci Total Environ. 2018 Nov 15;642:45–55.

23. Puig-Castellví F, Cardona L, Bureau C, Bouveresse DJ-R, Cordella CBY, Mazéas L, Rutledge DN, Chapleur O. Effect of ammonia exposure and acclimation on the performance and the microbiome of anaerobic digestion. Bioresour Technol Rep. 2020 Sep 1;11:100488.

24. Lanzén A, Epelde L, Blanco F, Martín I, Artetxe U, Garbisu C. Multi-targeted metagenetic analysis of the influence of climate and environmental parameters on soil microbial communities along an elevational gradient. Sci Rep. 2016 Jun 20;6(1):28257.

25. Costello EK, Lauber CL, Hamady M, Fierer N, Gordon JI, Knight R. Bacterial community variation in human body habitats across space and time. Science. 2009 Dec 18;326(5960):1694–7.

26. Gilbert JA, Jansson JK, Knight R. Earth Microbiome Project and global systems biology. mSystems. 2018 Jun 26;3(3).

27. Bolyen E, Rideout JR, Dillon MR, Bokulich NA, Abnet CC, Al-Ghalith GA, Alexander H, Alm EJ, Arumugam M, Asnicar F, Bai Y, Bisanz JE, Bittinger K, Brejnrod A, Brislawn CJ, Brown CT, Callahan BJ, Caraballo-Rodríguez AM, Chase J, Cope EK, Da Silva R, Diener C, Dorrestein PC, Douglas GM, Durall DM, Duvallet C, Edwardson CF, Ernst M, Estaki M, Fouquier J, Gauglitz JM, Gibbons SM, Gibson DL, Gonzalez A, Gorlick K, Guo J, Hillmann B, Holmes S, Holste H, Huttenhower C, Huttley GA, Janssen S, Jarmusch AK, Jiang L, Kaehler BD, Kang KB, Keefe CR, Keim P, Kelley ST, Knights D, Koester I, Kosciolek T, Kreps J, Langille MGI, Lee J, Ley R, Liu Y-X, Loftfield E, Lozupone C, Maher M, Marotz C, Martin BD, McDonald D, McIver LJ, Melnik AV, Metcalf JL, Morgan SC, Morton JT, Naimey AT, Navas-Molina JA, Nothias LF, Orchanian SB, Pearson T, Peoples SL, Petras D, Preuss ML, Pruesse E, Rasmussen LB, Rivers A, Robeson MS, Rosenthal P, Segata N, Shaffer M, Shiffer A, Sinha R, Song SJ, Spear JR, Swafford AD, Thompson LR, Torres PJ, Trinh P, Tripathi A, Turnbaugh PJ, Ul-Hasan S, van der Hooft JJJ, Vargas F, Vázquez-Baeza Y, Vogtmann E, von Hippel M, Walters W, Wan Y, Wang M, Warren J, Weber KC, Williamson CHD, Willis AD, Xu ZZ, Zaneveld JR, Zhang Y, Zhu Q, Knight R, Caporaso JG. Reproducible, interactive, scalable and extensible microbiome data science using QIIME 2. Nat Biotechnol. 2019 Aug;37(8):852–7.

28. Amir A, McDonald D, Navas-Molina JA, Kopylova E, Morton JT, Zech Xu Z, Kightley EP, Thompson LR, Hyde ER, Gonzalez A, Knight R. Deblur Rapidly Resolves Single-Nucleotide Community Sequence Patterns. mSystems. 2017 Mar 7;2(2).

29. Bokulich NA, Kaehler BD, Rideout JR, Dillon M, Bolyen E, Knight R, Huttley GA, Gregory Caporaso J. Optimizing taxonomic classification of marker-gene amplicon sequences with QIIME 2's q2-feature-classifier plugin. Microbiome. 2018 May 17;6(1):90.

30. Robeson MS, O'Rourke DR, Kaehler BD, Ziemski M, Dillon MR, Foster JT, Bokulich NA. RESCRIPt: Reproducible sequence taxonomy reference database management for the masses. bioRxiv. 2020 Oct 5;2020.10.05.326504.

31. Janssen S, McDonald D, Gonzalez A, Navas-Molina JA, Jiang L, Xu ZZ, Winker K, Kado DM, Orwoll E, Manary M, Mirarab S, Knight R. Phylogenetic placement of exact amplicon sequences improves associations with clinical information. mSystems. 2018 Jun 26;3(3).

32. Kruskal WH, Wallis WA. Use of ranks in one-criterion variance analysis. J Am Stat Assoc. 1952;47(260):583–621.

33. Anderson MJ. A new method for non-parametric multivariate analysis of variance. Austral Ecol. 2001;26(1):32–46.

34. Wickham H. ggplot2 - Elegant Graphics for Data Analysis [Internet]. 1st ed. Springer-Verlag New York; 2009. 213 p. (Use R). Available from: https://www.springer.com/gp/book/9780387981413

35. Vázquez-Baeza Y, Pirrung M, Gonzalez A, Knight R. EMPeror: a tool for visualizing high-throughput microbial community data. GigaScience. 2013 Dec 1;2(2047-217X-2–16).

36. Mandal S, Van Treuren W, White RA, Eggesbø M, Knight R, Peddada SD. Analysis of composition of microbiomes: a novel method for studying microbial composition. Microb Ecol Health Dis. 2015;26(1):27663.

37. Yu D, Zhang Z, Glass K, Su J, DeMeo DL, Tantisira K, Weiss ST, Qiu W. New statistical methods for constructing robust differential correlation networks. Sci Rep. 2019;9:3499.

38. Mantel N. The detection of disease clustering and a generalized regression approach. Cancer Res. 1967;27(2 Part 1):209–20.

39. Danczak R. Modified bNTI script for Shale S3 [Internet]. GitHub. Available from: https://github.com/danczakre/ShaleViralEcology

40. Stegen JC, Lin X, Fredrickson JK, Chen X, Kennedy DW, Murray CJ, Rockhold ML, Konopka A. Quantifying community assembly processes and identifying features that impose them. ISME J. 2013 Nov;7(11):2069–79.

41. Xu ZZ, Amir A, Sanders J, Zhu Q, Morton JT, Bletz MC, Tripathi A, Huang S, McDonald D, Jiang L, Knight R. Calour: an interactive, microbe-centric analysis tool. mSystems. 2019 Feb 26;4(1).

42. Pedregosa F, Varoquaux G, Gramfort A, Michel V, Thirion B, Grisel O, Blondel M, Prettenhofer P, Weiss R, Dubourg V, Vanderplas J, Passos A, Cournapeau D, Brucher M, Perrot M, Duchesnay É. Scikit-learn: Machine Learning in Python. J Mach Learn Res. 2011;12(85):2825–30.

CONCLUSIONS

The studies in this dissertation range a wide variety of research fields and industries, from built environment design to forensic science. In this work, I first demonstrated how microbial communities assemble in food processing facilities, showing that the microbiome present within the facilities is closely linked to the site of introduction, the temperature and other environmental conditions in a space, and the physical barriers separating rooms of different functions. Then, I presented our research on the microbiome of chicken spoilage, and how it can be impacted by the chilling method. This research could lead to improvements in product shelf-life and reduction of food waste due to spoilage. Finally, I show two research projects that investigate the patterns of microbial succession in postmortem remains and associated soils. These studies present novel findings regarding the mechanisms by which microbial communities assemble in postmortem environments, the microbial role in nutrient cycling during vertebrate decomposition, and the potential relationships between specific organisms and their environments. These data also demonstrate the utility of microbial succession patterns as a forensic investigation tool to estimate the postmortem interval of human remains.

Despite the diversity of these experiments, they all provide insight about how microbial communities assemble in different environments and how nutrient availability and environmental conditions impact microbial succession over time. In two of these studies, I demonstrate potential routes by which microbes are introduced to the environmental systems. In a meat processing facility, the animals and human employees of the space introduce organisms from feces and skin. In decomposition environments, evidence suggests that the microorganisms are already present in the environment. The microorganisms associated with the host are introduced into this environment, but the human signature is lost during the decomposition period. There are several differences between these environments that contribute to the differences in microbial origin and the persistence of the signature. Foremost is likely the cleanliness of the environment, as the meat processing facility is cleaned and sanitized daily, and the microbial diversity of the environment. But, taken together, these studies show that microbes present in an

environment are introduced by occupants of the environment, but the background communities can drive whether the newly introduced organisms remain part of the community.

Patterns in microbial succession are also evident in all of the studies in this dissertation. Microbial communities in a given space change over time, but how they change is driven by the environment. Sudden shifts or pulses in nutrients cause different organisms to dominate. For example, during human decomposition the input of high-quality nutrients into the soil from the remains cause a bloom in copiotrophic organisms such as *Clostridiales* and *Xanthamonadales*. In the other environments presented here, nutrient availability is more consistent, leading to fewer changes in the community based on the organism metabolism. However, I also showed the impact of other environmental factors on community succession. Temperature is an important variable for community formation. In the meat processing environment, the microbial communities assembled differently based on the room function, with one of the major differences between these spaces being room temperature. In cold rooms, *Pseudomonas* and other thermophilic organisms dominated the community, while animal-associated organisms thrived in warm spaces. In chicken spoilage environments, both temperature and nutrients contribute to the community. The high-protein environment coupled with chilled produce in aerobic packaging also contributed to the dominance of *Pseudomonas* in the decomposition community.

Interestingly, the microbiome of decay is similar, regardless of the decomposition environment. In both chicken product spoilage and human decomposition, the microbial community formation is driven by nutrients, oxygen availability, and temperature, as described above. Moreover, similar organisms are involved in decomposition, as similar metabolisms must be present in both situations. Namely, proteolysis must occur to fully breakdown the remains, which makes organisms like *Pseudomonas* spp very important to the microbial community. The human decomposition microbiome is more diverse, especially due to the contribution of soil microorganisms, which are intentionally excluded from chicken spoilage environments. The decreased diversity in chicken products contributed to *Pseudomonas* dominating the environment while the human decomposition environments maintain a broader community.

In this dissertation, I demonstrate that studies from multiple fields can be combined to answer important ecological research questions. Moreover, I present practical applications for our understanding of microbial ecology. Future research based on these studies could inform the future of food processing facility design, poultry processing systems, food waste reduction, and forensic investigations. I also further establish the value of microbiome analysis as a research tool to answer questions across disciplines.

APPENDIX A: CHAPTER 3 SUPPLEMENTARY MATERIALS

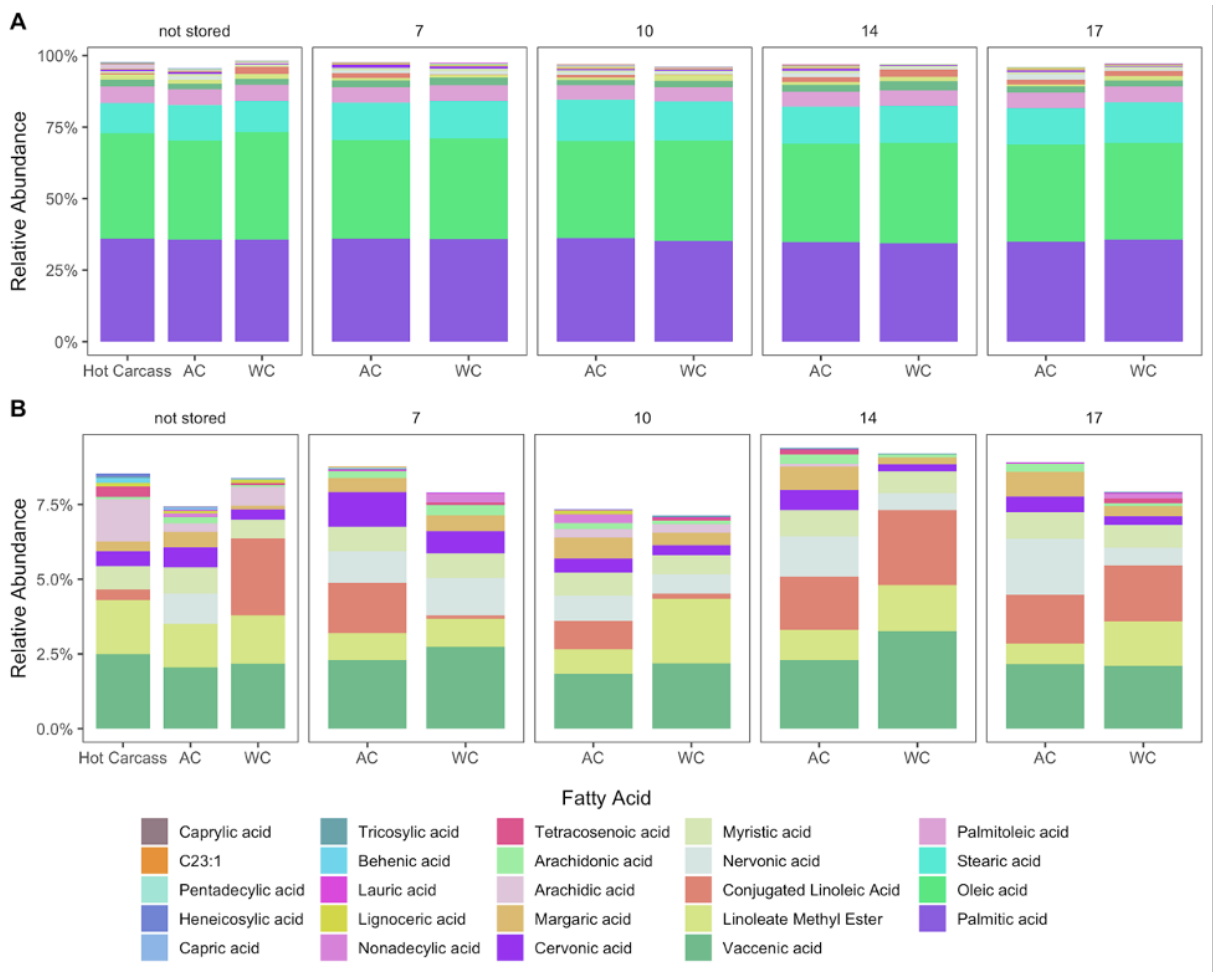

SI Figure 3.1. Relative abundances of fatty acids present in air (AC) and water chilled (WC) chicken meat. A) All fatty acids present in the samples. B) The 'rare' fatty acids present at <10% relative abundance.

This resource was prepared by the author(s) using Federal funds provided by the U.S. Department of Justice. Opinions or points of view expressed are those of the author(s) and do not necessarily reflect the official position or policies of the U.S. Department of Justice.

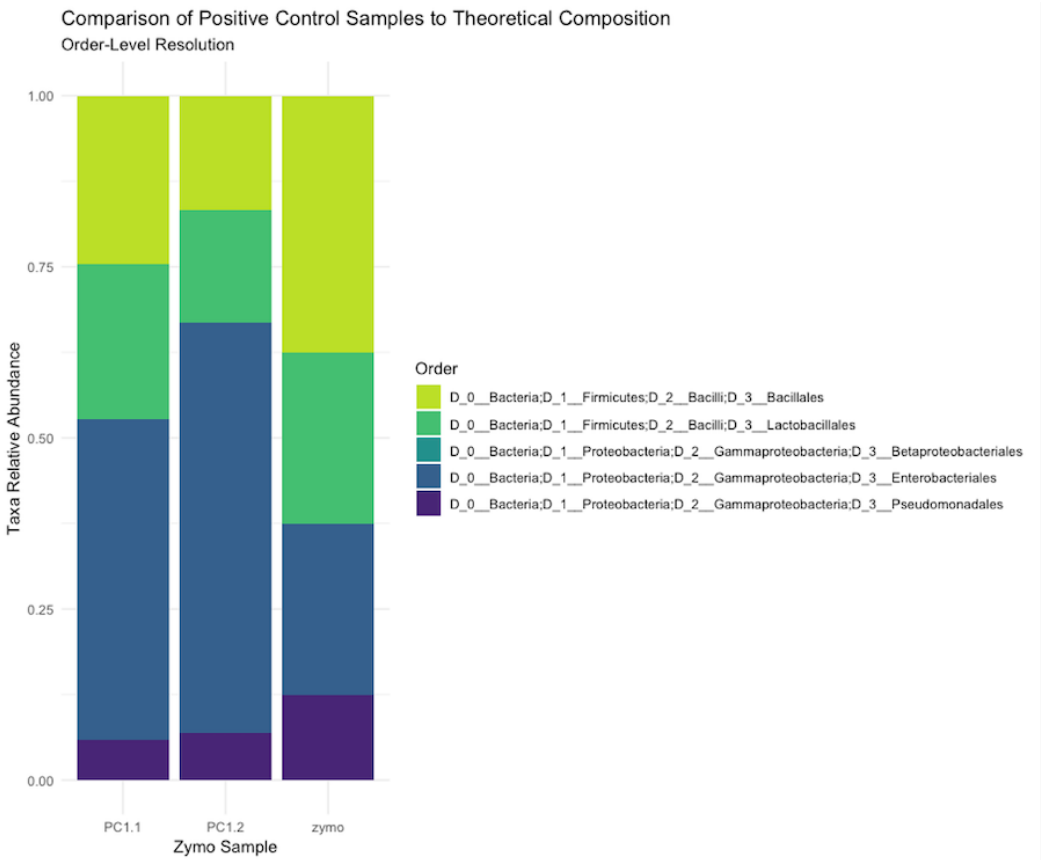

SI Figure 3.2. A comparison of positive control samples (ZymoBIOMICS D6300) and the standard expected composition as described by the company.

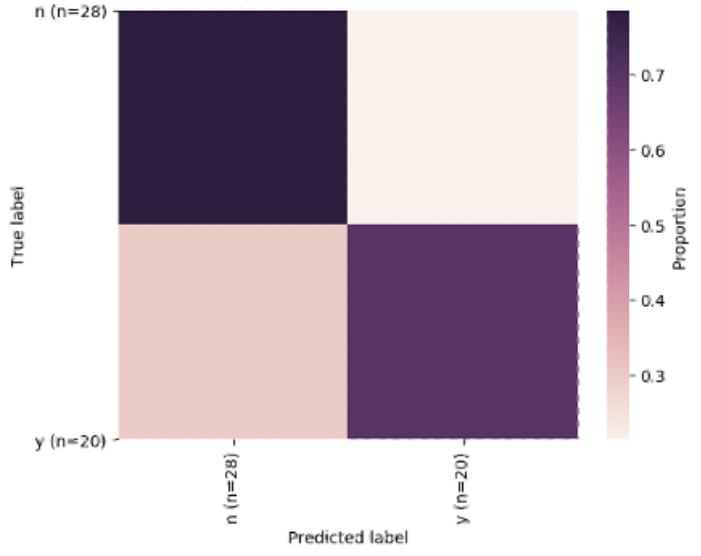

SI Figure 3.3. Model prediction errors using the microbiome data as a predictor and spoilage indicators as response variables. Model predicting whether the product has reached a spoilage state based on psychrotrophic bacterial counts. Model testing resulted in an accuracy score of 75%.

This resource was prepared by the author(s) using Federal funds provided by the U.S. Department of Justice. Opinions or points of view expressed are those of the author(s) and do not necessarily reflect the official position or policies of the U.S. Department of Justice.

SI Figure 3.4. Phylogenetic tree showing the evolutionary relationship between ASVs found in this study that assigned to the *Pseudomonas* genus.

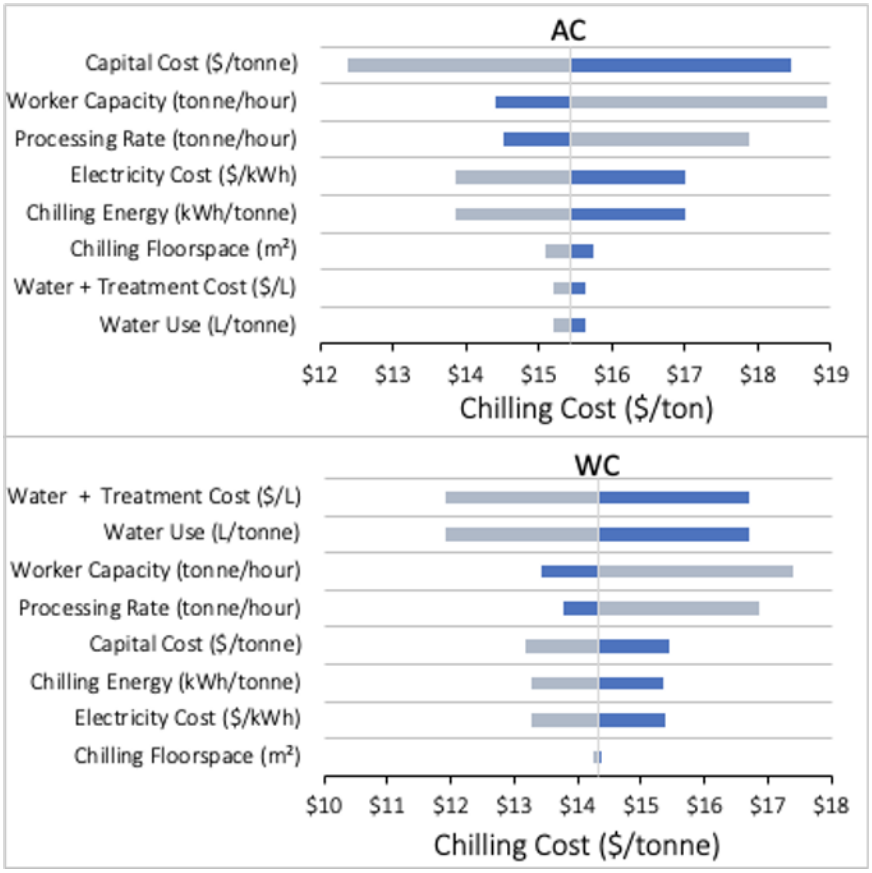

SI Figure 3.5. The sensitivity analyses varied the following model values by ±50%: capital cost ($/tonne), chilling floorspace (m^2), processing rate (tonne/hour), chilling energy (kWh/tonne), worker capacity (tonne/hour), water use (L/tonne), water price plus water treatment cost ($/L), and electricity cost ($/kWh). The resulting levelized costs for AC (upper panel) and WC (lower panel) systems demonstrate which aspects of each system have the most influence over the total levelized cost of chilling. For AC systems capital costs and labor costs have the most impact on the total levelized chilling cost, while water and labor costs have the most impact on WC systems.

SI table 3.1. Average weight loss of chicken carcasses prior to and following chilling by either air chilling (AC) or water chilling (WC). On average the WC carcasses gained 5% of their pre-chilling weight while AC carcasses lost 1.6% of their pre-chill weight.

Time	Air Chilled	Water Chilled
Pre-Chilling weight (g)	1966.53	2008.51
Post-Chilling weight (g)	1933.33	2115.30
Total weight lost or gain (g)	-33.2	+106.79

This resource was prepared by the author(s) using Federal funds provided by the U.S. Department of Justice. Opinions or points of view expressed are those of the author(s) and do not necessarily reflect the official position or policies of the U.S. Department of Justice.

SI Table 3.2. Least square means of Mesophilic bacterial counts (log cfu/g) for bone-in and boneless chicken breast cooled by either air chilling or water chilling pre- and post-fabrication, pre and post chilling, during storage, during and after display.
a-e Least square within a column with different superscripts differ (P<0.05)

		Springiness	Cohesiveness of Mass	Moistness	Chicken Flavor Intensity	Off Flavor Intensity
AC	Bone-in	54.8 (1.83)^{A}	51.2 (2.01)^{A}	52.9 (2.26)^{A}	63.5 (1.58)^{A}	3.04 (0.77)^{A}
	Boneless	53.3 (1.83)^{A}	52.2 (2.01)^{A}	46.0 (2.26)^{A}	61.5 (1.58)^{A}	3.33 (0.77)^{A}
WC	Bone-in	56.6 (1.83)^{A}	52.9 (2.01)^{A}	51.7 (2.26)^{A}	61.3 (1.58)^{A}	2.17 (0.77)^{A}
	Boneless	53.7 (1.83)^{A}	52.4 (2.01)^{A}	47.2 (2.26)^{A}	61.1 (1.58)^{A}	3.08 (0.77)^{A}

	Odor Selection	Purchase Decision
Phase One		
Water-chill bone-in	2.54^{a} (0.08)	8.37^{a} (0.10)
Water-chill boneless	2.47^{a} (0.08)	8.24^{ab} (0.10)
Air-chill bone-in	2.32^{b} (0.08)	8.17^{b} (0.10)
Air-chill boneless	2.00^{c} (0.08)	7.62^{c} (0.10)
Phase Two		
Water-chill	2.91^{a} (0.06)	8.93^{a} (0.08)
Air-chill	2.67^{b} (0.06)	8.64^{b} (0.08)

SI Table 3.3. Trained panelists were asked to evaluate chicken breasts for texture and flavor attributes on a 100-point scale. Within a column, values with the same letter were not significantly different ($P > 0.05$).

Time	Fabrication	
	Bone-in (BI)	**Boneless (BL)**
Pre-Fabrication (D00)	4.01^{b} (0.10)	4.01^{b} (0.12)
Post-Fabrication (D0)	4.32^{b} (0.10)	3.11^{a} (0.12)
7 day – storage (D7)	4.80^{c} (0.09)	3.58^{ab} (0.12)
End of Display (D10)	6.44^{d} (0.11)	5.01^{c} (0.12)
14 day – storage (D14)	7.15^{e} (0.09)	6.12^{d} (0.12)
End of Display (D18)	7.30^{e} (0.09)	6.72^{e} (0.12)

SI Table 3.4. Analysis of nutrient composition (proximate analysis) values. Data are organized first by chilling method, including hot carcass (HC), air chilled (AC) and water chilled (WC) samples. Within day, data are then organized by sampling day, which includes not stored (day 0), 7 or 14 days of dark storage, and 3 days of retail display after removal from dark storage (day 10 and day 17). Within day, data is organized by fabrication method, including unfabricated carcass, bone-in breasts, and boneless breasts. Values with the same letter within a column are not significantly different (P > 0.05).

			Dry Matter	Moisture	Ash	Crude Fat
HC	**Day 0**	Carcass	25.8 (0.337) A	74.2 (0.337) B	1.095 (0.061) AB	1.270 (0.085) G
AC	**Day 0**	Carcass	25.8 (0.477) AB	74.2 (0.477) AB	0.965 (0.086) AB	1.191 (0.120) EFG
		Bone-in	28.3 (0.477) AB	71.7 (0.477) A	1.140 (0.086) AB	1.429 (0.121) G
		Boneless	24.7 (0.477) A	75.3 (0.477) B	1.075 (0.086) AB	0.481 (0.121) ABC
	Day 7	Bone-in	27.0 (0.477) AB	73.0 (0.477) AB	1.195 (0.086) AB	1.178 (0.121) DEFG
		Boneless	25.1 (0.477) A	74.9 (0.477) B	1.250 (0.086) AB	0.506 (0.121) ABCD
	Day 10	Bone-in	26.9 (0.477) AB	73.1 (0.477) AB	1.078 (0.086) AB	1.089 (0.121) BCDEFG
		Boneless	25.2 (0.477) A	74.8 (0.477) B	1.158 (0.086) AB	0.445 (0.121) ABC
	Day 14	Bone-in	27.2 (0.502) AB	72.8 (0.502) AB	1.015 (0.091) AB	1.201 (0.127) DEFG
		Boneless	25.4 (0.477) A	74.6 (0.477) B	1.126 (0.086) AB	0.415 (0.120) AB
	Day 17	Bone-in	26.7 (0.477) AB	73.3 (0.477) AB	0.940 (0.086) A	1.033 (0.121) ABCDEFG
		Boneless	26.9 (0.477) AB	73.1 (0.477) AB	1.440 (0.086) AB	0.589 (0.121) ABCDEF
WC	**Day 0**	Carcass	25.6 (0.477) AB	74.4 (0.477) AB	1.160 (0.086) AB	1.109 (0.121) CDEFG
		Bone-in	26.3 (0.502) AB	73.7 (0.502) AB	1.077 (0.091) AB	1.131 (0.127) CDEFG
		Boneless	25.0 (0.477) A	75.0 (0.477) B	1.366 (0.091) AB	0.353 0.1207 A
	Day 7	Bone-in	27.1 (0.477) AB	72.9 (0.477) AB	1.164 (0.086) AB	1.260 (0.121) FG
		Boneless	24.9 (0.477) A	75.1 (0.477) B	1.327 (0.086) AB	0.543 (0.121) ABCDE
	Day 10	Bone-in	27.4 (0.502) AB	72.6 (0.502) AB	1.226 (0.091) AB	1.188 (0.127) DEFG
		Boneless	25.4 (0.502) A	74.6 (0.502) B	1.210 (0.091) AB	0.426 (0.127) ABC
	Day 14	Bone-in	26.5 (0.477) AB	73.5 (0.477) AB	1.250 (0.086) AB	1.092 (0.121) BCDEFG
		Boneless	25.5 (0.477) A	74.5 (0.477) B	1.223 (0.086) AB	0.484 (0.121) ABC
	Day 17	Bone-in	26.8 (0.477) AB	73.2 (0.477) AB	1.062 (0.086) AB	0.986 (0.1207) ABCDEFG
		Boneless	25.4 (0.477) A	74.6 (0.477) B	1.347 (0.086) B	0.412 (0.1207) AB

SI Table 3.5. The most abundant *Pseudomonas*-associated ASVs associated with each chilling and storage group. The relative abundance of each ASV was averaged across samples within the group.

Day	Chilling Method	ASV	Average Percent
10	AC	ASV10	0.017998
10	AC	ASV20	0.000684
10	AC	ASV7	0.054059
10	WC	ASV10	0.164519
10	WC	ASV20	0.003918
10	WC	ASV7	0.001833
14	AC	ASV10	0.039777
14	AC	ASV20	0.00117
14	AC	ASV7	0.049584
14	WC	ASV10	0.188287
14	WC	ASV20	0.013212
14	WC	ASV7	0
17	AC	ASV10	0.035419
17	AC	ASV20	0
17	AC	ASV7	0.02821
17	WC	ASV10	0.094772
17	WC	ASV20	0.00855
17	WC	ASV7	0.001355
7	AC	ASV10	0.012105
7	AC	ASV20	0
7	AC	ASV7	0.146024
7	WC	ASV10	0.076009
7	WC	ASV20	0.001751
7	WC	ASV7	0.0021
not stored	AC	ASV10	0.01177
not stored	AC	ASV20	0
not stored	AC	ASV7	0.002082
not stored	Hot Carcass	ASV10	0.005359
not stored	Hot Carcass	ASV20	0
not stored	Hot Carcass	ASV7	0.005298
not stored	WC	ASV10	0.002398
not stored	WC	ASV20	0
not stored	WC	ASV7	0.012768

This resource was prepared by the author(s) using Federal funds provided by the U.S. Department of Justice. Opinions or points of view expressed are those of the author(s) and do not necessarily reflect the official position or policies of the U.S. Department of Justice.

APPENDIX B CHAPTER 4 SUPPLEMENTARY MATERIALS

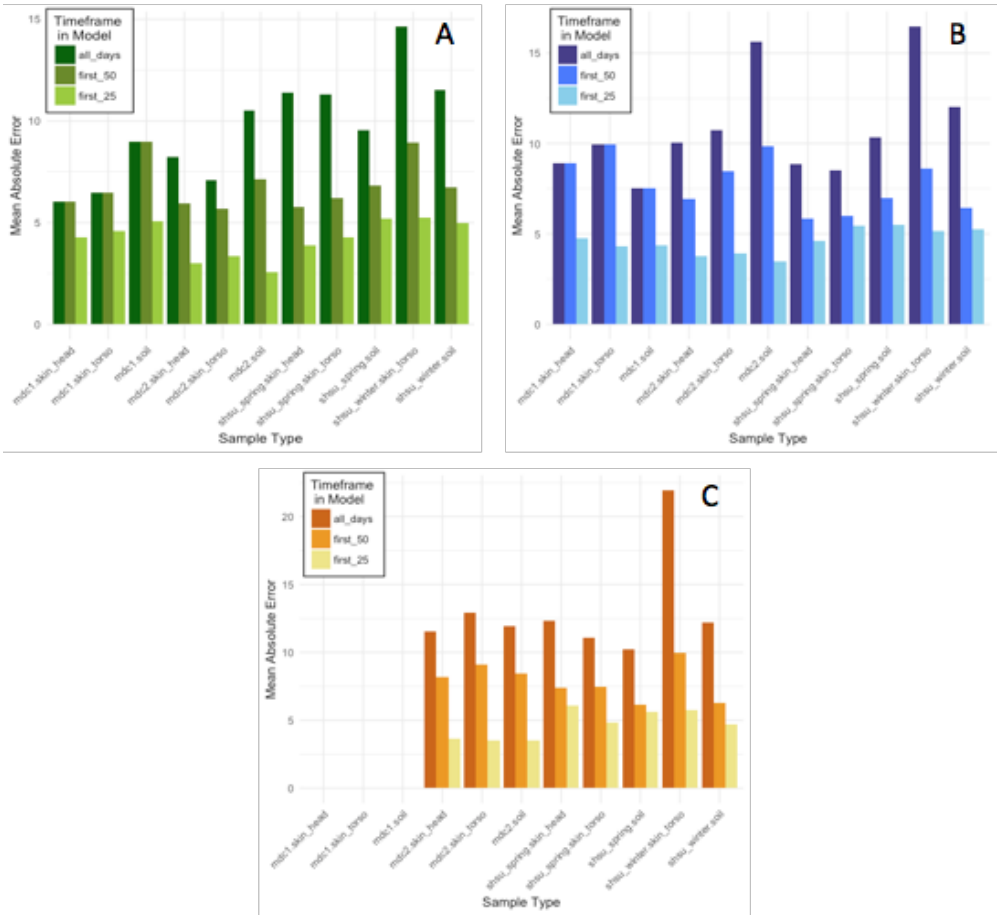

Figure S4.1. Plots of the Mean Absolute Error (MAE) of each model generated. For each marker type, models were generated for 3 sample types (skin_head, skin_torso, and soil) from each of 4 studies (mouse decomposition 1 (mdc1), mouse decomposition 2 (mdc2), SHSU human April (shsu_spring), SHSU human February (shsu_winter)). Skin of the head samples were not collected for the SHSU human winter experiment. Models were built using multiple time frames, including all sample days (mdc1: 48d, mdc2: 70d, shsu_spring: 132d, shsu_winter: 82d), only the first 50 days of decomposition, and only the first 25 days of decomposition. Models were built using Random Forest regression, trained on a subset of individuals within each sample type and tested on another individual. The MAE represents the best model for each sample type. (a) within study MAE for models trained on 16S rRNA data; (b) within study MAE for models trained on 18S rRNA data; (c) within study MAE for models trained on ITS data.

This resource was prepared by the author(s) using Federal funds provided by the U.S. Department of Justice. Opinions or points of view expressed are those of the author(s) and do not necessarily reflect the official position or policies of the U.S. Department of Justice.

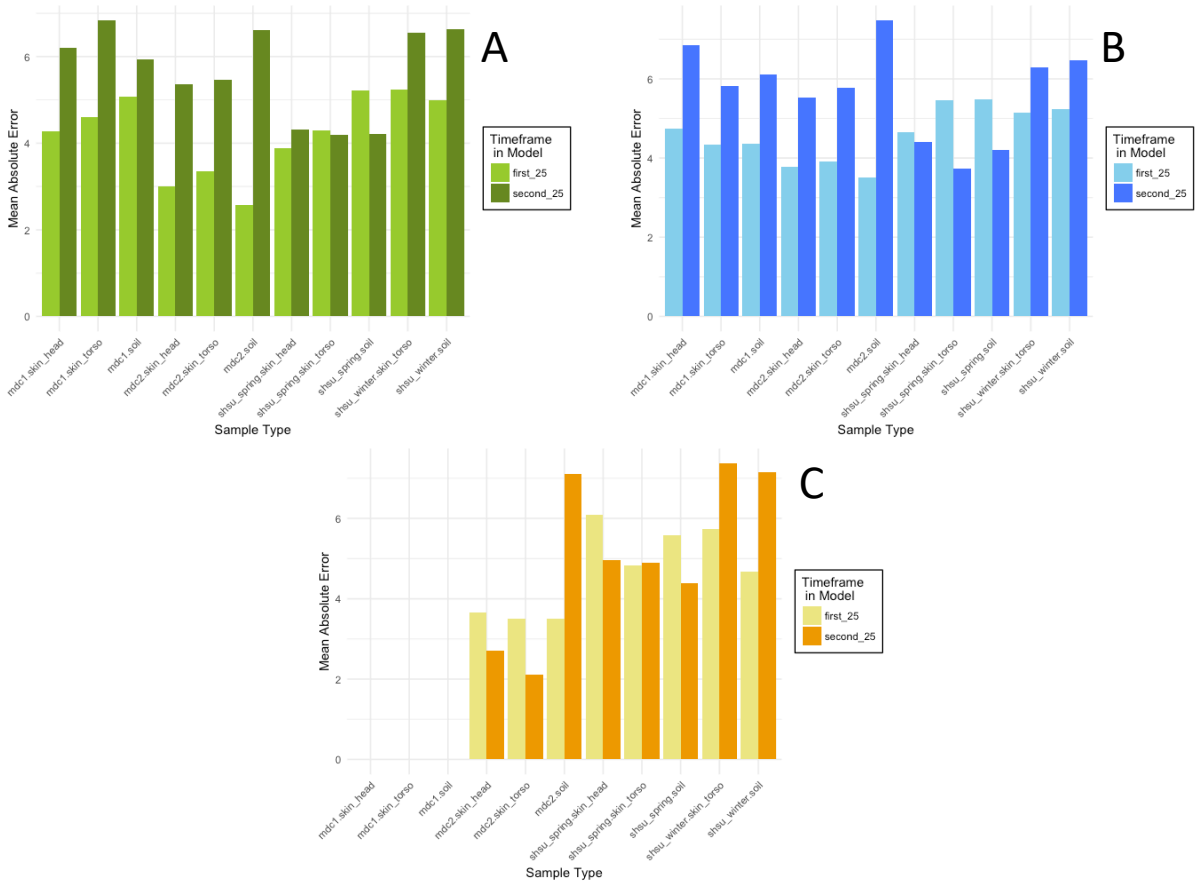

Figure S4.2. Plots of the Mean Absolute Error (MAE) for models generated on subsets of the data containing only the first 25 sampling days or sampling days 26-50. For each marker type, models were generated for 3 sample types (skin_head, skin_torso, and soil) from each of 4 studies (mouse decomposition 1 (mdc1), mouse decomposition 2 (mdc2), SHSU human April (shsu_spring), SHSU human February (shsu_winter)). Skin_head samples were not collected for shsu_winter. Models were built using random forest classifiers, trained on a subset of individuals within each sample type and tested on another. The MAE represents the best model for each sample type. (a) MAE for models trained on 16S rRNA data; (b) MAE for models trained on 18S rRNA data; (c) MAE for models trained on ITS data.

This resource was prepared by the author(s) using Federal funds provided by the U.S. Department of Justice. Opinions or points of view expressed are those of the author(s) and do not necessarily reflect the official position or policies of the U.S. Department of Justice.

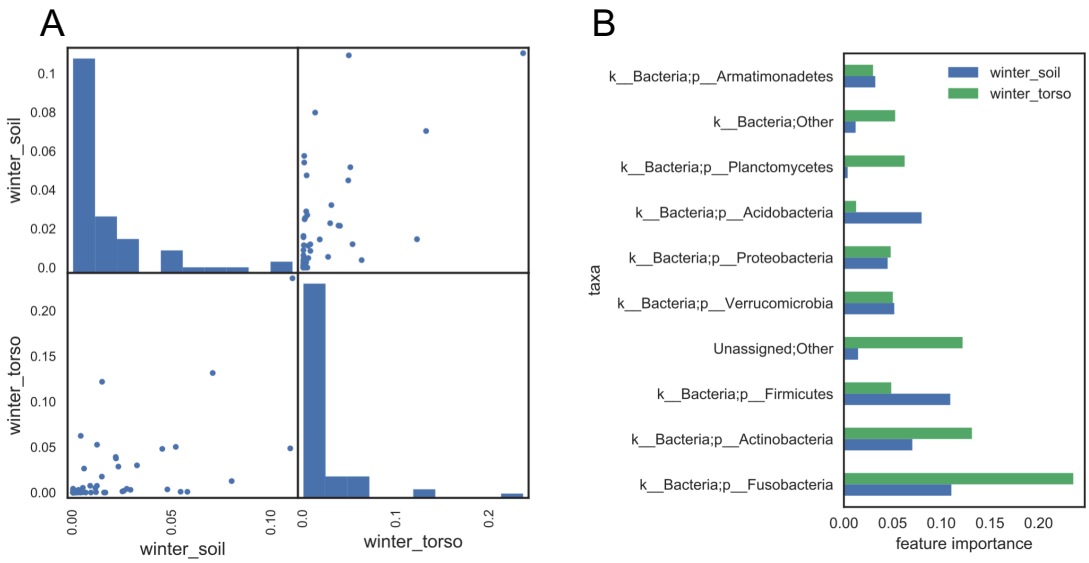

Figure S4.3. The feature importance of the phyla that measures the contribution of each phylum to the PMI regression model (results from SHSU winter study). (A) The feature importance is correlated across 3 sample types. Each scatter plot shows the correlation between feature importances of every pair of models built from each sample type. Each dot represents a phylum and its value on the x- or y-axis represents its feature importance in the 2 models of sample types. The Spearman correlation coefficients for torso vs. soil is 0.68, with a p-values << 0.01. The diagonal histogram plots show that most of phyla do not contribute much to regression models of each sample type. (B) The top 10 phyla that are most informative for PMI prediction within each sample type.

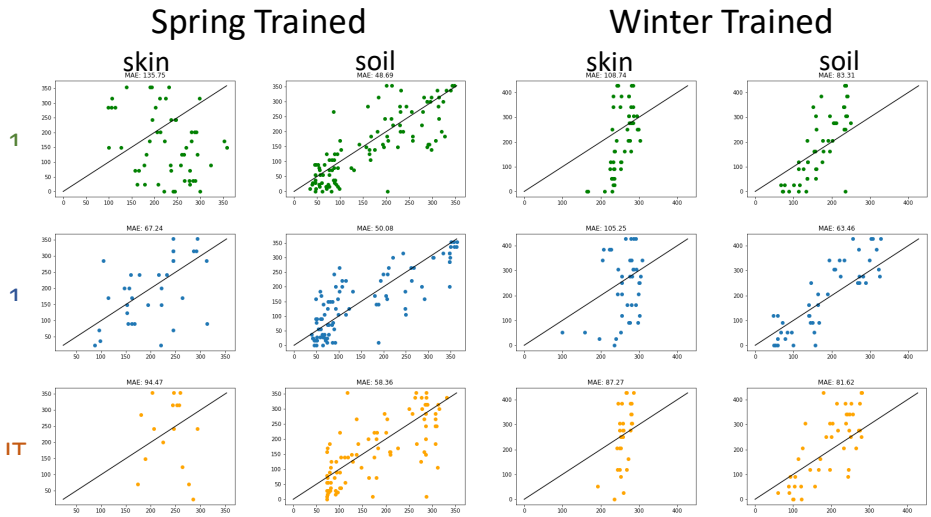

Figure S4. Random Forest regression models built from 16S rRNA, 18S rRNA, and ITS phylum data from models build using the human decomposition studies. Models in column 1 were trained on Spring body skin samples and tested on Winter body skin samples. Models in column 2 were trained on Spring body soil samples and tested on Winter body soil samples. Models in column 3 were trained on Winter body skin samples and tested on Spring body skin samples. Models in column 4 were trained on Winter body soil samples and tested on Spring body soil samples.

This resource was prepared by the author(s) using Federal funds provided by the U.S. Department of Justice. Opinions or points of view expressed are those of the author(s) and do not necessarily reflect the official position or policies of the U.S. Department of Justice.

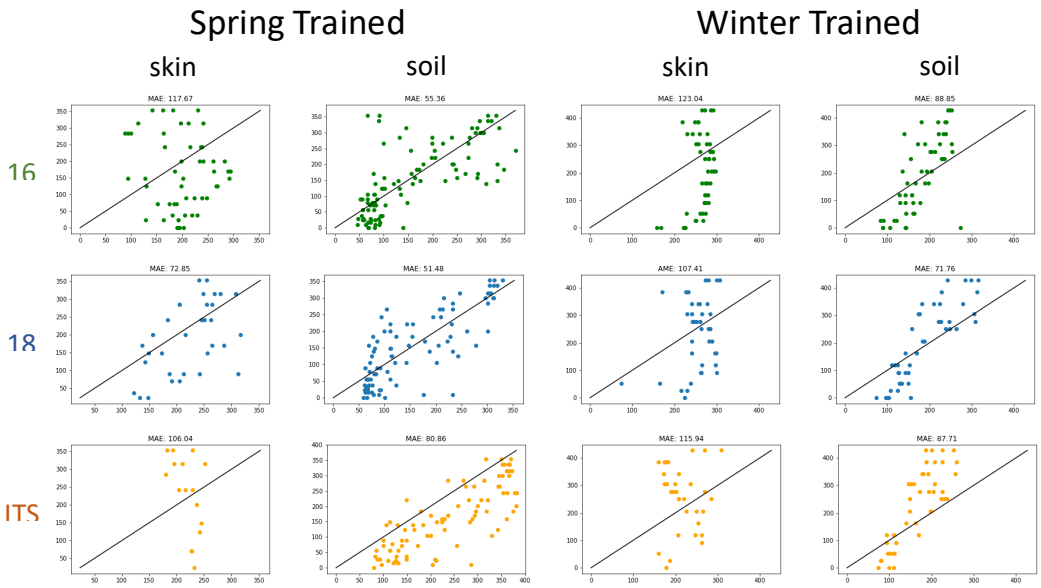

Figure S4.5. Random Forest regression models built from 16S rRNA, 18S rRNA, and ITS class data from models build using the human decomposition studies. Models in column 1 were trained on Spring body skin samples and tested on Winter body skin samples. Models in column 2 were trained on Spring body soil samples and tested on Winter body soil samples. Models in column 3 were trained on Winter body skin samples and tested on Spring body skin samples. Models in column 4 were trained on Winter body soil samples and tested on Spring body soil samples.

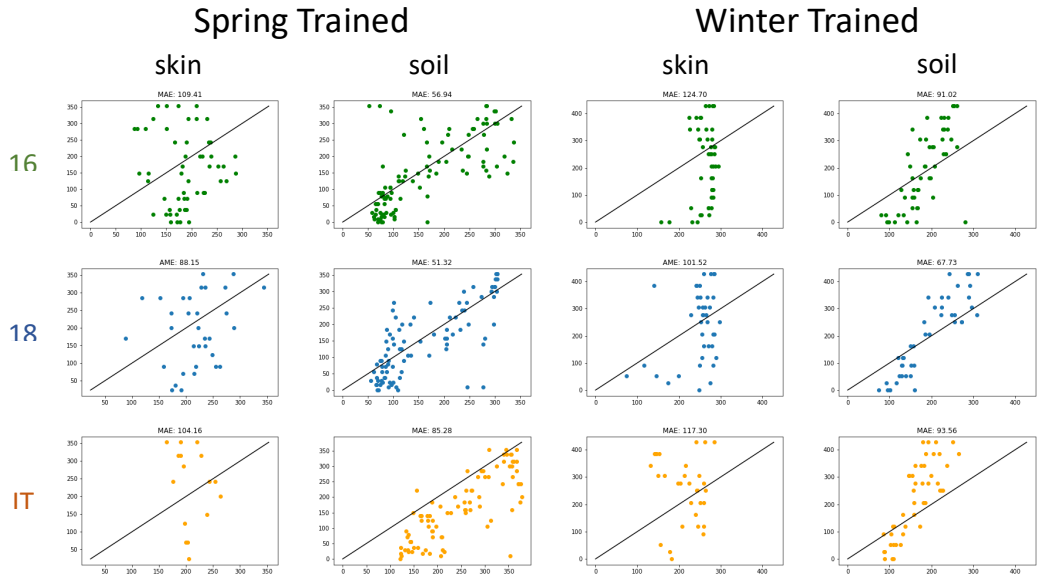

Figure S4.6. Random Forest regression models built from 16S rRNA, 18S rRNA, and ITS order data from models build using the human decomposition studies. Models in column 1 were trained on Spring body skin samples and tested on Winter body skin samples. Models in column 2 were trained on Spring body soil samples and tested on Winter body soil samples. Models in column 3 were trained on Winter body skin samples and tested on Spring body skin samples. Models in column 4 were trained on Winter body soil samples and tested on Spring body soil samples.

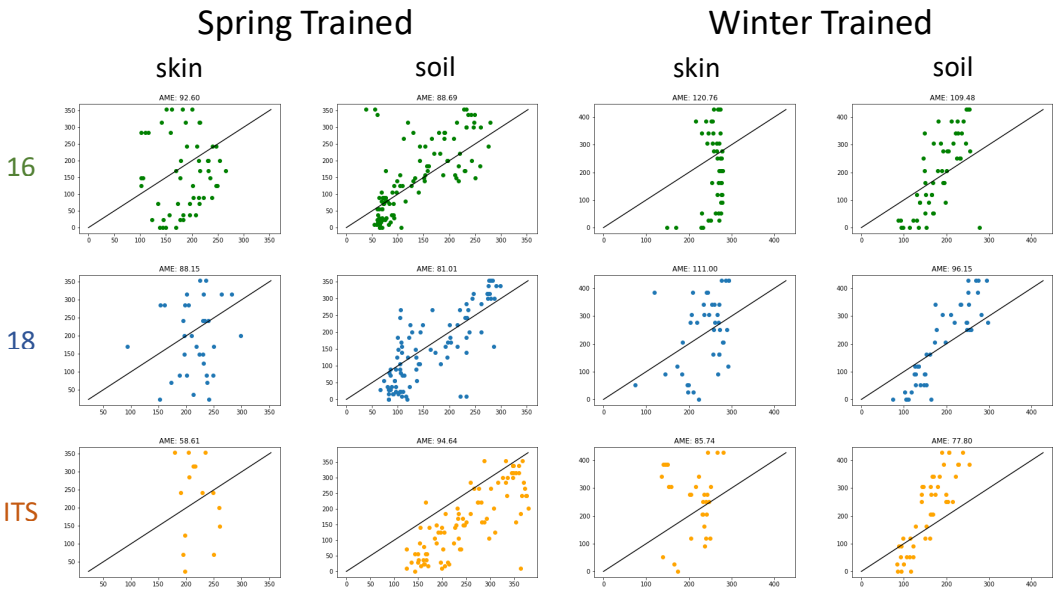

Figure S4.7. Random Forest regression models built from 16S rRNA, 18S rRNA, and ITS family data from models build using the human decomposition studies. Models in column 1 were trained on Spring body skin samples and tested on Winter body skin samples. Models in column 2 were trained on Spring body soil samples and tested on Winter body soil samples. Models in column 3 were trained on Winter body skin samples and tested on Spring body skin samples. Models in column 4 were trained on Winter body soil samples and tested on Spring body soil samples.

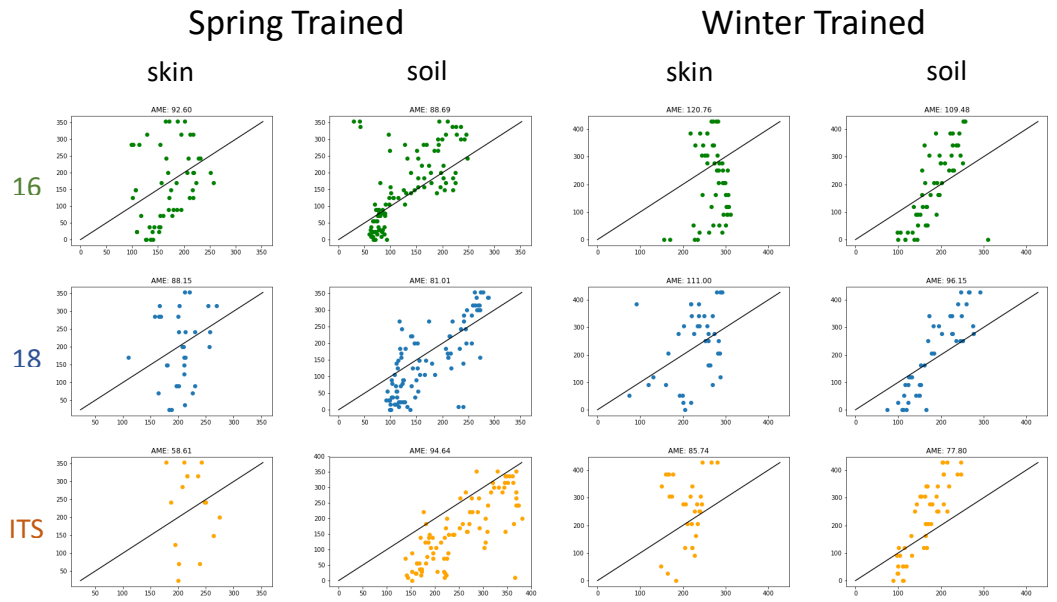

Figure S4.8. Random Forest regression models built from 16S rRNA, 18S rRNA, and ITS genus data from models build using the human decomposition studies. Models in column 1 were trained on Spring body skin samples and tested on Winter body skin samples. Models in column 2 were trained on Spring body soil samples and tested on Winter body soil samples. Models in column 3 were trained on Winter body skin samples and tested on Spring body skin samples. Models in column 4 were trained on Winter body soil samples and tested on Spring body soil samples.

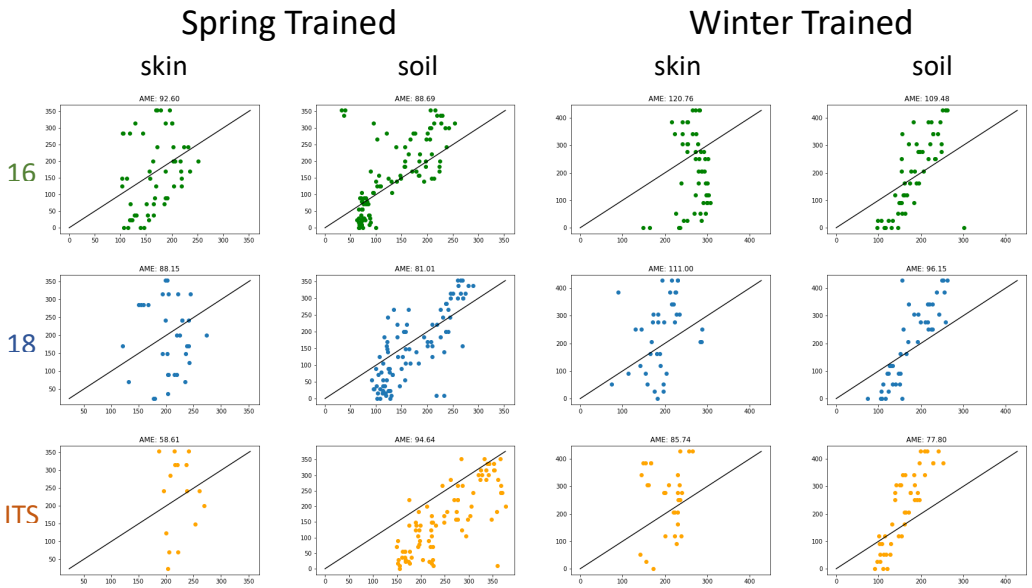

Figure S4.9. Random Forest regression models built from 16S rRNA, 18S rRNA, and ITS species data from models build using the human decomposition studies. Models in column 1 were trained on Spring body skin samples and tested on Winter body skin samples. Models in column 2 were trained on Spring body soil samples and tested on Winter body soil samples. Models in column 3 were trained on Winter body skin samples and tested on Spring body skin samples. Models in column 4 were trained on Winter body soil samples and tested on Spring body soil samples.

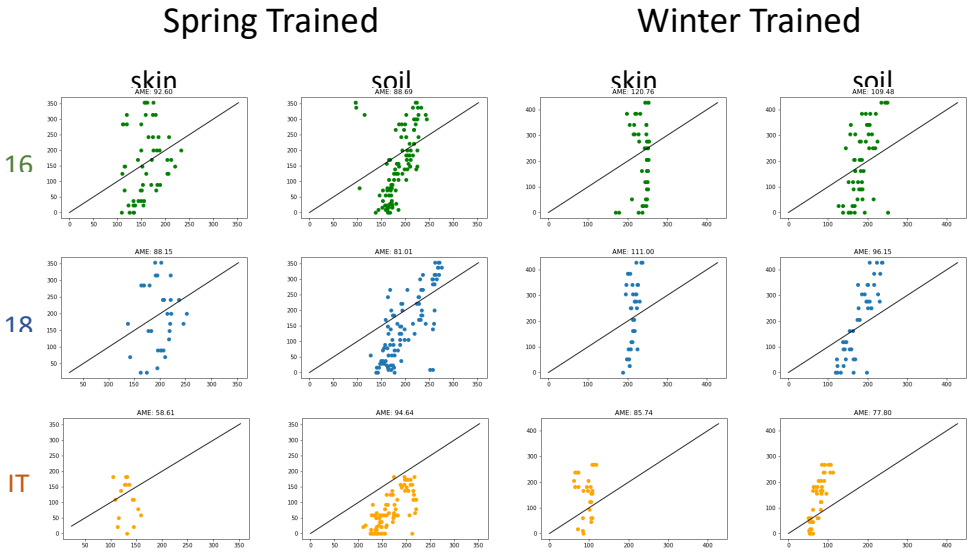

Figure S4.10. Random Forest regression models built from 16S rRNA, 18S rRNA, and ITS sequence variant data from models build using the human decomposition studies. Models in column 1 were trained on Spring body skin samples and tested on Winter body skin samples. Models in column 2 were trained on Spring body soil samples and tested on Winter body soil samples. Models in column 3 were trained on Winter body skin samples and tested on Spring body skin samples. Models in column 4 were trained on Winter body soil samples and tested on Spring body soil samples.

This resource was prepared by the author(s) using Federal funds provided by the U.S. Department of Justice. Opinions or points of view expressed are those of the author(s) and do not necessarily reflect the official position or policies of the U.S. Department of Justice.